Freshwater and nutrient distributions in contrasting coastal domains of Hudson Bay and James Bay

by

Alessia Guzzi

A thesis submitted to the Faculty of Graduate Studies of

The University of Manitoba

In partial fulfillment of the requirements of the degree of

MASTER OF SCIENCE

Department of Environment and Geography

University of Manitoba

Winnipeg

Abstract

In Arctic marine environments, the renewal of surface nutrient stocks through physical and biogeochemical processes during winter is critical to support primary production later in the season when solar irradiance is sufficient. Landfast sea-ice and river discharge in the riverine coastal domain influence not only the structure of the coastal water column, but also impact the movement and distribution of nutrients within the system. Over the last several decades, both climate change and anthropogenic activities have caused shifts in both sea-ice and riverine cycles. Winter freshwater tracer and nutrient data from Canadian Arctic coastal areas, such as in Hudson Bay are extremely scarce. In this thesis I begin to fill this gap, focusing on three coastal regions: northeast James Bay (NEJB), northwest Hudson Bay (NWHB), and southeast Hudson Bay (SEHB). The objective is to evaluate the relationships between freshwater sources and nutrient distributions, during ice-covered and ice-free seasons, across the selected coastal domains. I present new nutrient (nitrate, phosphate, and silicate) and freshwater tracer (oxygen isotope ratio, salinity) data for water samples collected during ice-covered conditions, and additionally, data from open-water conditions in NEJB. Samples were collected with the help of numerous community members and guides between 2016-2019. Each region was distinct in terms of freshwater composition and influence, with NEJB strongly influenced by La Grande River, as its large under-ice plume (because of regulation) drove surface nutrient concentrations in winter (high nitrate, low phosphate). The sea-ice cycle (withdrawal of freshwater and release of brine during formation) was the dominant influence on NWHB coastal waters. Here there are large concentration ranges of nutrients within a small salinity range, possibly due to an alternate source water, or recirculation of HB outflow. SEHB coastal waters are largely influenced by

riverine input from local rivers, and from the upstream James Bay outlet. Nutrient ratios showed potential nitrate limitation at salinities > 10 across all regions. Overall, this thesis provides new data that characterize a multitude of relationships between coastal freshwater sources, marine source waters, and the distribution of nutrients during winter and summer across three oceanographically different coastal regions of Hudson Bay.

Extended Abstract

In Arctic marine environments, the renewal of surface nutrient stocks through physical and biogeochemical processes during winter is critical to support primary production later in the season when solar irradiance is sufficient. Landfast sea-ice and river discharge in the riverine coastal domain (RCD) influence not only the structure of the coastal water column, but also impact the movement and distribution of nutrients within the system. Over the last several decades, observed changes in the environment due to climate and anthropogenic activities have caused shifts in both sea-ice and riverine cycles, which may ultimately impact the nutrient renewal and other processes associated with the RCD. Winter freshwater tracer and nutrient data from Canadian Arctic coastal areas, such as in Hudson Bay are extremely scarce. In this thesis I begin to fill this gap of knowledge, focusing on three coastal regions of the Hudson Bay system: northeast James Bay (NEJB), northwest Hudson Bay (NWHB), and southeast Hudson Bay (SEHB). In the following chapters, I present new nutrient (nitrate, phosphate, and silicate) and freshwater tracer data ($\delta^{18}O$) for water samples collected during ice-covered conditions for all three regions, and for NEJB, I present data from open-water conditions, as well. Data collection spanned the years 2016 to 2019 and sampling was achieved with the help of numerous community members and guides.

I examine the $\delta^{18}O$ – salinity relationship in each region and associated sub-region to identify the dominant sources of freshwater in these coastal water masses. I further examine the nutrient concentrations, ratios, and stocks to assess the relationships between the freshwater content and nutrient distribution during winter, and in the case of NEJB, summer. Each region is found to be distinct in terms of freshwater composition and influence, with NEJB being strongly influenced by the La Grande River, as its large under-ice plume drives surface nutrient concentrations in winter. At present, because of regulation, La Grande River experiences spring-freshet-like conditions in winter, and in spring, the discharge rates of La Grande are relatively low. The winter SEHB coastal waters are largely influenced by riverine input from local rivers (Great Whale River and the Nastapoca River), but also from the upstream James Bay outlet, in terms of large-scale circulation. The dominant influence on NWHB coastal waters is from the sea-ice cycle, including the processes of sea-ice formation and brine production. Variation in source seawater during winter is inferred from observations of a phosphate-rich water type in NWHB (concentrations up to 3.3 μM). This water type contained both brine and river water but had low nitrate concentrations, leading to a low N/P ratio and nitrate limitation at the start of the growing season. Phosphate concentrations showed conservative behaviour against salinity in late winter for both SEHB and NEJB. La Grande River discharge supplied nitrate at higher concentration (~5 μM) than those typical of NEJB coastal waters. Silicate concentrations were highest in NEJB and lowest in NWHB. Nutrient ratios showed potential phosphate limitation at salinities < 10 and potential nitrate limitation at salinities > 10 across all regions. Overall, this thesis provides new data that characterize a multitude of relationships between coastal freshwater sources (river discharge and sea-ice), marine source waters, and the distribution of nutrients during

winter and summer across three oceanographically different regions of Hudson Bay. It is a significant first step towards a comparative understanding of the coastal oceanographic domains of Hudson Bay and James Bay and the relationships between freshwater-mediated processes and nutrients cycling.

Acknowledgments

I would first like to express my immense gratitude to my co-advisors Drs. Zou Zou Kuzyk, and Jens Ehn, for their support, guidance, and motivation to continually learn. I am forever grateful for the opportunities I had during my graduate program that allowed me to gain new skills and grow not only as a student, but also as a person.

I would like to thank my committee members Drs. Robie Macdonald, and Christine Michel, for sharing their invaluable expertise and knowledge, and for their continual support, advisement and encouragement.

I would like to acknowledge our partnership with the Arctic Eider Society (Joel Heath) and thank the communities and the countless community members and guides that worked closely with us during the research campaigns, as well as the Arctic Eider Society liaisons including: the Cree Nation of Chisasibi (CNC; John Lameboy), Sanikiluaq (Lucassie Arragutainaq), Inukjuak (Allie Nalukturuk), Umiujaq (Annie Kasudluak) and Kuujjuaraapik (Peter Paul Cookie). I would also like to thank the Inuit communities of Naujaat and Chesterfield Inlet, with a special thank you to our Naujaat guides Johnny Tagornak and Laurent Kringayark.

A special thank you to the team that spent countless hours during field campaigns gathering and processing samples and data: Michelle Kamula, Chris Peck, Annie Eastwood, Misha Warbanski, and Drs. Kuzyk and Ehn. Also, thank you to everyone that helped with logistical and technical support, including Stephen Ciastek (who had multiple roles).

This work was financially supported by the Cree Nation of Chisasibi (contract with Arctic Eider Society), and grants to Kuzyk and Ehn from ArcticNet, Natural Sciences and Engineering Council of Canada (NSERC), Niskamoon Corporation, and Polar Knowledge Canada. The University of Manitoba Graduate Fellowship Program and the Government of Canada Northern Scientific Training Program also provided financial support.

Last but not least, I would like to thank my family and friends, and fellow students (who have become friends along the way) who have endlessly supported and encouraged me throughout my program. I couldn’t have done it without you!

Dedication

To my parents, Rosanna and Frank, for your unwavering support and encouragement to pursue my passions and discover new ones.

To my mom, especially, for teaching me to be strong, courageous, and resilient in the face of adversity.

Table of Contents

List of Tables

List of Figures

List of Copyrighted Materials

1.0 Introduction

Coastal zones, the portions of coastal shelves closest to the land, are recognized globally as having great ecological, societal and economic importance. These zones represent the areas where freshwater inputs from various sources merge and interact with coastal marine water. Where terrestrial freshwater enters the marine system, the density gradient between water masses creates a sharp halocline and buoyant surface plume, which mixes and moves as a result of physical processes and conditions that the coastal zone is susceptible to.

The Riverine Coastal Domain (RCD), a domain type defined by Carmack et al. (2015) for coastal zones in the circumpolar Arctic, is defined as a contiguous feature along continental coasts, including Hudson Bay, which lies in the sub-Arctic (Figure 1.1). This domain is characterized by relatively shallow water depths (< 10 m) and is generally less than 15 km in distance from the coast (Carmack et al., 2015). The RCD plays an important role in biogeochemical processes, as this is where terrestrial components are incorporated in the marine environment (Holmes et al., 2012) affecting light availability, nutrients and overall carbon regimes, which consequently impacts primary production (Carmack et al., 2015). The properties of the RCD, which acts essentially as a pathway for coastal waters, can be influenced by many factors acting both locally and regionally, weather events, the bathymetry of the region and coastline topography, and the seasonal variation of processes known to Arctic coastal areas (e.g., river discharge, sea-ice) (Carmack et al., 2015).

Figure 1.1 The Riverine Coastal Domain (RCD) identified by the red outline and direction of flow in the northern hemisphere. From Carmack et al., 2015 © 2020 Elsevier

The Arctic Ocean is fresher (average salinity of 31.7) in comparison to other oceans such as the Pacific and the Atlantic with average salinities of 32.5 and 34.8 respectively (Azetsu-Scott et al., 2012). The Arctic receives ~10% of the global ocean's freshwater discharge into a volume that represents only 1% of all oceans (Bianchi et al., 2014), which highlights the strength and unique character of the RCD across Arctic coastal areas. The Canadian Arctic Archipelago alone receives a mean annual riverine discharge estimated at 200-300 km^3 (Alkire et al., 2017). This relatively high volume of riverine inflow is one of the reasons why the Arctic experiences density-driven stratification, in contrast to coastal areas at lower latitudes where water temperature typically drives the stratification (McClelland et al., 2012).

Density-driven stratification is also a result of the presence of seasonal sea ice cover, i.e., ice that forms during winter withdrawing freshwater from the surface layer and melts each summer adding freshwater back into the surface layer. The ice growth and melt processes occur at different rates in various places, and indeed ice drift leads to freshwater transfers between the RCD and offshore areas. It has been estimated that approximately 10,000 km^3 worth of freshwater is stored annually in the sea ice of the Arctic Ocean and released again during the period of melt (Serreze et al., 2006).

In addition to the sea-ice cycle, the seasonality in freshwater addition and stratification in these coastal areas is influenced by the riverine discharge cycle. Natural Arctic and sub-Arctic Rivers experience an annual pattern where there are low flows in winter, high flows in spring (freshet) and low flows during late summer and fall (Figure 1.2).

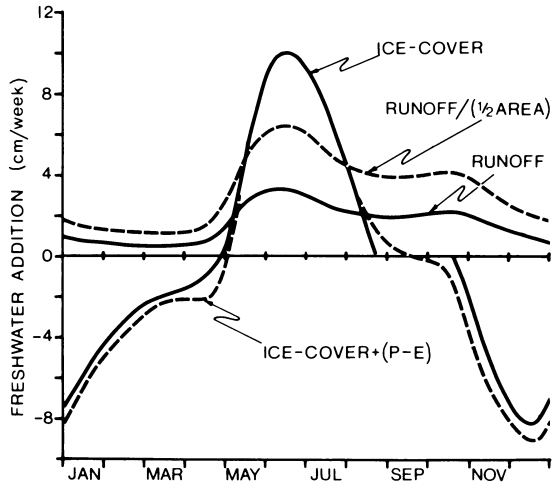

Figure 1.2 Freshwater addition to Hudson Bay from January to December, using a 1.6 m maximum ice-cover thickness. P = Precipitation, E = Evaporation. From Prinsenberg, 1988.

In Arctic and sub-Arctic coastal areas, the seasonality in freshwater also drives seasonality in biogeochemical processes. During spring and summer, when sea-ice melting and river discharge lead to peaks in freshwater additions (Figure 1.2), there is a strengthening of the halocline, which restricts vertical mixing and reduces nutrient supply from deep waters, which could be used by primary producers during the growing season (Tremblay et al., 2008; Ferland et al., 2011). Throughout the summer, the surface nutrients in ice-free waters tend to be used up; then in fall, a breakdown of stratification occurs with more weather perturbations before freezing begins (Alkire et al., 2019). At the time of ice formation, brine is released into the system, driving deep mixing and the breakdown of the surface pycnocline (Granskog et al., 2011). Sea ice can also act as a barrier to outside forces, such as wind or weather events, and light, which is why there is low production occurring in winter, in comparison to the ice-free period, apart from ice algae which grows either at the ice-water interface or within the interstitial waters in the ice (Maestrini et al., 1986). Therefore the fall-winter period is a critical time for nutrients to be renewed in the surface waters (Ferland et al., 2011), resetting the nutrient condition for when the productive season begins.

Areas near major river outlets, however, can have more complicated seasonal freshwater and nutrient cycles. Most simply, river water is different from sea ice melt in that it contains nutrients and other dissolved constituents. Furthermore, in these areas, the river inflow may be incorporated into landfast ice as it forms, delaying freshwater transports to other areas and resulting in less brine release. These areas may also develop under-ice river plumes, which vary in extent and depth depending on factors such as topography, shelf size, and volume of discharge (e.g., Ingram et al., 1996; Carmack and Macdonald, 2002). There

can be strong stratification and very low surface salinities associated with under-ice river plumes and, for an equivalent discharge, river plumes can spread over much larger areas under ice than they would in ice-free areas (cf., Ingram and Larouche, 1987a, b). Figure 1.3 provides an example of one way that the ice cover and river discharge can interact to modify the structure of the water column in the RCD and how the interaction of the freshwater components changes during different seasons. These processes are specific to the Canadian Beaufort Shelf (Carmack and Macdonald, 2002). Indeed, the interaction between the ice cover and underlying water column is likely different in its specifics all along the RCD with variation in river inflow and ice environment, and additional study is needed because only a few locations have been studied in any detail.

Arctic sea ice cover shows inter-annual variability when it comes to both extent and volume, which has increasingly been changing over the last few decades, along with the overall shortening of the annual ice cover period (Andrews et al., 2018; Solomon et al., 2021). This change has implications for the freshwater budgets of Arctic and sub-Arctic seas. It could also change the timing and magnitude of surface nutrient renewal in the RCD, as suggested by Ferland et al. (2011).

The biogeochemistry, particularly the cycling of freshwater and nutrients, in the Canadian Arctic RCD remains poorly characterized, particularly for the winter period. Only a few coastal Arctic locations have received intensive oceanographic study during the winter period, e.g., Mackenzie estuary (Macdonald et al., 1987) and the Great Whale River (Ingram et al., 1996; Legendre et al., 1996). In other places, such as in Hudson Bay, intensive studies were conducted during 1970s but major environmental changes related to climate change and/or hydroelectric development have occurred subsequent to these early studies (e.g., La

Grande, Freeman et al., 1982; Messier et al., 1986; Lalumiere et al., 1994; Hernandez-Henriquez et al., 2010). The complexity of the RCD and its sensitivity to changing environmental conditions make these regions important to study and understand the potential consequences of change to freshwater sources. In order to understand nutrient distribution and seasonality in the Arctic and subarctic RCD, freshwater contributions and their role in structuring the system needs to be understood and quantified. By applying water isotope tracers in addition to salinity, new perspectives have been gained on the cycling of sea ice and river water in the Arctic Ocean (cf., Alkire et al. 2017) and subarctic seas such as Hudson Bay (Granskog et al. 2011), and in a few Arctic estuaries (cf., Alkire et al., 2019; Macdonald et al., 1995; Kuzyk et al. 2008; Pavlov et al., 2016). However, considering the diversity of the RCD along the tens of thousands of kilometers of Arctic coastline, further studies that assess the contributions of freshwater sources and their influences on nutrients are certainly needed.

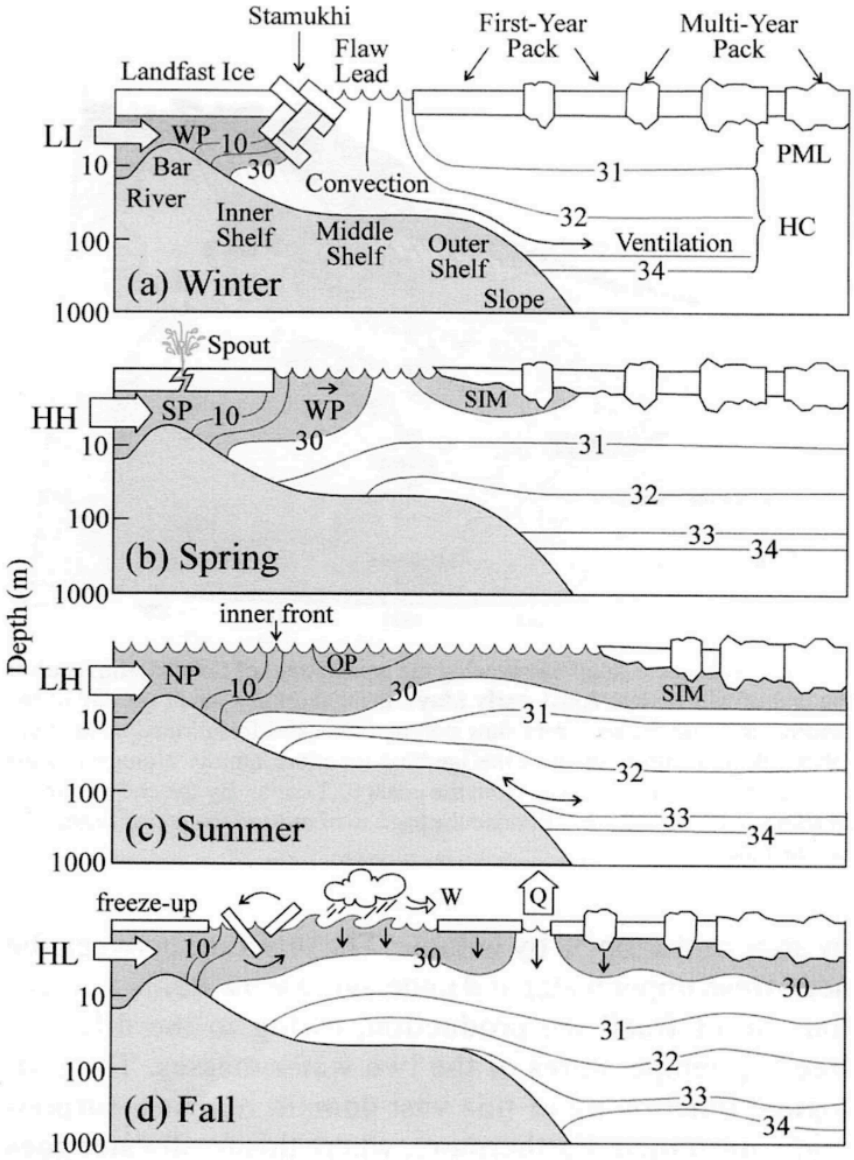

Figure 1.3 Schematic sections of ice cover and water column structure across the Canadian Shelf for (a) the end of winter; (b) spring freshet and break-up; (c) summer open water season; and (d) fall mixing and freeze-up. Abbreviations: HH = higher high river discharge; HL = higher low river discharge; LW = lower high river discharge; LL = lower low river discharge, NP = new plume water; OP = old plume water; Q = surface heat flux; SIM = sea ice melt; SP = spring inflow (warm and turbid); W =winter; WP = winter inflow (cold and clear). Taken from Carmack and Macdonald, 2002.

1.1 Research Objectives

The overarching objective of this thesis is to evaluate the relationships between freshwater sources and nutrient distributions, during both ice-covered and ice-free seasons, across three selected coastal domains of the Hudson Bay-James Bay system. The water oxygen isotopic ratio is used together with salinity to estimate the contributions of ice melt and river water and their influence on nutrients during different seasons. Inuit research partners from communities in each coastal area were involved in designing and conducting the field sampling.

A motivation for conducting this research is that coastal Hudson Bay and James Bay is home to thirty-nine communities that are predominantly populated by Inuit and Cree, and represent the largest population (~50,000 individuals) of any region of the Canadian Arctic (Andrews et al. 2018). The coastal domain is utilized by community members as a means of travel, in both ice-cover and ice-free conditions. Inuit hunt marine mammals and polar bears in these coastal areas, and the offshore islands within the RCD along James Bay are used by Cree for hunting marine mammals as well, berry picking and harvesting migratory birds, especially Canada Geese. Inuit and Cree land users have seen the environment change rapidly over the last few decades. Changes have been observed in species as well, for example, in seal body conditions, seabird diets, stomach contents of hunted animals, and even declining eelgrass (vascular rooted plant) condition and extent (local observations; Gaston et al., 2007; Gaston et al., 2012). Within this context of rapid change and despite the need for baseline information to inform marine monitoring and protection of these areas, coastal Hudson Bay and James Bay still have limited or no biogeochemical data collected,

especially during winter months, which is in part due to the difficulty in sampling the coastal domain during winter.

In this study, I examine the seasonality of freshwater and nutrient relationships at sites distributed among three distinct coastal regions of Hudson Bay and James Bay which I distinguish as: northwest Hudson Bay (NWHB), southeast Hudson Bay (SEHB), and northeast James Bay (NEJB). NWHB lies in the "Hudson Bay" marine ecoregion defined by Fisheries and Oceans Canada (Figure 1.4). It is located along one of the passageways that connects Hudson Bay to adjacent water bodies (Foxe Basin and Hudson Strait) and it has a relatively low degree of local river influence with the first major source of river water discharged at Chesterfield Inlet from Baker Lake (a combination of the Thelon and Kazan Rivers) (Figure 1.4). Most of NWHB's freshwater is supplied with inflowing Pacific-origin, Arctic-derived water masses and/or the seasonal sea-ice cycle (Tan and Strain, 1996). NEJB and SEHB lie in the "James Bay and eastern Hudson Bay" marine ecoregion (Stewart and Lockhart, 2005; Figure 1.4). Northeast James Bay is distinctly estuarine and dominated by river discharge from the La Grande River Complex, which typically discharges 5000 m^3 s^{-1} during winter and thus constitutes the largest single source of freshwater to the Hudson Bay-James Bay system during winter (Figure 1.4). The winter discharge of the La Grande River is, in fact, among the largest winter river discharges of the entire circumpolar Arctic (Peck et al., submitted).

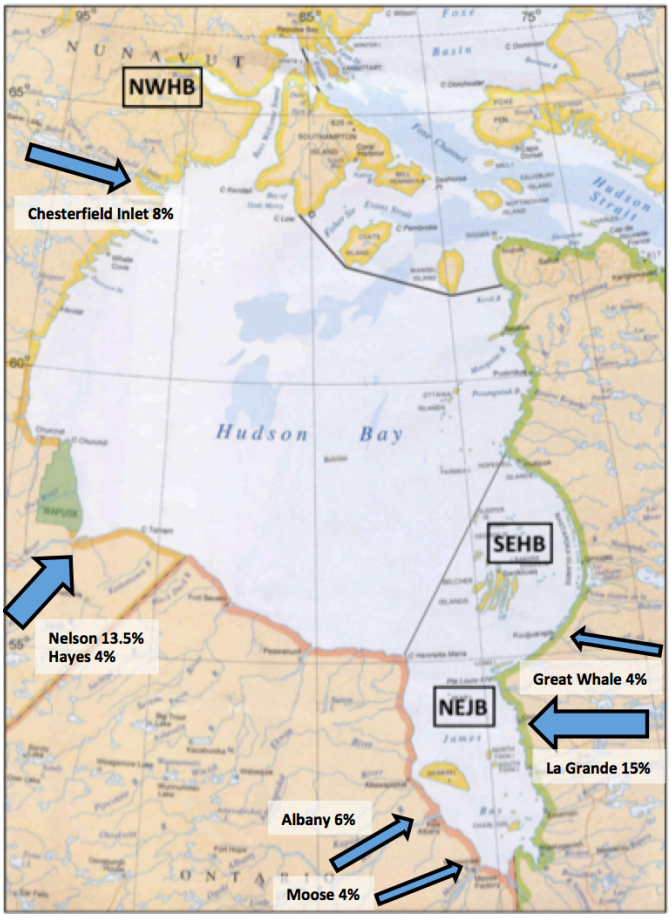

Figure 1.4 Hudson Bay Ecoregions as defined by Stewart and Lockhart (2005). Annotations indicate the three study regions of this thesis. Percentage of total average streamflow of all Hudson Bay rivers (from Déry et al., 2011) is noted along with a blue arrow indicating direction of river outlet. Size of arrows indicate relative percentage.

To accomplish the main objective, the following sub-objectives were established for this thesis:

1. Quantify and describe the distribution of freshwater supplied by river water *versus* sea-ice melt in the coastal study areas using oxygen isotope tracer and salinity data.
2. Examine nutrient distributions with respect to the supply provided by different water sources and evaluate the conservative *versus* non-conservative behaviour of the properties.

3. Where data allow, calculate nutrient inventories in winter and summer surface waters, and compare among sites and with previously published data. This third sub-objective applies only to the NEJB region, as substantial summer data was collected in addition to winter data, which is not the case for SEHB and NWHB.

1.2 Thesis Structure

This thesis contains five chapters. Section one introduces the topic and significance of the research from a large-scale perspective, outlines the research objectives, and details the thesis structure. Section two provides relevant scientific knowledge through a comprehensive review of the literature around the topics of freshwater and nutrient dynamics in the Arctic and subarctic as well as a review of what is known of the oceanographic setting of Hudson and James Bays. Section three focuses on the northeast James Bay (NEJB) region and examines the seasonal freshwater composition and the influence it has on nutrient distributions. Section four covers the same objectives as section three but in regards to the winter condition of coastal northwest Hudson Bay (NWHB) and southeast Hudson Bay (SEHB). The last section synthesizes key research findings and discusses their implications.

References

Alkire, M.B., A. Jacobson, G.O. Lehn, R.W. Macdonald, and M.W. Rossi. (2017). On the geochemical heterogeneity of rivers draining into the straits and channels of the Canadian Arctic Archipelago. *Journal of Geophysical Research – Biogeosciences* 122: 2527– 2547. https://doi.org/10.1002/2016JG003723.

Alkire, M. B., Jacobson, A., Macdonald, R. W., & Lehn, G. (2019). Assessing the Contributions of Atmospheric/Meteoric Water and Sea Ice Meltwater and Their Influences on Geochemical Properties in Estuaries of the Canadian Arctic Archipelago. *Estuaries and Coasts*, *42*(5), 1226–1248. https://doi.org/10.1007/s12237-019-00562-w

Andrews, J., Babb, D., & Barber, D. G. (2018). Climate change and sea ice: Shipping in Hudson Bay, Hudson Strait, and Foxe Basin (1980–2016). *Elem Sci Anth*, *6*(1), 19. https://doi.org/10.1525/elementa.281

Azetsu-Scott, K., Petrie, B., Yeats, P., & Lee, C. (2012). Composition and fluxes of freshwater through Davis Strait using multiple chemical tracers. *Journal of Geophysical Research: Oceans*, *117*(12), 1–12. https://doi.org/10.1029/2012JC008172

Bianchi, T.S., Allison, M.A., & Cai, W.-J. (2014). An introduction to the biogeochemistry of river coastal systems. In T.S. Bianchi, M.A. Allison, & W.-J. Cai (Eds.), Biogeochemical Dynamics at Major River-Coastal Interfaces: Linkages with Global Change (3-18). Cambridge: Cambridge University Press.

Carmack, E. C., & Macdonald, R. W. (2002). Oceanography of the Canadian shelf of the Beaufort Sea: A setting for marine life. *Arctic*, *55*(SUPPL. 1), 29–45. https://doi.org/10.14430/arctic733

Carmack, E., Winsor, P., & Williams, W. (2015). The contiguous panarctic Riverine Coastal Domain: A unifying concept. *Progress in Oceanography*, *139*, 13–23. https://doi.org/10.1016/j.pocean.2015.07.014

Déry, S. J., Mlynowski, T. J., Hernández-Henríquez, M. A., & Straneo, F. (2011). Interannual variability and interdecadal trends in hudson bay streamflow. *Journal of Marine Systems*, *88*(3), 341–351. https://doi.org/10.1016/j.jmarsys.2010.12.002

Ferland, J., Gosselin, M., & Starr, M. (2011). Environmental control of summer primary production in the hudson bay system: The role of stratification. *Journal of Marine Systems*, *88*(3), 385–400. https://doi.org/10.1016/j.jmarsys.2011.03.015

Freeman, N. G., Roff, J. C., & Pett, R. J. (1982). Physical, chemical, and biological features of river plumes under an ice cover in James and Hudson Bays. *Le Naturaliste Candien*, *109*, 745–764.

Gaston, A. J., Smith, S. A., Saunders, R., Storm, G. I., & Whitney, J. A. (2007). Birds and marine mammals in southwestern Foxe Basin, Nunavut, Canada. *Polar Record*, *43*(1), 33–47. https://doi.org/10.1017/S0032247406005651

Gaston, A. J., Mallory, M. L., & Gilchrist, H. G. (2012). Populations and trends of Canadian Arctic seabirds. *Polar Biology*, *35*(8), 1221–1232. https://doi.org/10.1007/s00300-012-1168-5

Granskog, M. A., Kuzyk, Z. Z. A., Azetsu-Scott, K., & Macdonald, R. W. (2011). Distributions of runoff, sea-ice melt and brine using δ18o and salinity data - a new view on freshwater cycling in hudson bay. *Journal of Marine Systems*, *88*(3), 362–374. https://doi.org/10.1016/j.jmarsys.2011.03.011

Hernández-Henríquez, M. A., Mlynowski, T. J., & Déry, S. J. (2010). Reconstructing the Natural Streamflow of a Regulated River: A Case Study of La Grande Rivière, Québec, Canada. *Canadian Water Resources Journal*, *35*(3), 301–316. https://doi.org/10.4296/cwrj3503301

Holmes, R. M., McClelland, J. W., Peterson, B. J., Tank, S. E., Bulygina, E., Eglinton, T. I., … Zimov, S. A. (2012). Seasonal and Annual Fluxes of Nutrients and Organic Matter from Large Rivers to the Arctic Ocean and Surrounding Seas. *Estuaries and Coasts*, *35*(2), 369–382. https://doi.org/10.1007/s12237-011-9386-6

Ingram, R. G., & Larouche, P. (1987a). Changes in the under-ice characteristics of la grande rivière plume due to discharge variations. *Atmosphere - Ocean*, *25*(3), 242–250. https://doi.org/10.1080/07055900.1987.9649273

Ingram, R. G., & Larouche, P. (1987b). Variability of an under-ice river plume in Hudson Bay. *Journal of Geophysical Research*, *92*(C9), 9541-9547.

Ingram, R. G., Wang, J., Lin, C., Legendre, L., & Fortier, L. (1996). Impact of freshwater on a subarctic coastal ecosystem under seasonal sea ice (southeastern Hudson Bay, Canada). I. Interannual variability and predicted global warming influence on river plume dynamics and sea ice. *Journal of Marine Systems*, *7*(2–4), 221–231. https://doi.org/10.1016/0924-7963(95)00006-2

Kuzyk, Z. A., Macdonald, R. W., Granskog, M. A., Scharien, R. K., Galley, R. J., Michel, C., … Stern, G. (2008). Sea ice, hydrological, and biological processes in the Churchill River estuary region, Hudson Bay. *Estuarine, Coastal and Shelf Science*, *77*(3), 369–384. https://doi.org/10.1016/j.ecss.2007.09.030

Lalumière, R., Messier, D., Fournier, J. J., & Peter McRoy, C. (1994). Eelgrass meadows in a low arctic environment, the northeast coast of James Bay, Québec. *Aquatic Botany*, *47*(3–4), 303–315. https://doi.org/10.1016/0304-3770(94)90060-4

Legendre, L., Robineau, B., Gosselin, M., Michel, C., Ingram ', R. G., Fortier, L., … Monti, D. (1996). Impact of freshwater on a subarctic coastal ecosystem under seasonal sea ice (southeastern Hudson Bay, Canada) II. Production and export of microalgae *. *Journal of Marine Systems*, *7*, 233–250.

Macdonald, R. W., Wong, C. S., & Erickson, P. E. (1987). The distribution of nutrients in the southeastern Beaufort Sea: Implications for water circulation and primary production. *Journal of Geophysical Research: Oceans*, *92*(C3), 2939–2952. https://doi.org/10.1029/JC092iC03p02939

Macdonald, R.W., D.W. Paton, and E.C. Carmack. (1995). The freshwater budget and under-ice spreading of Mackenzie River water in the Canadian Beaufort Sea based on salinity and 18O/16Omeasurements in water and ice. *Journal of Geophysical Research 100*(C1): 895– 919.

Maestrini, S. Y., Rochet, M., Legendre, L., & Demers, S. (1986). Nutrient limitation of the bottom-ice microalgal biomass (southeastern Hudson Bay, Canadian Arctic). *Limnology and Oceanography*, *31*(3), 969–982.

McClelland, J. W., Holmes, R. M., Dunton, K. H., & Macdonald, R. W. (2012). The Arctic Ocean Estuary. *Estuaries and Coasts*, *35*(2), 353–368. https://doi.org/10.1007/s12237-010-9357-3

Messier D, Ingram RG, Roy D. (1986). Chapter 20: Physical and biological modifications in response to La Grande hydroelectric complex. *Elsevier Oceanography Series* 44:403-424.

Pavlov, A. K., Stedmon, C. A., Semushin, A. V., Martma, T., Ivanov, B. V., Kowalczuk, P., & Granskog, M. A. (2016). Linkages between the circulation and distribution of dissolved organic matter in the White Sea, Arctic Ocean. *Continental Shelf Research*, *119*, 1–13. https://doi.org/10.1016/j.csr.2016.03.004

Peck, C. J., Kuzyk, Z. Z. A., Heath, J. P., Lameboy, J., Ehn, J. K. (submitted). Under-ice hydrography of the La Grande River plume in relation to a ten-fold increase in wintertime discharge.

Prinsenberg, S. J. (1988). Ice-Cover and Ice-Ridge Contributions to the Freshwater Contents of Hudson Bay and Foxe Basin. *Arctic*, *41*(1), 6–11.

Serreze, M. C., Barrett, A. P., Slater, A. G., Woodgate, R. A., Aagaard, K., Lammers, R. B., … Lee, C. M. (2006). The large-scale freshwater cycle of the Arctic. *Journal of Geophysical Research: Oceans*, *111*(11), 1–19. https://doi.org/10.1029/2005JC003424

Solomon, A., Heuzé, C., Rabe, B., Bacon, S., Bertino, L., Heimbach, P., … Tang, H. (2021). Freshwater in the Arctic Ocean 2010-2019. *Ocean Science*, *17*(4), 1081–1102. https://doi.org/10.5194/os-17-1081-2021

Stewart, D.B., and W.L. Lockhart. 2005. An Overview of the Hudson Bay Marine Ecosystem. Can. Tech. Rep. Fish. Aquat. Sci. 2586: vi + 487 p.

Tan, F. C., & Strain, P. M. (1996). Sea ice and oxygen isotopes in Foxe Basin, Hudson Bay, and Hudson Strait, Canada. *Journal of Geophysical Research C: Oceans*, *101*(C9), 20869–20876. https://doi.org/10.1029/96JC01557

Tremblay, J. É., Simpson, K., Martin, J., Miller, L., Gratton, Y., Barber, D., & Price, N. M. (2008). Vertical stability and the annual dynamics of nutrients and chlorophyll fluorescence in the coastal, southeast Beaufort Sea. *Journal of Geophysical Research: Oceans*, *113*(7), 1–14. https://doi.org/10.1029/2007JC004547

2.0 Background and Literature Review

2.1 Freshwater in the Arctic and Subarctic

In high-latitude marine environments, freshwater input is not limited to meteoric sources such as precipitation and riverine input. Due to the characteristic climate of Arctic and subarctic regions, where in winter months it is consistently below freezing, there is significant sea-ice formation, which withdraws freshwater from the surface of the ocean. In summer, there is sea-ice melt, which contributes to the freshwater content of the surface waters. Because ice growth and melt do not necessarily occur at the same location, the sea-ice cycle has a complicated influence on local freshwater budgets even if it balances out in any given year for seasonal ice (i.e., growth = melt) at the large scale.

The Arctic Ocean is the ocean most influenced by riverine input of all the world's oceans, with lower overall surface salinities and the detection of terrigenous chemical signals across the entire basin indicating riverine influence to some degree (Tank et al., 2012). The Arctic Ocean receives approximately 10% of the global freshwater discharge (Bianchi et al., 2014), which has been increasing in both volume and variability (Tank et al., 2012). Riverine input at these high latitudes not only impacts the immediate coastal area where a river outlets, but also further 'downstream' throughout the riverine coastal domain (RCD). In this context, "downstream" is in reference to the direction of flow of the RCD, which is impacted by the Coriolis Effect, where river plumes generally appear to "turn to the right" once exiting a river mouth and flow in that direction along the coast in the Northern Hemisphere. Other processes such as wind/storms, or dense water formation during winter also can move river water from the coastal domain across the shelf into, for example, the halocline of the Arctic Ocean

(Aagaard et al., 1981; cf., Bauch et al. 2011). Examining the freshwater content of marine regions in the Arctic is important because salinity is what influences stratification patterns of the water column, as opposed to the temperature of the water mass, which drives stratification in more temperate regions (McClelland et al., 2012). Riverine discharge, and sea ice vary seasonally in the Arctic, and are influenced by a variety of factors dependent upon geographic location and climate (Figure 2.1), which would have implications for biogeochemical processes. For example, high-latitude rivers that outlet to coastal areas may freeze and have an overall lower flow (negligible in the case of small streams) during winter months, and as melt begins, there is a large pulse of freshwater known as the spring freshet, which brings much larger volumes of meteoric water to the coast. Canadian drainage basins vary quite widely in terms of the geology and climate and these differences are reflected in their respective hydrographs (Figure 2.1). Quantifying the contributions of freshwater sources to coastal water masses allows us to have a better understanding of the environment and biogeochemical processes that ultimately influence nutrient availability and primary production.

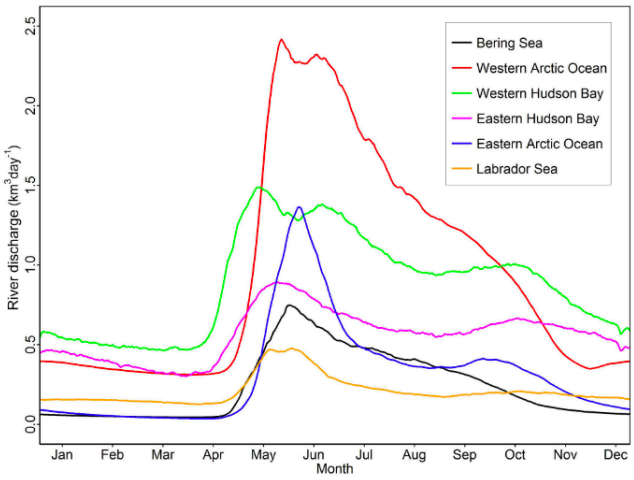

Figure 2.1 Climatological hydrographs of daily mean river discharge for six major drainage basins of northern Canada, 1964-2013. From Déry et al., 2016. © 2019 Copernicus Publications

2.1.1 Freshwater source identification (Tracers)

In order to quantify different freshwater source contributions to a system (i.e. sea-ice melt versus meteoric waters) sets of conservative or semi-conservative tracers must be used in addition to salinity. Tracers commonly used include alkalinity (Jones and Anderson, 1994), nutrient concentrations (Yamamoto-Kawai et al., 2008), and most commonly, stable oxygen isotope ratios ($\delta^{18}O$). Salinity paired with oxygen isotope ratios have been used widely in the Arctic in the past forty years (Östlund and Hut, 1984; Granskog et al., 2011, Eastwood et al., 2020), and are used in this study to quantify the water types in our study area. In the natural environment, ^{16}O and ^{18}O are the most abundant isotopes (99.8% and 0.2% respectively) and are most often used when calculating oxygen isotope ratios. With a heavier molecular weight, ^{18}O is precipitated out at lower latitudes, in comparison to ^{16}O, and thus precipitation (rain, snow) and river water is characteristically isotopically depleted (depleted of the heavy isotope) in the Arctic. We are able to identify the source of freshwater, through the use of isotope ratio comparisons. $\delta^{18}O$ is a value, with units ‰ ("per mil"), calculated as the deviation of the measured $^{18}O/^{16}O$ ratio from the recognized standard isotopic composition of ocean water, the Vienna Standard Mean Ocean Water, (V-SMOW, $\delta^{18}O = 0‰$), (Östlund and Hut, 1984). The $\delta^{18}O$ of a water sample may be calculated with Equation 1.

$$\delta_{\text{V-SMOW}}{}^{18}(\text{sample}) = \left[\frac{{}^{18}O/{}^{16}O\ (\text{sample})}{{}^{18}O/{}^{16}O\ (\text{V-SMOW})} - 1\right] \times 1000‰ \qquad \text{(Equation 1)}$$

Typical Arctic and subarctic river water has $\delta^{18}O$ values between about -20‰ and -12‰, whereas ocean water has $\delta^{18}O$ values near 0‰. Thus, the more negative the $\delta^{18}O$ value of a coastal water sample (more depleted), the more meteoric water influence that water has had.

The number of tracers needed to quantify source waters is one less than the number of water types in the system. Therefore, to identify three water types (meteoric water, sea ice melt (SIM), and seawater), two tracers are needed. Sea-ice melt water does not differ much in isotopic composition from the seawater from which it has been formed, however it has much lower salinity due to the expulsion of brine during formation (Tan and Strain. 1980). This is why salinity and $\delta^{18}O$ can be used as tracers to distinguish SIM from seawater and meteoric waters. Östlund and Hut (1984) used $\delta^{18}O$ and salinity to differentiate freshwater sources by identifying a set of three linear equations (Equation 2) where F = kg of water, S = Salinity, and X = $\delta^{18}O$; and where subscripts a = Atlantic water, r = continental runoff and precipitation, and i = ice meltwater.

$$F_a + F_r + F_i = 1$$

$$F_a S_a + F_r S_r + F_i S_i = S$$

$$F_a X_a + F_r X_r + F_i X_i = X$$

(Equation 2 – From Östlund and Hut, 1984)

When these equations are used with the appropriate end-member values representative of the data set, the fractionation of three water types in a water sample would be calculated as a unique algebraic solution. Selection of end-members should reflect the average observed salinity and $\delta^{18}O$ values of the water masses being differentiated between. While this may be simple enough with source water samples, different processes that may alter the water mass

need to be taken into account, one being the sea ice cycle. Sea ice melt has low salinity and is generally around 0‰ in its isotopic composition (Tan and Strain, 1996) but the isotopic composition varies depending on the seawater from which it is formed. If sea ice itself has not been sampled, fractionation factors (usually between 1.5-2‰) are often applied to seawater $\delta^{18}O$ values to determine the sea ice melt end-member, as sea ice is less depleted (less negative of a value) than the seawater from which is was formed (Granskog et al., 2011; Eastwood et al., 2020). Time of sample collection may also influence the accuracy of end-members, as $\delta^{18}O$ values that have been measured in large Arctic rivers have reflected seasonality with highest values in summer and lowest (most depleted) values during late winter and spring (Cooper et al., 2008). For example, the Northern Dvina River in the Eurasian Arctic exhibits $\delta^{18}O$ differences in the order of ~3‰ between seasons (Pavlov et al., 2016). Seasonal variability in $\delta^{18}O$ also has been reported for Hudson Bay rivers (Granskog et al., 2011). Marine deep waters are not expected to have seasonally variable end-members. With this being said, caution needs to be used when assigning values as end-members. Tan and Strain (1996) state that using deep water data to estimate the mixing line underestimates the amount of sea ice melt, as deep water usually contains brine in high latitude bodies of water. This error ultimately increases with the progression of the melting season, with the introduction of more freshwater into the system (Tan and Strain, 1996).

The use of $\delta^{18}O$ and salinity as tracers for identifying freshwater sources has been applied to the Hudson Bay system in a few studies. Tan and Strain (1996) applied this approach in Foxe Basin, Hudson Strait, and northern Hudson Bay, north of 60°N (See Figure 2.2 for sampling locations). Tan and Strain (1996) observe varying $\delta^{18}O$–salinity relationships related to the timing in sampling where there are different stages of melting,

however they establish that $\delta^{18}O$ values for what they describe as northern Hudson Bay range from -3.4 to -4.1‰, accompany salinity values of about 31-33, indicating a relatively low influence from riverine sources (Figure 2.2). However, of all their sampling stations in and around northern Hudson Bay, Foxe Basin, and Hudson Strait, the most depleted surface values were located in northeast Hudson Bay, indicating more riverine influence, most likely reflecting Hudson Bay outflow (Figure 2.2). Surface $\delta^{18}O$ values in Foxe Basin were found to range -2.2 to -2.5‰, with salinity of 31-32, which is indicative of sea ice melt freshening the water without strongly altering the $\delta^{18}O$ values (Figure 2.2). This is consistent with Northern Hudson Bay being a very active melting area (Tan and Strain, 1996). Freshwater found in the Foxe Basin water mass is known to be majorly composed of isotopically heavy sea ice melt (Tan and Strain, 1996).

Southern, central, and coastal Hudson Bay is the focus of a study conducted by Granskog et al. (2011), which uses the Östlund and Hut (1984) method (Equation 2). Not only are riverine source water and sea-ice melt quantified, but their distribution patterns are discussed in terms of water mass interactions during both winter and summer. $\delta^{18}O$ values for rivers discharging to the Hudson Bay system vary between -10.5‰ and -19.5‰. Surface waters in the southeast and near-shore areas were found to contain some of the highest fractions of RW (15-25%) (Figure 2.3) (Granskog et al., 2011). They found that positive SIM, or excess sea-ice melt, is only present in the surface layer, and that high negative SIM, or excess brine, is found on the west and southeast shelves extending in some places to bottom waters (Granskog et al. 2011). Their results suggest that large amounts of brine are stored in intermediate waters, specifically in the central basin. The deep waters, > 100 m, contain higher than expected RW fractions which implies that there is mixing of surface

waters to depth through physical processes and the mechanism of brine rejection (Granskog et al. 2011). These authors also studied the fractional composition of the winter surface mixed layer (WSML), where brine would be expected to accumulate. They found that the area of highest brine accumulation in the WSML is in northwest Hudson Bay, followed by south-central Hudson Bay and northern James Bay (Figure 2.3). The distributions of river water in the winter SML suggest strong associations between accumulation of river water and brine.

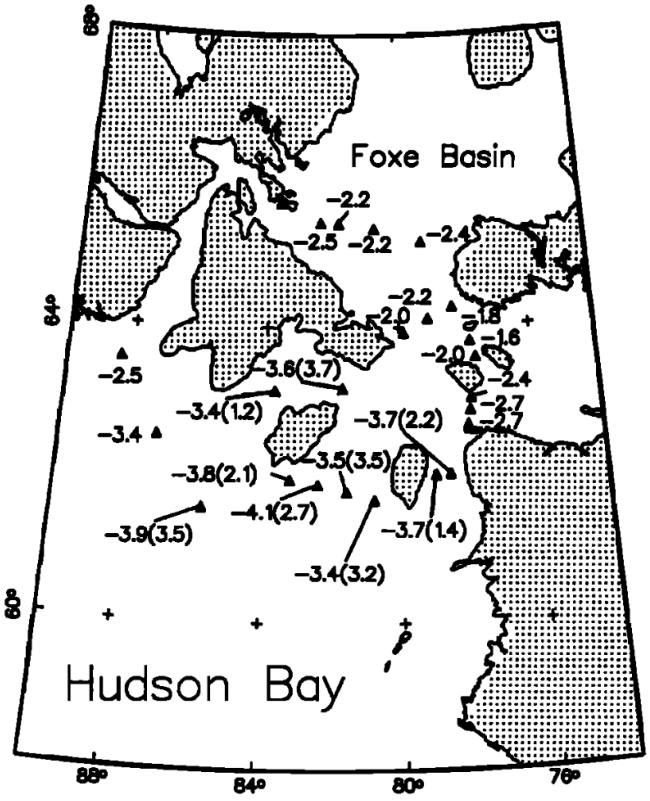

Figure 2.2 Surface water $\delta^{18}O$ values for northern Hudson Bay, western Hudson Strait, and southern Foxe Basin. From Tan and Strain, 1996. © 2019 American Geophysical Union

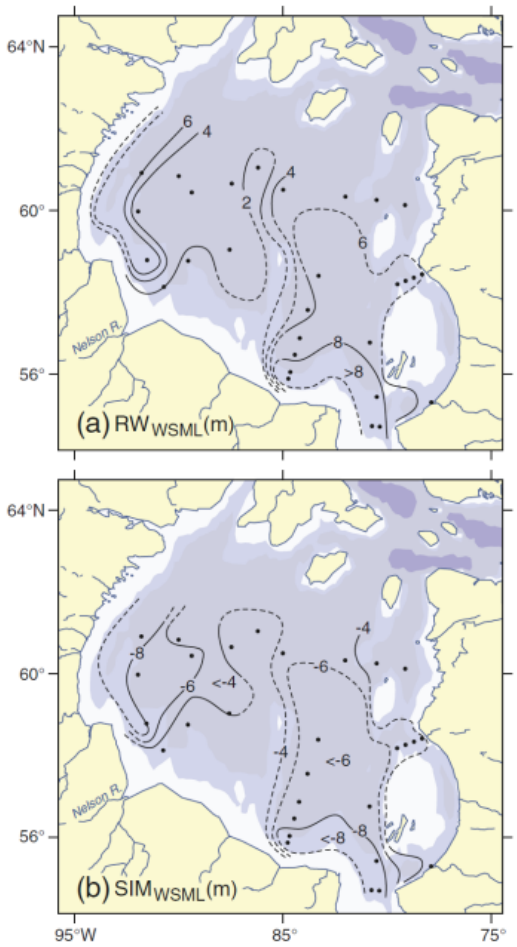

Figure 2.3 Estimate of total (a) RW and (b) SIM inventories (meters) in the WSML at the end of winter from Granskog et al. (2011). Note that more negative numbers in (b) reflect higher proportions of brine or lower proportions of ice melt. © 2019 Elsevier B. V.

2.2 Nutrients in Arctic and Subarctic Aquatic Environments

Nutrients, also known as essential elements, are a critical aspect of aquatic systems as they are one of the main controllers of biological production (Mann and Lazier, 2005; Tremblay and Gagnon, 2009; Tremblay et al., 2015). The most widely studied in Arctic marine environments are macronutrients nitrogen (N), phosphorus (P), and silicic acid (Si) (Redfield, 1958; Moore et al., 2013; Tremblay et al., 2002). The availability of nutrients has been shown to limit abundance and activity of primary producers in the euphotic zone of

water bodies (Moore et al. 2013). The way a nutrient cycles within the natural environment and becomes bioavailable depends on its elemental composition and chemical speciation. The three nutrients that this thesis will focus on are N, P and Si.

The marine nitrogen cycle is the most complex in comparison to phosphorus and silicon because there are many sources and sinks of the element, as well as many different bioavailable chemical species that exist in nature including nitrate (NO_3^-), nitrite (NO_2^-), ammonium (NH_4^+), and ammonia (NH_3). The highest rates of supply to seawater of bioavailable nitrogen are in coastal waters, through river runoff, benthic nitrogen fixation, deposition, or atmospheric diffusion at the air-water interface (Libes, 2009; Tremblay et al., 2015). Riverine nitrate specifically comes from the leaching of soils and terrestrial surface run-off within a watershed, and thus is variable dependent upon the geological and biological composition of the watershed (Le Fouest et al., 2013). Primary producers use nitrogen in the form of ammonium, or oxidized to the forms of nitrite and nitrate (Tremblay et al., 2015). Nitrogen can be transformed in an aquatic system through oxidation reactions such as remineralization, ammonification, nitrification, denitrification, and nitrogen fixation (Libes, 2009). Arctic shelves at least along the Pacific margin are believed to be host to substantial nitrogen loss through benthic denitrification (Granger et al., 2011).

Unlike nitrogen, phosphorus is almost only ever found in natural environments as phosphate (PO_4^{3-}). In coastal areas, the primary source of P is riverine input (Libes, 2009) in the form of particulate inorganic P (PIP), particulate organic P (POP), dissolved organic P (DOP), and dissolved inorganic P (DIP) (Slomp, 2011). This mainly comes from weathering of crustal minerals, which, in high latitude regions, often means phosphorus is the most limiting element in rivers (Le Fouest et al., 2013). Fertilizers used for agricultural purposes

are also large contributors to phosphate input, and have drastically increased in use over the last century due to the growing agricultural sector (Slomp, 2011). Groundwater discharge is also a source of DIP to coastal waters; however, influential contribution is only really ever found in regions where groundwater flow rates are high such as near volcanic islands and karstic aquifers (Slomp, 2011). What makes the P cycle less complicated in aquatic settings is the fact that the only form of phosphorus that is bioavailable is dissolved inorganic phosphate (Libes, 2009). DIP is taken up by organisms in the photic zone of the water column which are then either eaten by larger organisms or become detritus, sink and are buried through sedimentation, and phosphate is then possibly released when the organic matter is remineralized. Inorganic phosphorus species are often measured and presented as soluble reactive phosphorus (SRP). The distribution of P in aquatic system is highly dependent upon physical processes but also biological uptake and cycling.

The major source of Si in marine waters comes mainly from the weathering of sedimentary and crystalline rocks, which leads to silicon being carried in soluble form by river runoff to coastal waters (Turner et al. 2003; Libes, 2009). Si in the form of silicate (or silicic acid, $Si(OH)_4$) is an important compound for diatom populations in marine environments as they take it up to form shell-like structures called frustules (Turner et al., 2003). Because of this requirement for diatoms, silicon is hypothesized to limit diatom populations in some regions (Moore et al. 2013). As diatoms become detritus and sink to the seabed, they may be buried in the sediment and remain there until there is benthic disturbance through physical processes and remineralization of nutrients occurs (Libes, 2009). Dissolved Si returns to the marine environment as silicate with the dissolution

of diatomaceous frustules, while sinking, making up the majority of silicate's cycle in the marine environment (Libes, 2009).

Despite a variation in the elemental make up of plankton species, a C:N:P molar ratio of 106:16:1 has been generally used as the reference for the average elemental composition of plankton as first identified by A. Redfield in 1958. Silica had been found by Brzezinski (1985) to have a weighted average Si:N ratio of diatom species to be 1.05, meaning diatoms consume Si and N at almost a one to one molar rate. These ratios vary by species type, physiological adaptations, as well as species composition.

Specific average nutrient ratios have been used to identify different water masses in the past, particularly on a large ocean-wide scale (i.e. Atlantic vs. Pacific) due to the different nutrient compositions of these water bodies (Jones et al., 1998; Yamamoto-Kawai et al., 2008). Pacific-source waters are known to be generally depleted in nitrate, and have a large pool of phosphate, resulting in low NP ratios (< 15) (Yamamoto-Kawai et al., 2008; Tremblay et al., 2008). Whereas, areas in Baffin Bay, which sees a mixture of Atlantic and Pacific waters, have higher NP ratios, closer to the Redfield ratio (Tremblay et al., 2015). A variety of biogeochemical processes are responsible for these differences. In the eastern Pacific Ocean, processes that contribute to the lowering of the N:P ratio of waters that eventually enter the Arctic include upwelling which supplies remineralized P from P-rich organic matter, denitrification, and anaerobic ammonium oxidation (Tremblay et al., 2014). In the Arctic, denitrification that occurs on shallow shelves further impacts the nitrate stock and reduces the NP ratio (Granger et al., 2011).

Using the 106:16:1 ratio as a baseline for the phytoplankton production requirement, what is observed in the environment in terms of nutrient composition can provide insights

into which nutrient may become a limiting factor with the occurrence of primary production. In marine waters, carbon, as carbonate, is found in great excess (C:N:P of 1000:15:1) and may be transformed very easily within the complex carbon cycle (Redfield 1958). Silicate is also largely abundant in the marine environment, especially in coastal areas. This of course varies by species, but examining the ratios of Si:N and Si:P in water is also a means of assessing the potential nutrient limitation as a result of diatom blooms. In estuarine areas Si:P ratios are expected to be high, and have been measured to be as high as 32:1 in the Mackenzie estuary (Macdonald et al., 1987). The Si:N consumption ratio has been found to vary depending on region (0.5 to 2; Tremblay et al. 2008; Simpson et al. 2008). Nitrate and phosphate are known as biolimiting nutrients, as they have been observed to limit production in aquatic systems, however the classic view on nutrient limitation is that only one nutrient may be considered limiting at one time (the nutrient that is depleted from the water column first) (Tremblay et al., 2015). In marine settings, nitrate is typically that element, and in freshwater bodies phosphate is usually the more limiting nutrient (Redfield 1958, Taylor et al. 2013). N:P has been found to vary quite a lot in marine environments, between 11.0 and 21.0 (Simpson et al., 2008; Tremblay et al., 2015); however, N is primarily the limiting nutrient in the western (North American) Arctic Ocean with ratios generally <16 (Tremblay and Gagnon, 2009). The actual ratio also varies throughout the year as nutrients are consumed, and after the primary limiting nutrient is exhausted (Tremblay et al., 2015). The assessment of potential nutrient limitation becomes more complex in coastal regions, especially near river outlets, due to the mixing of meteoric (riverine) and sea-source waters, which have different elemental composition.

2.2.1 Nutrient conditions in high latitude river systems

Riverine nutrient supplies vary strongly by location mainly due to the differences in a watershed's geology and population density. Lower latitude regions with high population density and widespread agricultural activity almost always have different riverine nutrient composition than higher latitude areas. This is mainly due to the difference in total wastewater generated, as well as contamination of water sources associated with runoff from applied agricultural fertilizers. Higher population density, the greater use of fertilizers, and overall greater agricultural activity taking place tends to be associated with higher nitrate and phosphate loading to freshwater bodies (Turner et al., 2003). These factors do not impact the amount of silicate entering and being transported through rivers systems. Despite the location of high latitude rivers, their watersheds often include tributaries found much further south, in boreal and even prairie regions. This makes it more difficult to extrapolate the conditions of one Arctic river to another.

On a pan-Arctic scale, there are fewer than ten large Arctic rivers that have received much attention in the last few decades. Nitrate values vary widely across these major pan-Arctic rivers, with distinct differences between those located in Eurasia and those in North America. The Lena River specifically, located in Russia, is known to be enriched in nitrate and silica because it's drainage basin not only encompasses tundra but also Siberian forest which is rich in organic matter (Cauwet and Sidorov, 1996). These differences are also reinforced when looking at flow-weighted average dissolved inorganic nitrogen (DIN) concentrations between large Eurasian Arctic rivers (4-14 μM) and large North American Arctic rivers (6-9 μM) (Tank et al., 2012). Because these rivers are located at high latitudes, seasonality plays a role in the nutrient concentration levels as well. Typically in winter,

nitrate concentrations are quite high with maximum concentrations observed under the ice in what would be considered late winter (March/April), which is seen in Hudson Bay rivers (cf., Kazmiruk et al., 2021). Previous measures of major Eurasian and North American Arctic rivers in the late winter period have shown a range of nitrate concentrations between 5.3-21.5 μM (Le Fouest et al., 2013). During the spring freshet period, these concentrations drop, in part due to the dilution effect from the pulse of runoff from melting snow and ice, and also potentially due to any primary production which would use up the nutrients (Le Fouest et al., 2013). Some examples of summer nitrate concentrations in large Arctic rivers include 3.3 μM in the Mackenzie, ~2.1 μM in the Kolyma, and 2.7 μM in the Indigirka rivers (Le Fouest et al., 2013). Rivers found in the subarctic, such as those found around southern Hudson Bay, have shown varying nitrate concentrations in summer/fall that are generally low in comparison to the Arctic Rivers listed above (0.35-1.52 μM) but reaching levels up to 2.0 μM in the Churchill River and 6.3 μM in the Nelson River (Kuzyk et al., 2010).

Large Arctic Rivers are known to have very high silicate concentrations to support diatom production. Similarly to nitrate, silicate demonstrates seasonal patterns in concentrations in high latitude rivers. It is found at the highest concentrations during the winter or late winter months, with a corresponding decrease in concentrations in the spring and summer period (Holmes et al., 2012; Le Fouest et al., 2013). Silicate values from a compiled data set of seven major Arctic rivers indicate concentrations in late winter (April) ranging from 28.7 to 202.6 μM and in summer (August) ranging from 20.3 to 112.2 μM, with the highest values measured in the Yukon River (Le Fouest et al., 2013). In a separate study, the annual flow-rated concentrations of the six largest Arctic rivers ranged 66 to 121 μM (Holmes et al., 2012).

As previously discussed, densely populated areas, and agricultural activity tend to contribute high amounts of phosphorus to nearby water bodies. The phosphorus supply to freshwater systems is limited by erosion (Le Fouest et al., 2013), which means in a natural environment, without those outside factors, phosphate is almost always the limiting nutrient in rivers and freshwater bodies. It has been shown in many studies that rivers at high latitudes, and just general in-land waters, contain very little inorganic phosphorus or SRP (Carmack and Macdonald, 2002; Simpson et al., 2008; Holmes et al., 2012; Le Fouest et al., 2013). It is also hypothesized that the low levels of SRP are reflective of its removal from some rivers through reactions with iron, such as is seen in the Mackenzie River before discharging to the coast (Macdonald and Yu, 2006). Unlike nitrate and silicate, phosphate has not been shown to have a significant difference in riverine concentrations between seasons especially in large North American Arctic rivers. For context, the Yukon and Mackenzie Rivers are both much lower in SRP year-round (0.14 - 0.97 μM and 0.11 - 0.37 μM respectively) than Eurasian rivers such as the Ob, which measures some of the highest (0.60-2.83 μM) (Le Fouest et al., 2013). Based on the data compiled of nine northern rivers by Le Fouest et al. (2013) the majority of SRP values in late winter (April) remain < 1 μM and in summer all except the Ob are found to measure < 0.95 μM. Overall, the freshet does not seem to substantially influence phosphate content of rivers, which may also be reflective of the processes occurring in rivers before discharging into coastal waters.

Another process that alters nutrient ratios in inland waters is development (dams and diversions). Because of increased algal activity and particle trapping (sedimentation) in reservoirs, there are significant changes in the riverine N:P:Si ratios delivered to the coastal ocean (Maavara et al., 2017, 2020). In particular, the biogeochemical processes enhanced in

reservoirs above dams lead to the preferential removal of P over N thus increasing the N:P ratios delivered to the ocean.

2.2.2 Nutrient conditions of high latitude coastal and marine waters

Terrestrial waters that discharge into Arctic and subarctic Coastal areas are transported and transformed as they interact with the source seawater. The combination of water masses with distinct sets of properties that mix in coastal areas adds complexity when examining the nutrient conditions and winter nutrient recharge processes of coastal waters.

Nutrient concentrations can vary greatly both in space (e.g., with salinity and distance from the coast) and time in high latitude marine environments, in part due to the general seasonality of the sea-ice cycle, the natural riverine discharge cycle, as well as the overall seasonal nature of primary production. Deep waters typically have much higher concentrations of nutrients than surface waters because this is where remineralization occurs, and it is generally too dark for primary production to occur and consume nutrients. For example Hudson Bay deepwater is often referred to as being a large nutrient reservoir where average nitrate (> 12 mmol m^{-3}), phosphate (1.7 mmol m^{-3}) and silicate concentrations (30 mmol m^{-3}) (Matthes et al., 2021) are all much higher than those observed at the surface mixed layer (~0.35 mmol m^{-3}, ~0.60 mmol m^{-3}, and ~2.5 mmol m^{-3}, respectively) (Ferland et al., 2011). At the surface, especially in summer (as was the case in the above data) primary producers consume nutrients contributing to the low concentrations often recorded in literature for surface waters. There is also a difference between offshore/inshore areas, mainly due to the RCD and the influence of rivers on shallow inshore shelves, whereas offshore areas do not typically see much river water influence (Carmack et al., 2015). This inshore-offshore pattern can be seen in nutrient concentrations, for example silicate is

generally in excess closer inshore in Arctic coastal areas due to the higher riverine influence (Tank et al., 2012). Because silicate is mainly associated with the terrestrial environment and erosion, silicate found in surface waters is typically negatively correlated with salinity in coastal environments (Kattner et al., 1999; Macdonald and Yu, 2006). Some studies in southeastern and southwestern Hudson Bay have noted highest silicate concentrations closest to the coast, in the freshest samples, and decreasing as you move farther from shore (Kuzyk et al., 2008; Lapoussière et al., 2013).

Both physical and biological processes impact the distribution of nutrients in the marine setting. Biologically, nutrient conditions in coastal waters can be impacted by the uptake of inorganic nutrients by producers, and the renewal of nutrients through decomposition of detritus. The distribution of nutrients can also be impacted by the physical processes brought on by both the riverine discharge cycle and the sea-ice cycle. Since the RCD is a contiguous region of freshwater flow and transformation (Carmack et al., 2015) the conditions of riverine discharge from upstream are likely to impact a coastal region further downstream or even offshore areas. This is further complicated by the sea ice cycle in these high latitude areas.

Riverine input can provide high nutrient content in terms of nitrate and silicate to coastal surface waters via horizontal advection (Popova et al., 2012) but not so much for phosphate since riverine concentrations are low, but can also enhance density-driven stratification, the strength of which is determined by discharge rates, preventing the vertical exchange of nutrients and other components between water masses (Tremblay et al., 2008; Ferland et al., 2011). The sea ice cycle works in two main ways to impact nutrient distribution in coastal areas where landfast ice is present during winter. During the melting

period, freshwater enhances stratification, in a similar fashion as river input, but may also act as a diluent. By the beginning of the melt period, any nutrients that would have been incorporated in the sea-ice would be used up, meaning sea-ice would contain little to no nutrients (Granskog et al., 2005) and therefore the fresh meltwater would facilitate dilution. This is difficult to measure, however, due to the mobility and export of sea ice (Landy et al., 2017). During the open-water season, however, there is no barrier preventing wind and storms from mixing the water column. Once the sea-ice breaks up and instigates phytoplankton blooms, nutrients are consumed in the photic zone and depleted nutrient conditions are often reported (Carmack and Macdonald, 2002; Tremblay et al., 2008; Popova et al., 2012). Ice formation, from seawater, which produces brine, works in the opposite way, providing a means and mechanism for surface waters and nutrients to mix down to deep waters with the high-density brine (Granskog et al., 2011). Landfast ice, which provides a barrier to wind and storms, also means river plumes and associated nutrients, are spread further and wider along the RCD than during summer.

In offshore areas, the winter conditions of low light and consequently low production rates under ice, is a critical time for nutrients to resupply and set up the system for the spring bloom once the ice melts (Ferland et al., 2011; Popova et al., 2012; Heikkilä et al. 2013). The nutrients that are found in late winter waters, just before the ice break-up, then informs of the possible maximum production in a certain area, unless there is an additional source of nutrients such as through riverine discharge.

2.3 Study Area

The study area being examined here encompasses three general coastal regions of the Hudson Bay System. These will be termed the northwest Hudson Bay region, the southeast Hudson Bay region, and the northeastern James Bay region. Hudson Bay and James Bay are connected but because James Bay extends further south into Canada key differences arise when examining the biogeochemical conditions of its coastal regions.

2.3.1 Hudson Bay System

Hudson Bay is a large, shelf-like, inland sea located in Canada, with a surface area of $1.2x10^6$ km^2 (including James Bay) bordering three provinces and one territory. It also has a watershed that spans 3.7×10^6 km^2, three times the surface area itself and approximately one third the area of Canada's total land mass (Figure 2.4) (Déry et al., 2011), encompassing a landscape with vastly different climates. With an average depth of 125 m with some deeper areas in the north of the Bay, it is overall very shallow relative to other ocean bodies (Jones and Anderson, 1994), but is very similar in structure to coastal shelves. Hudson Bay is located at the southern limit of the Arctic, primarily in what would be considered a subarctic region, but the overall region experiences a similar climate and sea-ice cycle as the shelves of the Arctic Ocean (Hochheim and Barber, 2010; Andrews et al., 2018). The seawater found in Hudson Bay mainly comes from the Arctic Ocean where seawater flows through the Canadian Archipelago and enters the Bay through the northwest (Prinsenberg, 1982; Ridenour et al., 2019). Waters then generally circulate in a cyclonic direction through the system until it flows out in the northeast through Hudson Strait. It is also important to note that in recent years there have been model simulations that depict a weak reversal of the general circulation direction in spring and summer in eastern Hudson Bay, specifically near

the mouth of James Bay (Ridenour et al., 2019). The condition of waters exiting James Bay could then impact the southwestern coastal waters of Hudson Bay, along with the already established influence in the southeast.

This system experiences seasonal variation in ice-cover and is ice-free for a portion of the year, with ice break up beginning in late May and freeze up starting in late October, however this varies by region (Prinsenberg, 1984; Hochheim et al., 2011; Andrews et al., 2018). As sea ice is present across the Bay, sea ice melt contributes to the freshwater budget at a Bay-wide scale, producing on average 742 ± 10 km^3 of freshwater annually (Landy et al., 2017). The other large freshwater source to the Hudson Bay system comes from the rivers surrounding it, supplying 630-870 km^3 of freshwater annually, creating strong estuarine-like coastal regions (Saucier et al., 2004) and reinforcing the coastal current structure which transports river discharge around the Bay. This also contributes indirectly to enhanced new production in inshore areas through entrainment and consequent upwelling of deep nutrient-rich waters (Kuzyk et al., 2010). Precipitation in the form of rain and snow also occur, however are negligible in comparison to riverine discharge and sea ice melt, which are resultantly considered the two main sources of freshwater to the system (Granskog et al., 2011; Landy et al., 2017).

Coastal regions of Hudson Bay have not been extensively studied, especially in winter months, mainly because of the difficulty accessing shallow regions, and ice-covered areas with large ships. Using large ships to gather measurements for scientific analysis has long been used in Arctic marine areas, Hudson Bay included, however it does not allow for year-round monitoring. Many Indigenous communities lie along the Hudson Bay coastline and are currently experiencing changes in their coastal environments due to climate change,

and in some cases anthropogenic alterations to the natural environment. The three coastal regions of this study have been rarely studied in the past.

Figure 2.4 Map of the Hudson Bay Basin showing the location of rivers with outlets into Hudson Bay or James Bay. The inset shows the overall contributing drainage basin for Hudson Bay shaded in grey. From Déry et al. 2011. © 2019 Elsevier B. V.

2.3.2 James Bay System

Located off of the southern edge of Hudson Bay, James Bay is generally shallower and much smaller in area (6.8×10^{-4} km^2) than Hudson Bay however it plays an important role for freshwater introduction in the overall system. The area that encompasses James Bay extends

south (latitude of 51.2°N at its most southern point) into the boreal dominated zone of Canada. The area still experiences a relatively cold climate with average temperatures ranging from -23.2°C in winter to +14.2°C in summer (data compiled between 1981-2010 from Environment and Climate Change Canada). This pattern of air temperature results in a seasonal sea-ice cycle similar to Arctic regions and that of Hudson Bay, but where ice formation typically begins in November and breaks up beginning in June.

A very large percentage of freshwater introduced to Hudson Bay via river runoff comes from this southern region of James Bay. It has been documented as early as 1976 that the surface salinity of water entering James Bay at the west coast dilutes as much as three units by the time it circulates and exits the eastern coast back into Hudson Bay (Prinsenberg, 1984). In James Bay, La Grande River alone, which is located on the eastern coast, discharges on average 80.5 km^3 of freshwater per year (Déry et al., 2011), and contributes approximately 16% of the total annual gauged streamflow input to Hudson Bay (Hernandez-Henriquez et al., 2010). The region covered in this study encompasses a portion of the northeastern coast of James Bay, with particular focus on the region affected by the La Grande River plume. Many of the larger rivers located along this stretch of the coast have been altered for hydroelectric development, either developed or diverted since the 1970s. These developmental activities altered the natural outflow of the rivers, in some cases leading to year-round changes in volume and timing of discharge. La Grande River currently has its largest outflow during the winter season as opposed to the expected natural peak during the spring freshet, effectively flattening the hydrograph for this river (Déry et al., 2011). La Grande's winter river discharge has been suggested to effectively lower the winter surface

salinities of some parts of southeastern and eastern Hudson Bay by as much as 3 (Whittaker, 2006 in Déry et al., 2011).

There have been some scientific studies of James Bay in the past, with a large undertaking to gather data beginning in the 1970s in an effort to quantify the pre-development conditions of coastal James Bay (Prinsenberg, 1984). Since then, there have been very limited studies conducted of the coastal regions, and very little data collected between then and present day.

References

Aagaard, K., L. K. Coachman, and E. C. Carmack (1981), On the halocline of the Arctic Ocean, Deep Sea Research I, 28A(6), 529-545.

Andrews, J., Babb, D., & Barber, D. G. (2018). Climate change and sea ice: Shipping in Hudson Bay, Hudson Strait, and Foxe Basin (1980–2016). Elem Sci Anth, 6(1), 19. https://doi.org/10.1525/elementa.281

Bauch, D., M. Rutgers van der Loeff, N. Andersen, S. Torres-Valdes, K. Bakker, and E. P. Abrahamsen (2011), Origin of freshwater and polynya water in the Arctic Ocean halocline in summer 2007, Prog. Oceanogr., 91(4), 482-495, doi:10.1016/j.pocean.2011.07.017.

Bianchi, T.S., Allison, M.A., & Cai, W.-J. (2014). An introduction to the biogeochemistry of river coastal systems. In T.S. Bianchi, M.A. Allison, & W.-J. Cai (Eds.), Biogeochemical Dynamics at Major River-Coastal Interfaces: Linkages with Global Change (3-18). Cambridge: Cambridge University Press.

Brzezinski, M. A. (1985). The Si:C:N ratio of marine diatoms: Interspecific variability and the effect of some environmental variables. Journal of Phycology, 21, 347–357.

Carmack, E. C., & Macdonald, R. W. (2002). Oceanography of the Canadian shelf of the Beaufort Sea: A setting for marine life. Arctic, 55(SUPPL. 1), 29–45. https://doi.org/10.14430/arctic733

Carmack, E., Winsor, P., & Williams, W. (2015). The contiguous panarctic Riverine Coastal Domain: A unifying concept. Progress in Oceanography, 139, 13–23. https://doi.org/10.1016/j.pocean.2015.07.014

Cauwet, G., & Sidorov, I. (1996). The biogeochemistry of Lena River: Organic carbon and nutrients distribution. Marine Chemistry, 53(3–4), 211–227. https://doi.org/10.1016/0304-4203(95)00090-9

Cooper, L. W., McClelland, J. W., Holmes, R. M., Raymond, P. A., Gibson, J. J., Guay, C. K., & Peterson, B. J. (2008). Flow-weighted values of runoff tracers (δ18O, DOC, Ba, alkalinity) from the six largest Arctic rivers. Geophysical Research Letters, 35(18), 3–7. https://doi.org/10.1029/2008GL035007

Déry, S. J., Mlynowski, T. J., Hernández-Henríquez, M. A., & Straneo, F. (2011). Interannual variability and interdecadal trends in hudson bay streamflow. Journal of Marine Systems, 88(3), 341–351. https://doi.org/10.1016/j.jmarsys.2010.12.002

Déry, S. J., Stadnyk, T. A., MacDonald, M. K., & Gauli-Sharma, B. (2016). Recent trends and variability in river discharge across northern Canada. Hydrology and Earth System Sciences, 20(12), 4801–4818. https://doi.org/10.5194/hess-20-4801-2016

Eastwood, R. A., Macdonald, R. W., Ehn, J. K., Heath, J., Arragutainaq, L., Myers, P. G., … Kuzyk, Z. A. (2020). Role of River Runoff and Sea Ice Brine Rejection in Controlling Stratification Throughout Winter in Southeast Hudson Bay. Estuaries and Coasts, 43(4), 756–786. https://doi.org/10.1007/s12237-020-00698-0

Ferland, J., Gosselin, M., & Starr, M. (2011). Environmental control of summer primary production in the hudson bay system: The role of stratification. Journal of Marine Systems, 88(3), 385–400. https://doi.org/10.1016/j.jmarsys.2011.03.015

Granger, J., Prokopenko, M. G., Sigman, D. M., Mordy, C. W., Morse, Z. M., Morales, L. V., … Plessen, B. (2011). Coupled nitrification-denitrification in sediment of the eastern Bering Sea shelf leads to 15N enrichment of fixed N in shelf waters. Journal of Geophysical Research: Oceans, 116(11), 1–18. https://doi.org/10.1029/2010JC006751

Granskog, M. A., Kaartokallio, H., Thomas, D. N., & Kuosa, H. (2005). Influence of freshwater inflow on the inorganic nutrient and dissolved organic matter within coastal sea ice and underlying waters in the Gulf of Finland (Baltic Sea). Estuarine, Coastal and Shelf Science, 65(1–2), 109–122. https://doi.org/10.1016/j.ecss.2005.05.011

Granskog, M. A., Kuzyk, Z. Z. A., Azetsu-Scott, K., & Macdonald, R. W. (2011). Distributions of runoff, sea-ice melt and brine using δ18o and salinity data - a new view on freshwater cycling in hudson bay. Journal of Marine Systems, 88(3), 362–374. https://doi.org/10.1016/j.jmarsys.2011.03.011

Heikkilä, M., Pospelova, V., Hochheim, K. P., Kuzyk, Z. Z. A., Stern, G. A., Barber, D. G., & Macdonald, R. W. (2014). Surface sediment dinoflagellate cysts from the Hudson Bay system and their relation to freshwater and nutrient cycling. Marine Micropaleontology, 106, 79–109. https://doi.org/10.1016/j.marmicro.2013.12.002

Hernández-Henríquez, M. A., Mlynowski, T. J., & Déry, S. J. (2010). Reconstructing the Natural Streamflow of a Regulated River: A Case Study of La Grande Rivière, Québec, Canada. Canadian Water Resources Journal, 35(3), 301–316. https://doi.org/10.4296/cwrj3503301

Hochheim, K. P., & Barber, D. G. (2010). Atmospheric forcing of sea ice in Hudson Bay during the fall period, 1980-2005. Journal of Geophysical Research: Oceans, 115(5), 1–20. https://doi.org/10.1029/2009JC005334

Hochheim, K.P., J.V. Lukovich, and D.G. Barber. 2011. Atmospheric forcing of sea ice in Hudson Bay during the spring period, 1980-2005. Journal of Marine Systems, 88:476-487.

Holmes, R. M., McClelland, J. W., Peterson, B. J., Tank, S. E., Bulygina, E., Eglinton, T. I., … Zimov, S. A. (2012). Seasonal and Annual Fluxes of Nutrients and Organic Matter from Large Rivers to the Arctic Ocean and Surrounding Seas. Estuaries and Coasts, 35(2), 369–382. https://doi.org/10.1007/s12237-011-9386-6

Jones, E. P., & Anderson, L. G. (1994). Northern hudson bay and foxe basin: Water masses, circulation and productivity. Atmosphere - Ocean, 32(2), 361–374. https://doi.org/10.1080/07055900.1994.9649502

Jones, E. P., Anderson, L. G., & Swift, J. H. (1998). Distribution of Atlantic and Pacific waters in the upper Arctic Ocean: Implications for circulation. Geophysical Research Letters, 25(6), 765–768.

Kattner, G., Lobbes, J. M., Fitznar, H. P., Engbrodt, R., Nöthig, E. M., & Lara, R. J. (1999). Tracing dissolved organic substances and nutrients from the Lena River through Laptev Sea (Arctic). Marine Chemistry, 65(1–2), 25–39. https://doi.org/10.1016/S0304-4203(99)00008-0

Kazmiruk, Z. V., D. W. Capelle, C. M. Kamula, S. Rysgaard, T. Papakyriakou, and Z. A. Kuzyk (2021), High biodegradability of riverine dissolved organic carbon in late winter in Hudson Bay, Canada, Elementa: Science of the Anthropocene, 9(1), doi:10.1525/elementa.2020.00123.

Kuzyk, Z. A., Macdonald, R. W., Granskog, M. A., Scharien, R. K., Galley, R. J., Michel, C., … Stern, G. (2008). Sea ice, hydrological, and biological processes in the Churchill River estuary region, Hudson Bay. Estuarine, Coastal and Shelf Science, 77(3), 369–384. https://doi.org/10.1016/j.ecss.2007.09.030

Kuzyk, Z. Z. A., Macdonald, R. W., Tremblay, J. É., & Stern, G. A. (2010). Elemental and stable isotopic constraints on river influence and patterns of nitrogen cycling and biological productivity in Hudson Bay. Continental Shelf Research, 30(2), 163–176. https://doi.org/10.1016/j.csr.2009.10.014

Landy, J. C., Ehn, J. K., Babb, D. G., Thériault, N., & Barber, D. G. (2017). Sea ice thickness in the Eastern Canadian Arctic: Hudson Bay Complex & Baffin Bay. Remote Sensing of Environment, 200(August), 281–294. https://doi.org/10.1016/j.rse.2017.08.019

Lapoussière, A., Michel, C., Gosselin, M., Poulin, M., Martin, J., & Tremblay, J. É. (2013). Primary production and sinking export during fall in the Hudson Bay system, Canada. Continental Shelf Research, 52, 62–72. https://doi.org/10.1016/j.csr.2012.10.013

Le Fouest, V., Babin, M., & Tremblay, J. E. (2013). The fate of riverine nutrients on Arctic shelves. Biogeosciences, 10(6), 3661–3677. https://doi.org/10.5194/bg-10-3661-2013

Libes SM. (2009). An Introduction to Marine Biogeochemistry. John Wiley and Sons Ltd., New York, NY, United States.

Maavara, T., Lauerwald, R., Regnier, P., & Van Cappellen, P. (2017). Global perturbation of organic carbon cycling by river damming. Nature Communications, 8, 15347. https://doi.org/10.1038/ncomms15347

Maavara, T., Akbarzadeh, Z., & Van Cappellen, P. (2020). Global dam-driven changes to riverine N:P:Si ratios delivered to the coastal ocean. Geophysical Research Letters, 47, e2020GL088288. https://doi.org/ 10.1029/2020GL088288

Macdonald, R. W., & Yu, Y. (2006). The Mackenzie Estuary of the Arctic ocean. Handbook of Environmental Chemistry, Volume 5: Water Pollution, 5(PART H), 91–120. https://doi.org/10.1007/698-5-027

Mann, K. H., & Lazier, J. R. N. (2005). *Dynamics of Marine Ecosystems*. (K. H. Mann & J. R. N. Lazier, Eds.), *Dynamics of Marine Ecosystems* (3rd ed.). Dartmouth: Blackwell Publishing. https://doi.org/10.1002/9781118687901

Matthes, L. C., et al. (2021), Environmental drivers of spring primary production in Hudson Bay, Elementa: Science of the Anthropocene, 9(1), doi:10.1525/elementa.2020.00160.

McClelland, J. W., Holmes, R. M., Dunton, K. H., & Macdonald, R. W. (2012). The Arctic Ocean Estuary. Estuaries and Coasts, 35(2), 353–368. https://doi.org/10.1007/s12237-010-9357-3

Moore, C. M., Mills, M. M., Arrigo, K. R., Berman-Frank, I., Bopp, L., Boyd, P. W., … Ulloa, O. (2013). Processes and patterns of oceanic nutrient limitation. Nature Geoscience, 6, 701–710. https://doi.org/10.1038/NGEO1765

Östlund, H. G., & Hut, G. (1984). Arctic ocean water mass balance from isotope data. Journal of Geophysical Research, 89(4), 6373–6381.

Pavlov, A. K., Stedmon, C. A., Semushin, A. V., Martma, T., Ivanov, B. V., Kowalczuk, P., & Granskog, M. A. (2016). Linkages between the circulation and distribution of dissolved organic matter in the White Sea, Arctic Ocean. Continental Shelf Research, 119, 1–13. https://doi.org/10.1016/j.csr.2016.03.004

Popova, E. E., Yool, A., Coward, A. C., Dupont, F., Deal, C., Elliott, S., … Zhang, J. (2012). What controls primary production in the Arctic Ocean? Results from an intercomparison of five general circulation models with biogeochemistry. Journal of Geophysical Research: Oceans, 117(1), 1–16. https://doi.org/10.1029/2011JC007112

Prinsenberg, S. J. (1982). The variability of physical oceanographic parameters in Hudson Bay. *Le Naturaliste Candien*, *109*, 685–700.

Prinsenberg, S. J. (1984). Freshwater contents and heat budgets of James Bay and Hudson Bay. Continental Shelf Research, 3(2), 191–200. https://doi.org/10.1016/0278-4343(84)90007-4

Redfield, A. C. (1958). The biological control of chemical factors in the environment. American Scientist, 46(3), 205–221. Retrieved from https://www-jstor-org.uml.idm.oclc.org/stable/pdf/27827150.pdf?refreqid=excelsior%3Af11611d1b19a1553954ceaab2c8b383c

Ridenour, N. A., Hu, X., Sydor, K., Myers, P. G., & Barber, D. G. (2019). Revisiting the Circulation of Hudson Bay: Evidence for a Seasonal Pattern. Geophysical Research Letters, 46(7), 3891–3899. https://doi.org/10.1029/2019GL082344

Saucier, F.J., Senneville, S., Prinsenberg, S., Roy, F., Smith, G., Gachon, P., Caya, D., Laprise, R. (2004). Modelling the sea ice–ocean seasonal cycle in Hudson Bay, Foxe Basin and Hudson Strait, Canada. Climate Dynamics 23, 303–326.

Simpson, K. G., Tremblay, J. E., Gratton, Y., & Price, N. M. (2008). An annual study of inorganic and organic nitrogen and phosphorus and silicic acid in the southeastern Beaufort Sea. Journal of Geophysical Research, 113. https://doi.org/10.1029/2007JC004462

Slomp, C. P. (2011). Phosphorus Cycling in the Estuarine and Coastal Zones: Sources, Sinks, and Transformations. In E. Wolanski & D. S. McLusky (Eds.), Treatise on Estuarine and Coastal Science (pp. 201–229). Elsevier. https://doi.org/10.1016/B978-0-12-374711-2.00506-4

Tan, F. C., & Strain, P. M. (1980). The distribution of sea ice meltwater in the eastern Canadian Arctic. Journal of Geophysical Research, 85(C4), 1925–1932. https://doi.org/10.1029/jc085ic04p01925

Tan, F. C., & Strain, P. M. (1996). Sea ice and oxygen isotopes in Foxe Basin, Hudson Bay, and Hudson Strait, Canada. Journal of Geophysical Research C: Oceans, 101(C9), 20869–20876. https://doi.org/10.1029/96JC01557

Tank, S. E., Manizza, M., Holmes, R. M., McClelland, J. W., & Peterson, B. J. (2012). The Processing and Impact of Dissolved Riverine Nitrogen in the Arctic Ocean. Estuaries and Coasts, 35(2), 401–415. https://doi.org/10.1007/s12237-011-9417-3

Taylor, R. L., Semeniuk, D. M., Payne, C. D., Zhou, J., Tremblay, J. É., Cullen, J. T., & Maldonado, M. T. (2013). Colimitation by light, nitrate, and iron in the Beaufort Sea in late summer. Journal of Geophysical Research: Oceans, 118(7), 3260–3277. https://doi.org/10.1002/jgrc.20244

Tremblay, J.-É., & Gagnon, J. (2009). The effects of irradiance and nutrient supply on the productivity of Arctic waters: a perspective on climate change. In J. C. J. Nihoul & A. G. Kostianoy (Eds.), Influence of Climate Change on the Changing Arctic and Sub-Arctic Conditions (pp. 73–93). Elsevier. Retrieved from https://link-springer-com.uml.idm.oclc.org/content/pdf/10.1007%2F978-1-4020-9460-6_7.pdf

Tremblay, J. É., Gratton, Y., Fauchot, J., & Price, N. M. (2002). Climatic and oceanic forcing of new, net, and diatom production in the North Water. Deep-Sea Research Part II: Topical Studies in Oceanography, 49(22–23), 4927–4946. https://doi.org/10.1016/S0967-0645(02)00171-6

Tremblay, J. É., Simpson, K., Martin, J., Miller, L., Gratton, Y., Barber, D., & Price, N. M. (2008). Vertical stability and the annual dynamics of nutrients and chlorophyll fluorescence in the coastal, southeast Beaufort Sea. Journal of Geophysical Research: Oceans, 113(7), 1–14. https://doi.org/10.1029/2007JC004547

Tremblay, J. E., Raimbault, P., Garcia, N., Lansard, B., Babin, M., & Gagnon, J. (2014). Impact of river discharge, upwelling and vertical mixing on the nutrient loading and productivity of the Canadian Beaufort Shelf. Biogeosciences, 11(17), 4853–4868. https://doi.org/10.5194/bg-11-4853-2014

Tremblay, J. É., Anderson, L. G., Matrai, P., Coupel, P., Bélanger, S., Michel, C., & Reigstad, M. (2015). Global and regional drivers of nutrient supply, primary production and CO2 drawdown in the changing Arctic Ocean. Progress in Oceanography, 139, 171–196. https://doi.org/10.1016/j.pocean.2015.08.009

Turner, R. E., Rabalais, N. N., Justic, D., & Dortch, Q. (2003). Global patterns of dissolved N, P and Si in large rivers. Biogeochemistry, 64(3), 297–317. https://doi.org/10.1023/A:1024960007569

Yamamoto-Kawai, M., McLaughlin, F. A., Carmack, E. C., Nishino, S., & Shimada, K. (2008). Freshwater budget of the Canada Basin, Arctic Ocean, from salinity, δ18O, and nutrients. Journal of Geophysical Research: Oceans, 113(1), 1–12. https://doi.org/10.1029/2006JC003858

3.0 Influence of seasonal freshwater dynamics on nutrient distributions in the region of freshwater influence of the La Grande River, northeastern James Bay

Abstract

Winter in subarctic marine environments generally serves as a time when nutrient stocks are replenished through physical and biogeochemical processes. These nutrient stocks set a limit on the maximum new production possible during the ice-free period in the absence of other nutrient sources. The addition of river water, which contains different nutrient concentrations and ratios than marine water, adds complexity to the nutrient dynamics of coastal areas. Nutrient data from subarctic coastal areas are scarce, particularly data that span both winter and summer and include tracers for river water influence. In northeastern James Bay, the lack of data has hampered the understanding of changes over the last several decades being felt along this coast by local communities and land users due to both climate change and hydroelectric development of the La Grande River watershed. In this study we examine the seasonal relationships between oxygen isotope tracer data and salinity from early winter, late winter, and summer 2016-2017, to identify freshwater sources (sea-ice vs. river discharge) of the northeast James Bay coast. Additionally, we use nutrient concentrations and ratios (nitrate, phosphate, and silicate) to assess the influence each water type has on nutrient distribution in this region. Stocks of nitrate and phosphate in surface waters (5 m) are calculated for winter and summer periods to better understand the spatial extent of La Grande River's plume influence between the two seasons. In this region, the dominant source of freshwater was La Grande River. During both seasons, La Grande inflow had higher concentrations of nitrate (2.6 - 4.5 μM) than surrounding coastal waters (2.2 -

3.2 μM). The diluted Hudson Bay source waters (salinity of 20 - 25) had N:P ratios (~5) well below the classic Redfield ratios for phytoplankton (16), implying possible N limitation along the coast. In low salinity waters (< 10), especially within the river plume, NP ratios are very high because of low phosphate concentrations. As a result, nitrate stocks in the surface layer of this coastal region nearly double from summer to winter, whereas phosphate stocks increase from winter to summer. The shift in discharge and thus fluvial nitrate inputs from spring to winter with river regulation has produced a mismatch between high surface nitrate stocks available to support primary production, which now occur in winter, and the growing season, which can begin only after the return of light.

3.1 Introduction

Hudson Bay is a large inland sea in northern Canada characterized by oligotrophic conditions (low annual primary production ≤ 67 g C m^{-2} yr^{-1}; Matthes et al. 2021), attributed in part to massive freshwater inputs from river water and seasonal sea-ice melt, which stratify the offshore waters and suppress the supply of nutrients to the euphotic zone (Anderson and Roff, 1980; Roff and Legendre, 1986; Kuzyk et al., 2010; Ferland et al., 2011). Nutrients are resupplied to surface waters through vertical mixing during fall and winter and remain relatively unused until spring because of light limitation. This resupply sets a limit on maximum production, based on how much nitrogen is resupplied, as it is the would-be limiting nutrient during the open water period at least in offshore areas (Ferland et al., 2011). In inshore areas, entrainment forced by riverine inflow, which works to distribute nutrients, must also be considered.

Nutrient distribution patterns and the impacts of freshwater on production are expected to be much more complex in shallow coastal regions of Hudson Bay (also known as

the riverine coastal domain, or RCD). This is because the coastal regions directly receive large additions of river runoff, which in some cases significantly augment the concentrations of nutrients in ambient waters. There are more than 40 rivers that contribute significantly to the total discharge received by Hudson Bay each year (Déry et al., 2011; 2016). However, aside from one study of the Churchill River (Kuzyk et al. 2008), and several studies of the Great Whale River in southeastern Hudson Bay (Ingram et al., 1996 and references therein), the influence of meteoric freshwater on nutrient dynamics and production in coastal areas of Hudson Bay remains poorly known. In addition to this, these coastal regions have a complex ice cover, which not only modifies the disposition of river discharge along the coast in winter, but also provides additional freshwater to the surface layer in summer as sea ice melt (SIM).

The La Grande River discharges directly into James Bay, which is a shallow estuarine area of about 68,300 km^2 extending off the southern end of Hudson Bay (Figure 3.1). Subsequent to its development for hydropower (1970s – 2012) the La Grande River system has become the largest river discharging into the Hudson Bay system providing a yield of 4 m of river inflow annually (Prinsenberg, 1984). This development work has led to alteration of the natural seasonality of the La Grande river discharge. During recent years, flow regulation associated with the La Grande system has shifted peak river discharge into winter while suppressing the natural spring freshet and summertime flow (Déry et al., 2016). There have been studies of the hydrography of the river plume that forms along the coast showing that it is now more than ten-times the size of the natural (prior to development) winter plume found in this area (Ingram and Larouche, 1987; Peck et al., submitted). However, aside from a few measurements near the La Grande River mouth (Messier et al.,

1986; Grainger & McSween, 1976), there has been no previous study of how the altered freshwater distribution in time and space impacts nutrient distributions. Prior to diversion it was suggested that the La Grande provided minimal nitrate contribution to the estuary with maximum concentrations found at depth (Grainger and McSween, 1976). Following early stages of development, Messier et al. (1986; p.422) concluded that the diversion had limited impact on productivity because the La Grande "does not provide nutrients that are at limiting levels in James Bay". In contrast, recent studies in other systems have emphasized that altered nutrient fluxes *and* nutrient ratios along the land-ocean aquatic continuum of dammed rivers may impact the ecosystem functioning of receiving water bodies (cf., Maavara et al. 2020). James Bay experiences a similar climate to Hudson Bay overall, and is generally ice covered between December and June, with the length of the ice-covered season projected to continually decrease into the future (Hochheim and Barber, 2014; Galbraith and Larouche, 2011; Taha et al., 2019). The sea ice adds complexity to the meteoric water influence on nutrient distributions, as it adds additional freshwater to the system in the form of sea-ice melt, which has not been well quantified in this region, has different elemental composition than riverine discharge, and also contributes brine during ice growth that induces physical mixing processes (Granskog et al., 2011).

The main objective of this study is to assess how the La Grande River, under contemporary flow regimes, affects nutrient distributions in the coastal domain of northeastern James Bay, considering sea ice dynamics. The data set spans the early winter, late winter, and summer seasons of 2016 and 2017. First, we quantify freshwater source contributions during each season using salinity and oxygen isotope ratio ($\delta^{18}O$) tracer data. Second, we examine nutrient-salinity and nutrient-nutrient relationships to explore the fate of

the nutrients in the coastal waters (conservative mixing vs. biological drawdown). Third, we quantify the direct contribution of river water to nutrient stocks in both winter and summer. This is done to gain insight into how the reversed seasonality of discharge has affected the nutrient stocks potentially available to support primary production in this area in spring. A further motivation for this study was the question of whether the modifications to the La Grande River have contributed to a decline in eelgrass (*Zostera marina)* along the northeast James Bay coast, where it was once abundant in all sheltered inlets and bays (Curtis, 1976; Lalumiere et al., 1994). Although, the condition of eelgrass is not discussed in this study, our conclusions are expected to provide some oceanographic context for future studies into the decline in health and extent that has been recorded both in peer-reviewed literature and by Cree land users over the past several decades.

3.2 Study Area

James Bay, a large shelf-like southern embayment directly connected to Hudson Bay is located well below the Arctic Circle (considered a subarctic region) but it experiences a climate and sea-ice cycle similar to the shelves bordering the Arctic Ocean (Hochheim and Barber, 2010; Andrews et al., 2018). There are two main sources of freshwater to the Hudson Bay system and subsequently the James Bay System, which are sea-ice melt and riverine discharge. The majority of studies about sea-ice and rivers in this area are focused on the entire Hudson Bay system. Sea ice melt contributes a widespread input, averaging 742 ± 10 km^3 of freshwater annually to Hudson Bay (Landy et al., 2017), compared to multiple point-source rivers, which collectively discharge 630-870 km^3 annually to the Bay's shores (Saucier et al., 2004). Seawater within Hudson Bay originates mostly from the Arctic Ocean via the Canadian Arctic Archipelago (through Fury and Hecla Strait, Lapoussiere et

al., 2013) where freshwater inputs modulate water properties upstream of Hudson Bay leading to an average salinity of inflowing waters of about 32.8 (Granskog et al., 2011). There has also been evidence of seawater inflow coming from Baffin Bay through Hudson Strait (Lapoussiere et al., 2013) (Figure 3.1).

The direct contribution of nutrients by rivers to Hudson Bay as a whole has been recorded as more than an order of magnitude less than the supply that occurs through vertical mixing and inflows from other ocean areas throughout the year (Hudon et al., 1996). On the other hand, Kuzyk et al. (2010) propose that the general transport of Hudson Bay's large river inflow in a cyclonic coastal current around the Bay's margin contributes indirectly to enhance new production in inshore areas through entrainment and consequent upwelling of deep nutrient-rich waters. Despite nutrients associated with riverine discharge being low in comparison to deep water supply, these riverine nutrients can contribute to primary production at a more local scale within estuaries. The estuaries of Hudson Bay have long been assumed to be productive hot-spots as indicated by the great numbers of beluga (e.g., > 10,000 individuals living year-round in James Bay alone) that are observed here. The Hudson Bay coastal region is also home to many Inuit and Cree communities, especially near river outlets, which also attract seasonal visitors.

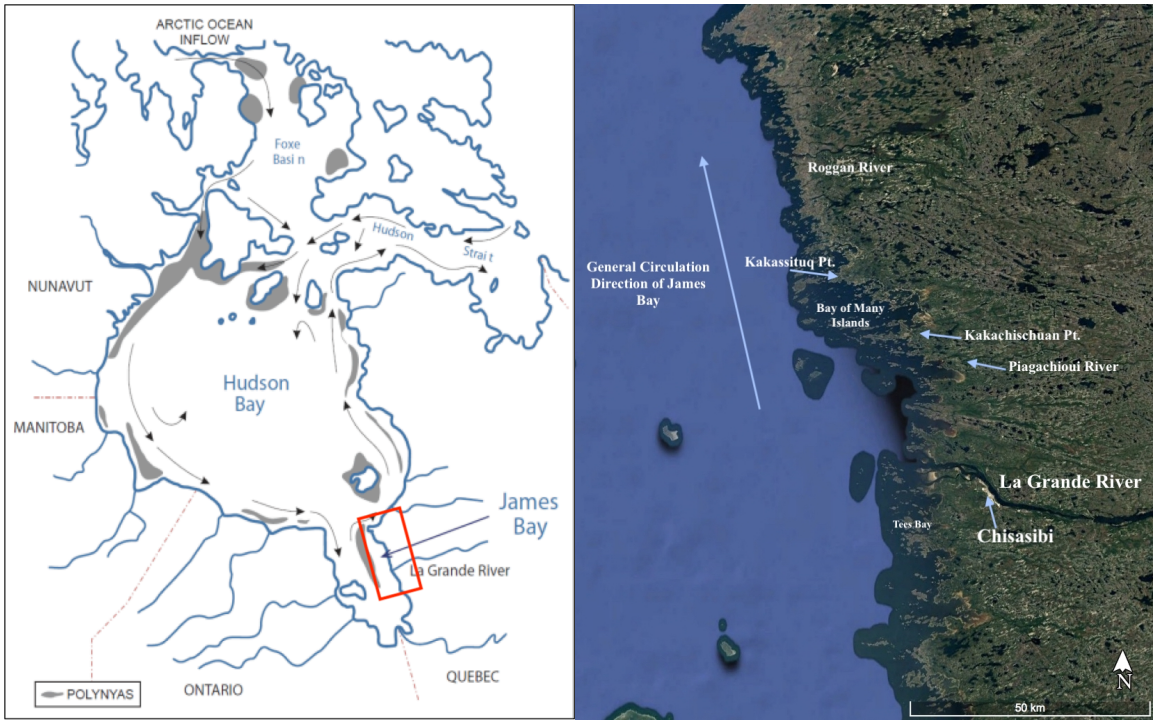

Figure 3.1 Map of Hudson Bay and James Bay (left) and satellite image of James Bay from Google Earth Pro with notable features labeled (right).

The study area is located along the eastern coast of northern James Bay between the latitudes 53.6°N and 54.6°N in the area influenced by the winter plume of the La Grande River (Figure 3.2). The area experiences a relatively cold climate with average annual temperatures ranging from -23.2°C in winter to +14.2°C in summer (data compiled between 1981-2010 from Environment and Climate Change Canada). Sea-ice formation typically begins in November and breakup occurs in June (Galbraith and Larouche, 2011; Taha et al., 2019). Source waters from Hudson Bay enter James Bay along the western coast and circulate within James Bay in a cyclonic manner, ultimately exiting along the eastern side back into Hudson Bay (Figure 3.1). As the waters circulate in James Bay, they continue to be transformed by addition of freshwater leading to lower surface salinity in both winter and

summer at the eastern mouth of the Bay in comparison to the values observed on the western side (Prinsenberg 1984).

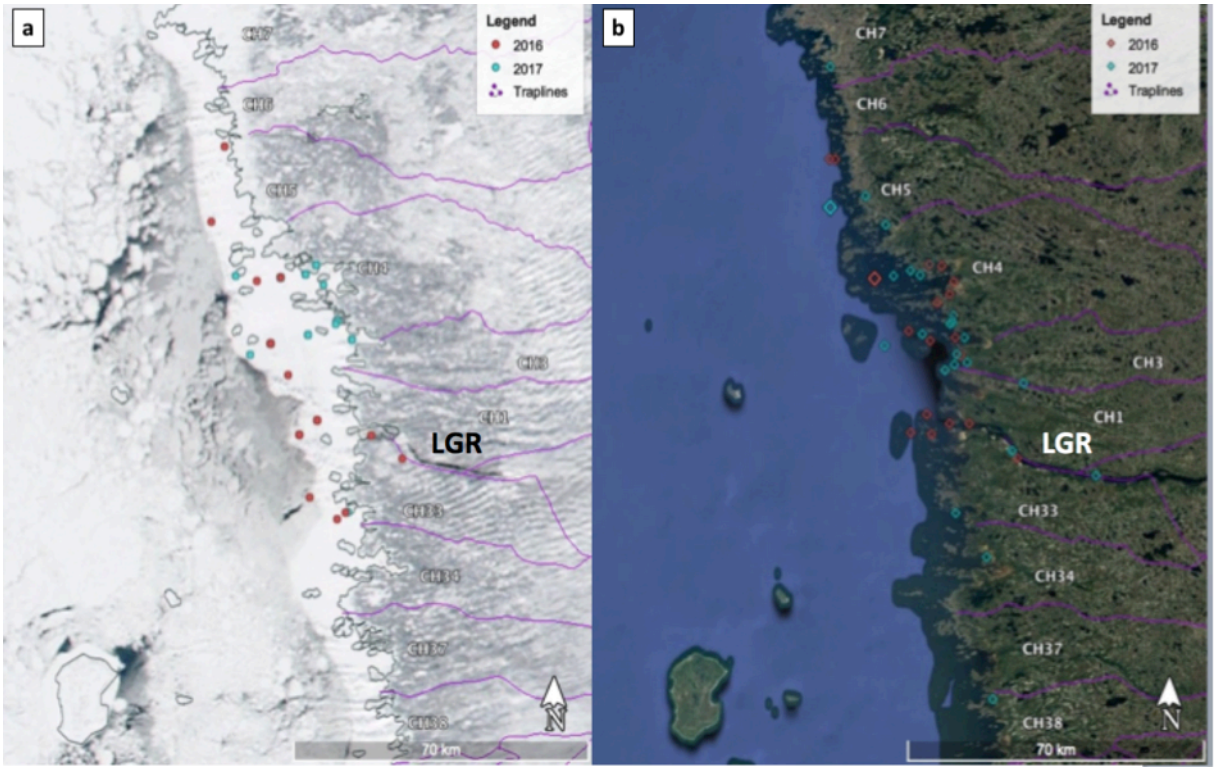

Figure 3.2 Winter (a) and summer (b) water sampling stations with colour distinguishing the year during which samples were collected. Ice image in (a) is sourced from Nasa World View and Google earth. Pink lines show boundaries of coastal traplines associated with the Cree Nation of Chisasibi (CH33-38 south of the river mouth, CH1-CH7 north of the river mouth). LGR label indicates the location of La Grande River.

James Bay, which represents roughly 5% of the surface area of Hudson Bay, receives a disproportionately large amount of the total river runoff to Hudson Bay: about 260 km^3 y^{-1} or 30%-40% of total runoff. The La Grande River alone contributes more than 16% of the total annual gauged streamflow input to Hudson Bay (Hernandez-Henriquez et al. 2010) and since the most recent phase of regulation, exceeds the Nelson River as the largest single river discharging to Hudson Bay (Déry et al. 2011; 2016). Flows that were specifically diverted to La Grande were from the Eastmain, Rupert, Caniapiscau, and Opinaca Rivers (Hernández-

Henríquez et al., 2010; Déry et al. 2016). Peak flows from La Grande River now occur between January and March and measure 4000-6000 m^3 s^{-1}; the sustained high flows result in a large under-ice river plume, which scales with discharge (Ingram and Larouche, 1987; Li and Ingram, 2007). Peak June flows (3094 ± 543 m^3 s^{-1} over 2013-2019; del Giorgio, pers. comm.) are at the low end of the observed natural range (2400 m^3 s^{-1} to 6100 m^3 s^{-1} for 1960-1978; Messier et al., 1986).

3.3 Methods

3.3.1 Sample Collection

This study was conducted in partnership with the Cree Nation of Chisasibi and community research partners contributed to the study design and field sampling. Bulk water samples were collected in early winter (January), late winter (April) and summer (August/early September) of 2016 and 2017 across the northeast James Bay coastal study region (Figure 2). All stations were < 25 km of shore within the limit of the landfast ice (Figure 3.2). In 2016, thirty-eight stations were visited during the course of three sampling trips in early winter, late winter, and summer. In 2017, forty-seven sites were sampled across four separate sampling trips but spanning the same three seasons. Stations varied spatially between the two years and seasonally because emphasis shifted from capturing the La Grande plume conditions in 2016 to across-plume sampling in 2017 (focusing on inshore-offshore conditions). Six locations visited in both late winter and summer, and some overlap of station locations between years but during the same season.

Upon arrival at a station, in winter, a hole was drilled through the landfast ice with an auger and the hole was clean free of slush prior to deployment of instruments and water sampler. In summer, sampling took place from freighter canoes and instruments and water

sampler were deployed directly from the canoe. Conductivity, temperature, depth profile were obtained with either, but most often with both, an Idronaut Ocean Seven 304 Plus or a Sontek Castaway CTD profiler. The accuracies of the Castaway results as stated by the manufacturer are ± 0.05°C for temperature, 0.25% ± 5 μS/C for conductivity, and ± 0.1 for salinity. The accuracies of the Idronaut Ocean Seven 304 Plus as stated by the manufacturer are ± 0.002°C for temperature and ± 0.003 mS/cm for conductivity. Various depths in the water column were sampled at each site with the use of a Kemmerer water sampler, which was deployed with a pre-marked rope (in 1 m intervals). Sampling depths were determined based upon the bottom depth of the site and the halocline observed, if one was present, via the Castaway CTD, which visualized the profiles immediately after deployment and retrieval. At stations < 5 m, only surface samples were collected with the exception of one station with bottom depth 3.5 m where surface and 3 m samples were collected. At all other stations, surface and near-bottom samples were collected. In addition, samples were collected within 1m above and below the halocline (usually at bottom) when one was observed

3.3.2 Sample Analysis

Bulk water samples were processed within a few hours in a temporary, clean laboratory space, free of materials that would contaminate samples. Samples were properly stored or frozen for later analysis in various university laboratories. All samples were analyzed for macronutrients (nitrate, phosphate, and silicate), salinity, and oxygen isotope ratio ($\delta^{18}O$). $\delta^{18}O$ samples were collected into new 20 mL scintillation vials, with no headspace, tightly capped, and then sealed around the cap with parafilm, and then stored at 4°C. The samples were analyzed at Ján Veizer Stable Isotope Laboratory (formerly GG Hatch) at the University of Ottawa using a Gasbench attached to a DeltaPlus XP isotope ratio

mass spectrometer (ThermoFinnigan, Germany). Subsamples (0.6 mL) were pipetted into an Exetainer, and, together with internal standards, flushed with a gas mixture of 2% CO_2 in helium using the Gasbench. Exetainers were left to equilibrate at +25°C for 18 h minimum. Values are expressed in standard $\delta^{18}O$ notation (in per mille or ‰ units) with the V-SMOW (Vienna Standard Mean Seawater) as reference value. Analytical instrument precision was ± 0.15‰. Salinity samples were collected into new or otherwise triple-rinsed and dried 125 mL Boston Round glass bottles, tightly capped and then covered with parafilm around the cap. Salinity was measured using a Guildline Autosal 8400 salinometer with a precision better than 0.002 at the Marine Productivity laboratory at the Freshwater Institute (FWI) – Department of Fisheries and Oceans (DFO), Winnipeg. Samples were standardized against IAPSO Standard Sea Water. Nutrient samples were collected by filtering water samples through a pre-combusted (5-8 hours at 500°C) glass fiber filter (Whatman GF/F 25mm, nominal pore size 0.7 um) held in an acid-washed syringe style filter holder. The filtrate was collected in triplicate into 15 mL polyethylene tubes that had been pre-cleaned in a 10% HCl acid bath. The vials were rinsed three times with the sample water, filled to three-quarters full, sealed, then frozen at -20°C until samples were analyzed. The concentrations of phosphate (PO_4^{3-}), nitrate (NO_3^-) and nitrite (NO_2^-), and silicic acid ($Si(OH)_4$) were determined using a Bran and Luebbe Autoanalyzer III following standard colorimetric methods (Grasshoff et al., 1999) at Jean-Éric Tremblay's lab at the Université Laval, Québec. Nutrient analytical detection limits are 0.02 μM for NO_2^-, 0.03 μM for NO_3^-, 0.05 μM for PO_4^{3-}, and 0.1 μM for $Si(OH)_4$. Despite slow thawing, samples with salinity between 0 and ~10 had unusually low concentrations of silicic acid, which furthermore exhibited a positive linear relationship with salinity. We suspect that for the fresher samples (salinity ≤ 10), silicic

acid (silicate) was not properly recovered from frozen samples after thawing (c.f., Macdonald and McLaughlin, 1982). Consequently silicate values reported for samples with salinity ≤ 10 were removed from the dataset.

3.3.3 Data Analysis

To ensure accuracy of sampling depths, bottle salinity was matched with CTD salinity readings. This was done to avoid discrepancies potentially caused by currents altering the depth at which the Kemmerer ultimately was closed because the CTD and Kemmerer sampler were deployed independently.

Statistical analysis was conducted with the use of R, within the RStudio interface. Relationships between seasons (early winter, late winter and summer) were analyzed for each parameter to determine seasonal patterns using regression analysis. Analysis of variance (ANOVA) was used to test the significance of the variance between slopes and y-intercepts of the winter and summer salinity- $\delta^{18}O$ relationships. Subsequently, paired T-tests were used to determine the significance of differences between water mass fractions calculated with salinity and $\delta^{18}O$ pairs and those fractions calculated with just salinity, to inform the final nutrient stock calculations (described in Section 3.3.4 in detail).

3.3.4 Water mass fraction calculations

To quantify the contributions of each freshwater type, traditional tracers, $\delta^{18}O$ and salinity, were used (Tan and Strain, 1980; Östlund and Hut, 1984). Tandem properties, $\delta^{18}O$ and salinity, provide a way to distinguish between the freshening influence of river water, which is isotopically lighter, and sea-ice melt, which is isotopically heavier (e.g., see Tan and Strain, 1980). We followed the method developed by Östlund and Hut (1984), wherein three linear equations are used together with a selection of end-members appropriate to the dataset

to calculate the fractional contributions of three source waters to each water sample (Östlund and Hut, 1984). In our case, the method was applied to calculate the fractions of runoff/riverine input (RW), sea-ice melt (SIM), and seawater (SW) for each sample. Sea-ice provides a different sort of signal than runoff, which can only add positive amounts of isotopically light water to the system. Sea ice freezes in winter, withdrawing freshwater and leaving salt behind (brine); during summer melt this brackish water is returned to the system. Accordingly, a calculated fraction of SIM may be either positive or negative with the latter indicating a higher than expected salinity, which is associated with brine production/rejection from sea ice growth (Granskog et al. 2011).

The equations are as follows, modified from Östlund and Hut (1984):

$$F_{SW} + F_{RW} + F_{SIM} = 1$$
$$F_{SW}S_{SW} + F_{RW}S_{RW} + F_{SIM}S_{SIM} = S$$
$$F_{SW}X_{SW} + F_{RW}X_{RW} + F_{SIM}X_{SIM} = X$$

Where F = fraction of the associated subscript, S = salinity, and X = $\delta^{18}O$; and where subscripts SW = ambient seawater, RW = riverine runoff, and SIM = sea ice melt water. Each S and X value above represents an appropriate water type end-member based on this dataset.

3.4 Results and Discussion

3.4.1 Seasonal distribution of salinity and $\delta^{18}O$

Surface salinity along the coast varied greatly between winter and summer (Figures 3.3a, e, i) partly because of changes in the extent of the under-ice plume of the La Grande River (cf., Ingram and Larouche, 1987; Messier et al., 1986; 1989) and partly due to the change in rate of inflow. During early and late winter of 2016 and 2017, the La Grande River

discharge spread out under the landfast ice cover forming a highly stratified plume, with a very fresh surface layer (salinity < 5), about 3-5 m thick, overlying brackish water (salinity > 15). The well-defined plume extended north of the river mouth to the south end of Bay of Many Islands (Kakashischuan Point, Figure 3.1) and south of the river mouth to Tees Bay covering an approximate area of 1200 km^2 (see also Peck et al., submitted). The region of freshwater influence (ROFI) defined here as immediately north of the core of the plume (between 30 and 50 km from the river mouth) was characterized by weak stratification and surface salinities of 8.8-13.6 during winter. Beyond the limit of our sampling, surface salinity along the coast generally increases northward to the entrance of James Bay where ~25 was recorded during winter 2015 (Eastwood et al. 2020) and similar values during winters 2016 and 2017 (Peck et al., submitted). The maximum salinity in the deepest waters within the study area (20-25 m), at 25.32 in early winter and 25.86 in late winter, were measured just beyond the La Grande river mouth (Figure 3.4a, f). Unusually low surface salinity observed in late winter at a site at 54.4°N (Figure 3.3e), in an area of otherwise brackish salinity (see Peck et al., submitted), is attributed to local influence of the Roggan River. With a mean annual flow of about 5 $km^3\ y^{-1}$, the Roggan River is the largest river discharging along the northeast James Bay coast north of the La Grande (del Giorgio, pers. comm.).

The distribution of $\delta^{18}O$ in surface waters along the coast during winter mirrored salinity, with low values (below -12.6‰) in surface waters near the La Grande river mouth and throughout the core area of the plume (salinity < 5). The $\delta^{18}O$ values of two samples collected from La Grande River (53.82°N, 78.99°W; and 53.78°N, 78.88°W) during winter were -13.86‰ and -14.28‰ respectively (Table 3-1). In the surrounding ROFI, $\delta^{18}O$ values in surface waters increased to about -8.79‰ and -9.4‰ in early winter and late winter

respectively (Figure 3.3b, f). The most saline subsurface samples had $\delta^{18}O$ values during winter of about -4.92‰ ± 0.5 (n=5) (Table 3-1).

During summer, both surface salinity and $\delta^{18}O$ show a much smaller river plume. The surface salinity was very low (< 5) only in a small area (~120 km^2) about ten-times smaller than winter, near the mouth of the La Grande River. Surface salinity increased rapidly with distance from the river mouth and surface salinity was slightly higher during summer than winter at almost every site that was resampled during both seasons (Figure 3.3i). In contrast, the maximum salinity of 22.45 ± 0.2 (n = 4) observed in deep waters during summer was about 3 lower than the maximum of 25.61 ± 0.2 (n = 5) found during winter (Table 3-1). La Grande River had a $\delta^{18}O$ value of -12.52 ± 0.2‰ (n = 4) during summer, significantly higher than winter values (Table 3-1). Similar to salinity, $\delta^{18}O$ of surface waters increased rapidly with distance from the river mouth reaching values as high as -5.2‰ in the area north of Kakassituq Point (Figure 3.3j). The most saline subsurface samples had an average $\delta^{18}O$ value of -5.05 ± 0.5‰ (n = 4) during summer (Table 3-1). The $\delta^{18}O$ value of the most saline samples was not significantly different during summer compared to winter despite the nearly three-unit difference in salinity of those samples as described above.

Table 3-1 summarizes the average properties of La Grande River and the most saline coastal samples during winter and summer, which were used as 'end-member values' for calculating water mass compositions from S- $\delta^{18}O$ data pairs. Early and late winter samples were combined due to low sample numbers and incomplete coverage of inshore and offshore samples during the two campaigns.

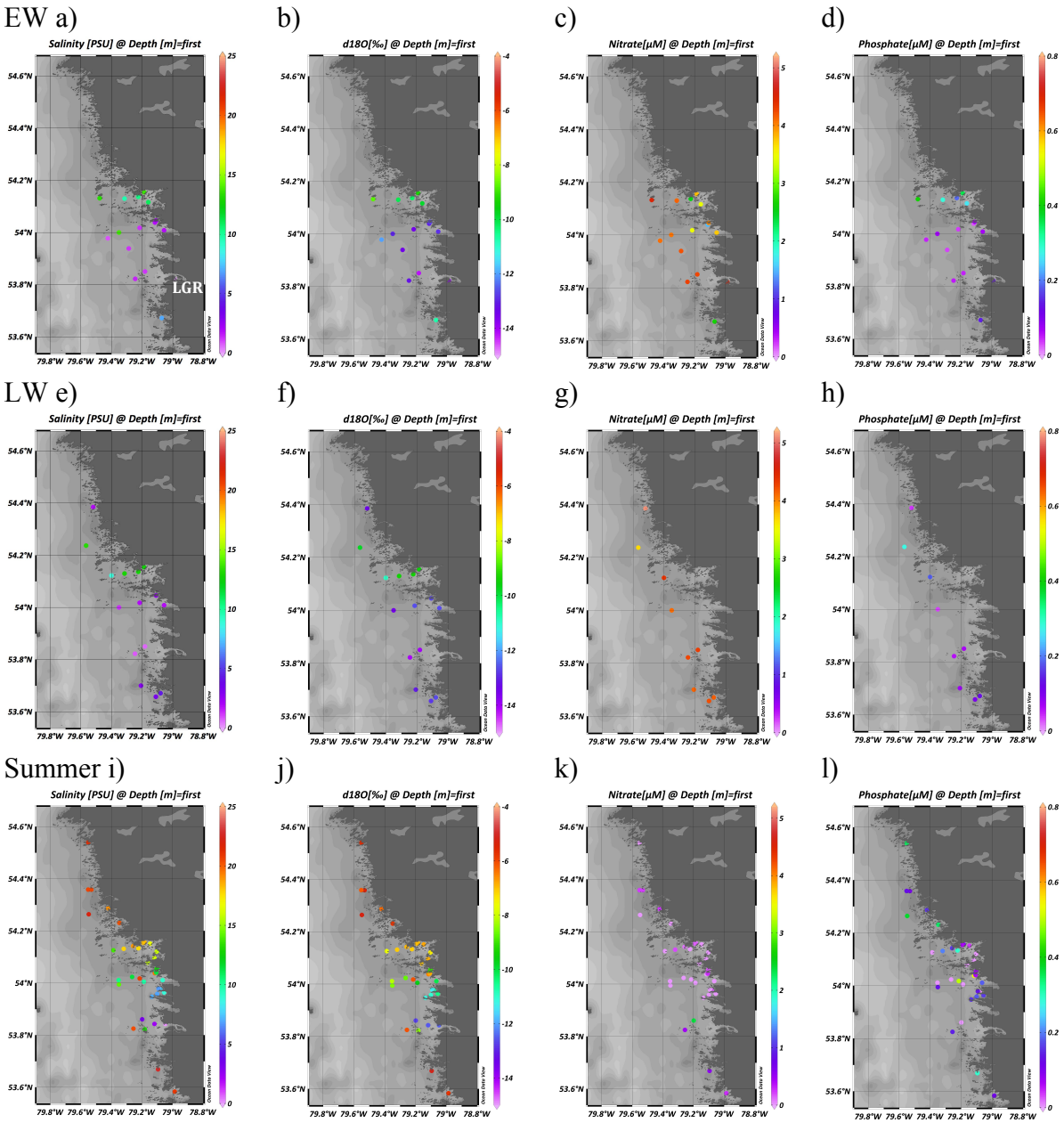

Figure 3.3 Maps of surface water salinity, d18O, nitrate, and phosphate, during field campaigns in early winter (a-d), late winter (e-h), and summer (i-l). La Grande River labeled as LGR in (a) for reference.

Table 3-1 Average and standard deviation for measured water properties in La Grande River water and undiluted seawater in the northeast James Bay study area during winter and summer. Early and late winter data were combined to calculate average winter values. Number of observations (n) is indicated in parentheses.

	Water Type	Salinity	$\delta^{18}O$ (‰)	Nitrate (µM)	Phosphate (µM)	Silicate (µM)
Winter	La Grande R.	0.03 ± 0.01 (2)	-14.07 ± 0.30 (2)	4.53 ± 0.001 (2)	0.11 ± 0.03 (2)	N/A
	Seawater	25.61 ± 0.2 (5)	-4.92 ± 0.5 (5)	3.18 ± 0.2 (5)	0.66 ± 0.04 (5)	13.26 ± 0.04 (5)
Summer	La Grande R.	0.03 ± 0.01 (4)	-12.52 ± 0.2 (4)	2.76 ± 0.3 (3)	0.07 ± 0.05 (3)	N/A
	Seawater	22.45 ± 0.2 (4)	-5.05 ± 0.5 (4)	2.29*	0.45*	15.92*

N/A = not available; *single sample

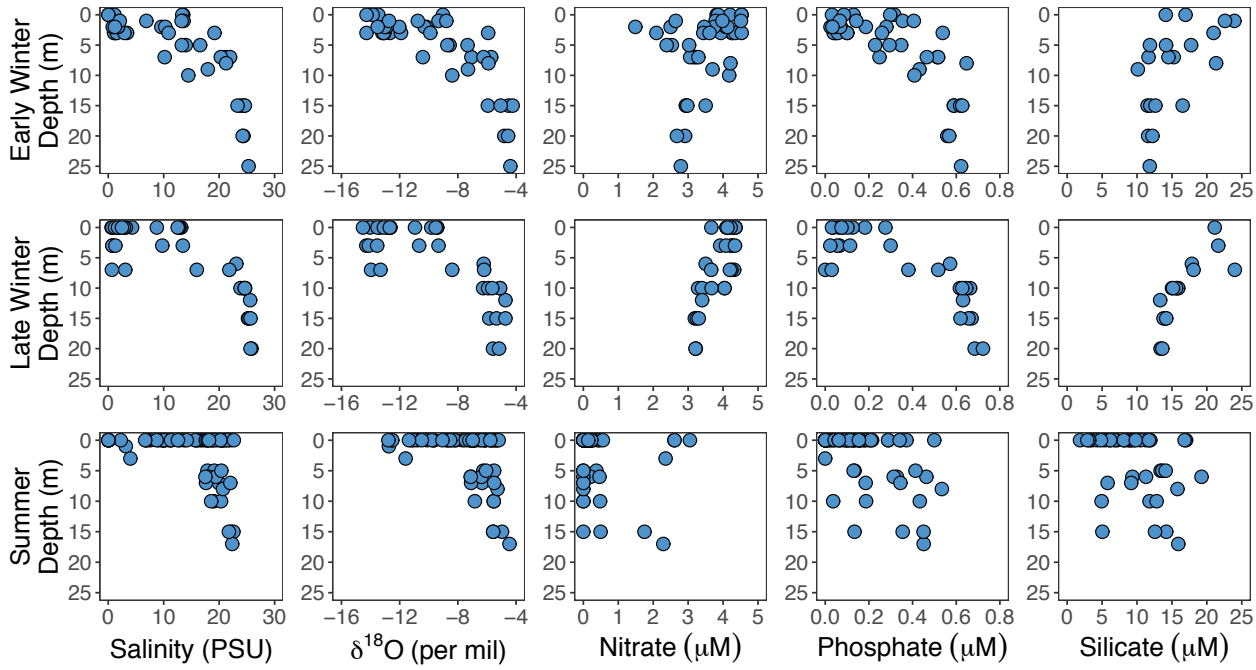

Figure 3.4 Northeast James Bay depth profiles of salinity, $\delta^{18}O$, nitrate and phosphate during early winter (a-e), late winter (f-j), and summer seasons (k-o).

3.4.2 Water mass composition

Salinity-$\delta^{18}O$ data pairs for samples from all three seasons (early winter, late winter, summer) are plotted in Figure 3.5a to assess deviations from simple mixing along the seawater - river water continuum. Such deviations indicate the contribution of sea-ice. Specifically, salinity increase or decrease unaccompanied by a change in $\delta^{18}O$, as observed between winter and summer, mentioned above, implies that SIM has been withdrawn or added to the system. This finding is expected based on the relative contributions of freshwater runoff and sea-ice melt estimated for the Hudson Bay system (cf., Prinsenberg, 1984).

Nevertheless, there remains a strong linear relationship overall between the two tracers during each sampling season showing dominance of the process of mixing river water with salt water. The relationship was very strong during both winter campaigns and when all winter data are combined (Table 3-2). The relationship was only slightly noisier during the summer campaign (Figure 3.5a, Table 3-2). The slopes of the linear regression relationships were not significantly different between winter and summer at 0.35‰ per unit salinity and 0.33‰ per unit salinity, respectively (Table 3-2). However, the y-intercept values of the linear regressions and thus the apparent zero-salinity $\delta^{18}O$ values differed significantly (p-value < 0.001) between winter (-13.83‰) and summer (-12.68‰) indicating isotopic enrichment of the apparent freshwater end-member from winter to summer. As described above and shown in Table 3-1, the average La Grande River $\delta^{18}O$ values aligned well with the y-intercepts of the seasonal regression lines and were more isotopically depleted during winter (-14.07 ± 0.3‰, n = 2) than summer (-12.52 ± 0.2‰, n = 4), which is typical for large northern rivers (Cooper et al., 2008; Pavlov et al., 2016) and for rivers in Hudson Bay, of

which several show similar magnitude changes (about 1.5‰) between winter and summer (Granskog et al., 2011).

Inspecting the $\delta^{18}O$-salinity relationships in Figure 3.5, the apparent mixing line is offset (shifted to the left) between winter and summer consistent with a difference in y-intercept but not regression slope (Figure 3.5a, Table 3-2). Because a change in river water $\delta^{18}O$ alone would have brought about a change in both intercept and slope, all else remaining the same, we attribute the unique winter and summer $\delta^{18}O$-salinity relationships to significant seasonal differences in the properties of *both* La Grande River *and* ambient seawater along the NEJB coast. A significant seasonal change in ambient seawater $\delta^{18}O$ and salinity is also supported by our data (Table 3-1), which showed freshening in the study area during summer, with salinity lower by ~3 without significant change in $\delta^{18}O$. The apparent change in ambient seawater composition in this coastal domain between winter and summer cannot be attributed to addition of river water considering the $\delta^{18}O$ values in La Grande River. Furthermore, all sampled rivers "upstream" of the study area (insofar as cyclonic circulation is concerned (Prinsenberg, 1988)) in southwest Hudson Bay have highly depleted $\delta^{18}O$ values (between -13.59‰ and -10.30‰) similar to La Grande (Granskog et al., 2011; Eastwood et al., 2020; Burt et al., 2016). A plausible source of the freshening with no change in $\delta^{18}O$ is SIM. Sea ice in southern Hudson Bay is formed annually and has low salinity (typically 0-6) and a $\delta^{18}O$ value only about 2‰ higher than that of the seawater from which it is formed (Eastwood et al., 2020). To quantify the approximate SIM percent contribution influencing summer freshening in the study area, we take the observed properties of sea ice in southern Hudson Bay as being representative of the composition of sea ice in the study area (i.e., salinity of 0-6, $\delta^{18}O$ between -4‰ and -0.5‰ (Eastwood et al., 2020)), and

combine them with the winter salinity and $\delta^{18}O$ values of La Grande River (0.03, -14.07‰), and the apparent winter properties of the ambient seawater (25.61, -4.92‰), to solve the linear equations of Östlund and Hut (1984). By representing the water masses in this region with the best available property measurements, we estimate that the ambient summer seawater in the study area could be produced by a mixture of about 10%-15% SIM with the ambient winter seawater. This estimate of the SIM fraction in the summer water mass in northeast James Bay significantly exceeds the previous estimate of 5% SIM in typical Hudson Bay surface waters during summer (Granskog et al., 2011). However, our estimate of 10%-15% SIM contribution to NE James Bay coastal waters is in good agreement with the ~10% SIM found in surface waters southeast of the Belcher Islands more recently in October 2014 (Eastwood et al., 2020). Significant contribution of SIM to summer surface waters in James Bay has long been proposed (cf., Prinsenberg, 1984) and is supported by recent observations of the long-lasting sea ice that tends to collect up and slowly melt throughout summer in southwest Hudson Bay and northwest James Bay (Barber et al., 2021). Because of its radiative properties and feedbacks to atmospheric forcings (e.g., albedo effect), the ice typically lasts in this area well into July, and sometimes into August (see, for example, Figure 2 in Etkin, 1991), although recent dates of ice loss have significantly advanced (cf., Andrews et al., 2018). Observations of the long-lasting sea ice cover in late June 2019 found that it contains very thick floes (up to 18 m) containing ice that has already rejected its brine and has salinity near zero (Barber et al., 2021). The extreme thickness and low salinity of the long-lasting ice support its role as a larger source of freshwater to James Bay than expected based on its areal extent. Protracted additions of sea-ice melt from the long-lasting ice mass into the surface water flowing into northwest James Bay could explain the 10-15% apparent

SIM contribution to summer seawater observed in the NEJB study area in August, which was more than a month after the local sea ice had disappeared.

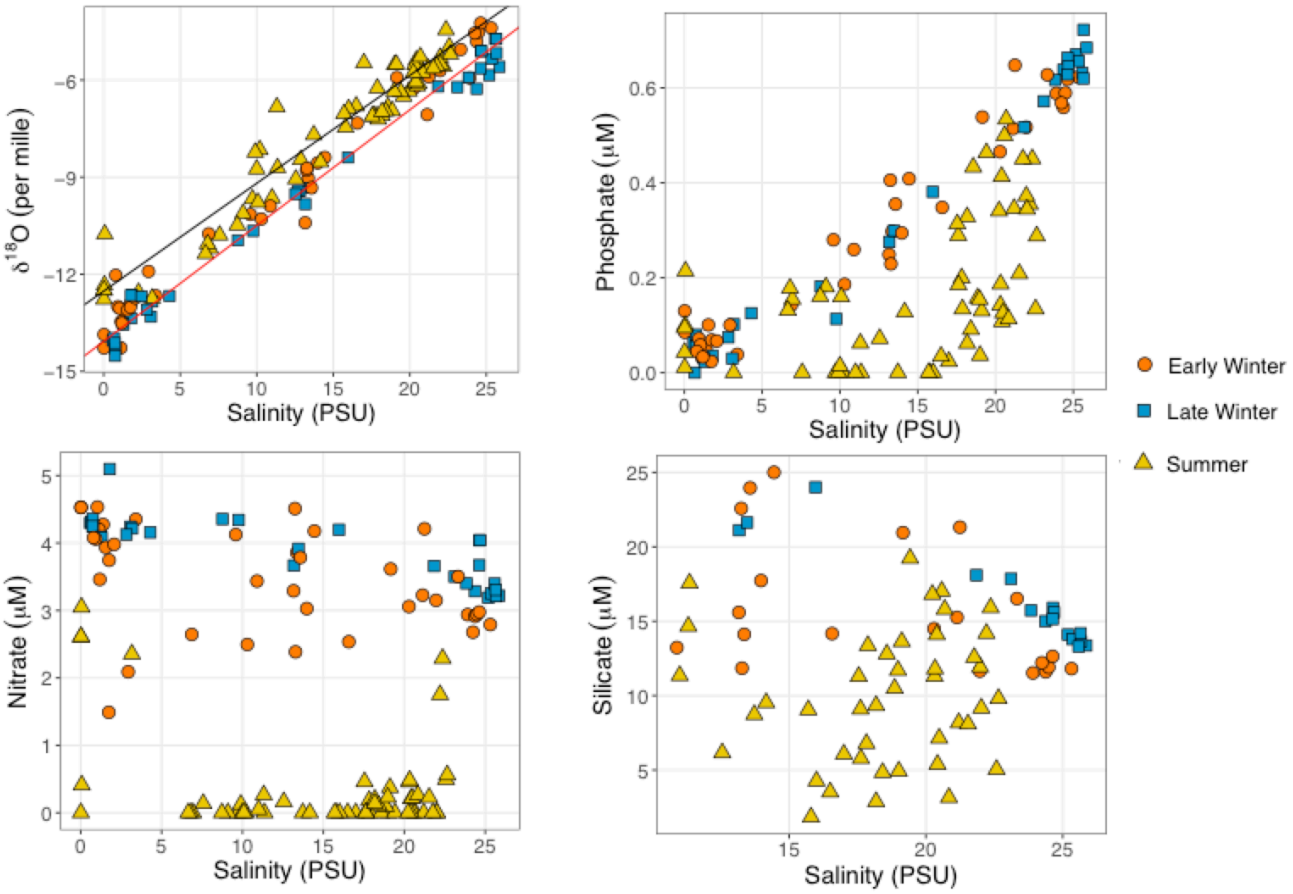

Figure 3.5 Relationships between salinity and $\delta^{18}O$ (a), phosphate (b), nitrate (c), and silicate (d). Apparent winter and summer mixing lines are shown in (a) determined by the average salinity and $\delta^{18}O$ of the two main water masses (La Grande River and James Bay source-water). Note that samples with low salinity (<10) are excluded from the silicate plot because of poor data quality. All points are coloured and shaped according to season of collection (early winter, late winter, summer).

Table 3-2 Statistical analysis of biochemical parameters' relationships with salinity during early winter (EW), late winter (LW), all winter data combined, and summer. Asterisk (*) indicates statistically significant relationship. n value indicates the sample size.

Parameter	Season	Slope (SE)	Intercept (SE)	p-value	R^2	n
$\delta^{18}O$	EW	0.36 (0.01)	-13.68 (0.14)	< 0.001*	0.98	42
	LW	0.35 (0.01)	-14.04 (0.10)	< 0.001*	0.99	36
	Winter	0.35 (0.01)	-13.83 (0.10)	< 0.001*	0.98	78
	Summer	0.33 (0.01)	-12.68 (0.19)	< 0.001*	0.93	66
Nitrate	EW	-0.03 (0.01)	3.86 (0.18)	0.01*	0.16	42
	LW	-0.04 (0.005)	4.39 (0.08)	< 0.001*	0.67	36
	Winter	-0.03 (0.01)	4.06 (0.12)	< 0.001*	0.22	78
	Summer	-0.04 (0.01)	0.93 (0.22)	0.005*	0.13	66
Phosphate	EW	0.02 ($9x10^{-4}$)	0.02 (0.01)	< 0.001*	0.95	42
	LW	0.03 ($7x10^{-4}$)	-0.003 (-0.20)	< 0.001*	0.98	36
	Winter	0.02 ($5x10^{-4}$)	0.01 (0.01)	< 0.001*	0.96	78
	Summer	0.01 (0.003)	-0.006 (0.04)	< 0.001*	0.27	66
Silicate	EW	-0.41 (0.18)	23.37 (3.54)	0.04*	0.17	24
	LW	-0.69 (0.07)	32.16 (1.72)	< 0.001*	0.85	19
	Winter	-0.41 (0.1)	24.47 (2.37)	< 0.001*	0.278	43
	Summer	0.11 (0.22)	7.81 (4.12)	0.61	0.02	47

Although all the winter data from both sampling campaigns were combined to compare water mass compositions between winter and summer, close inspection of the $\delta^{18}O$-salinity relationships in Figure 3.4a shows that during late winter, a number of high-salinity samples lie slightly under the mixing line, consistent with addition of brine (cf., Macdonald et al., 1995). To quantify this brine addition between early and late winter, we use the observed average winter salinity and $\delta^{18}O$ values as the end-members for river water and ambient seawater, a landfast sea ice end-member typical for southern Hudson Bay (4.0 and -2.92 ± 0.1‰) in the equations of Ostlund and Hut (1984). The landfast sea ice salinity

end-member is at the lower end of the range of values presented by Granskog et al. (2011) for Hudson Bay (5.0± 1.0), which is intended to reflect the general lower salinity of James Bay. The $\delta^{18}O$ value here is calculated from that of our ambient seawater value with a fractionation factor of 2‰ expected in southeast Hudson Bay (Eastwood et al., 2020). This method apportions each early winter and late winter water sample (given their salinity and $\delta^{18}O$) into the three water types: RW, SW, and SIM, with negative SIM indicating brine. Figure 3.6 shows the calculated fraction of river water (Frw), fraction of seawater (Fsw), and fraction of sea ice melt (Fsim) for samples from early winter and late winter. On a ternary diagram, the early winter samples lie distinctly closer to the Fsim vertex than the samples from late winter (Figure 3.6) indicating a relative decrease in Fsim or addition of brine between those two time periods. The relative decrease in Fsim from early winter to late winter is consistent with indication of sea ice growth and brine production. Mean values of Fsim across all samples decreased from 0.045 in early winter to -0.010 in late winter indicating a fractional increase in the brine content of 0.055. This fractional increase in brine represents the equivalent of 0.275 m of brine addition to a 5 m surface water layer (0.055 x 5 m = 0.275 m), or, allowing for the 10% expansion upon freezing, roughly 0.30 m of *in situ* sea-ice growth. The landfast ice thickness in the study area averaged 90 cm ± 14 cm (n = 10) in April 2016 and 74 cm ± 17 cm (n = 13) in April 2017. The relatively low estimate of sea-ice growth (only roughly 30% of the apparent *in situ* total ice growth) may be explained by advection of the brine formed earlier in the winter, which is reasonable given the short residence time of water along the northeast James Bay coast in winter (Eastwood et al., 2020). We calculate the river water residence time to be around 2.5 weeks for the core of the plume, based on a winter plume size of 1200 km^2, and April 2016 & 2017 average discharge

rates of La Grande River (~3800 ± 510 m^3 s^{-1} and ~3900 ± 300 m^3 s^{-1}). Lacking ice cores from the sampling sites during this time period, we cannot quantify the amount of river water that would have been incorporated into the landfast ice, which would cause a mismatch between observed ice thickness and the amount of ice growth inferred from the apparent brine in the water column (cf., Macdonald et al., 1995; Kuzyk et al., 2008). Results from ice cores taken in winter 2019, in the same study area, however indicate a range between 46% (furthest away from La Grande) to 80% meteoric water composition, with the station at the mouth of La Grande expected to be close to 100% meteoric water (no complete ice core here). The SIM end-member (Figure 3.6) is calculated, for simplicity, with the assumption that the landfast ice is composed entirely of SW, and thus we apply a fractionation factor to the mean SW. However, with this value and considering the ice core meteoric fractions and assuming they are similar to the ice conditions from 2016 & 2017, we are effectively over-estimating brine production, and under-estimating the RW contribution.

During summer, most of the scatter in the salinity- $\delta^{18}O$ relationship lies to the left of the line (Figure 3.5a), consistent with addition of sea-ice melt. However, with no ice having been present in the area during the month preceding our sampling, the unexplained variance could be due just as likely to influence of small local streams with different isotopic values from La Grande River. Indeed, the samples deviating the most from the linear mixing line include ones collected near the outlet of the Piagachioui River (Figure 3.1). An inland sample of a small unnamed river in the study area in summer 2017 yielded a higher $\delta^{18}O$ value than La Grande (-10.75‰), which indicates that the influence of small streams on the summer salinity- $\delta^{18}O$ relationship will be to shift samples above/to the left of the main trend-line, similar to the effect of addition of SIM. With only two tracers (salinity, $\delta^{18}O$), we can resolve

only three water types. Considering that only 7% of the variance in $\delta^{18}O$ during summer was *not* explained by salinity (according to the linear regression relationships, Table 3-2), we proceed with using salinity alone to trace freshwater influence in the study area within a particular season of study, and we assume a two-end-member mixing model (La Grande River and ambient seawater). This method also addresses the potential disconnect with negative SIM or brine over-estimation which comes from the use of a SIM value that may not reflect this complex estuarine system. We avoid quantitative comparisons of those samples for which the regression residuals indicate a third freshwater source might cause large error.

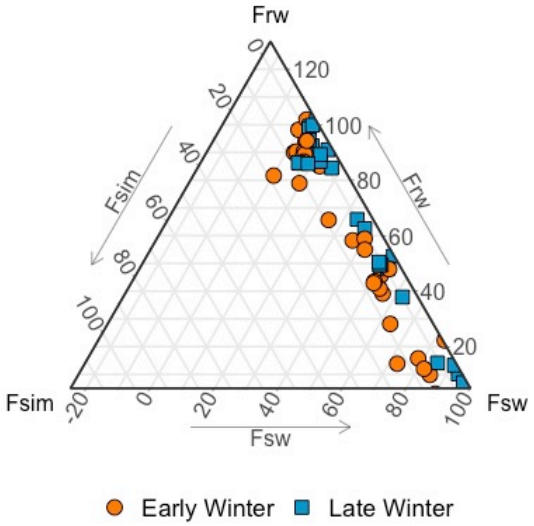

Water type	Salinity	$\delta^{18}O$ (‰)
RW	0.03 ± 0.01	-14.07 ± 0.3
SIM	4.00	-2.92 ± 0.1
SW	25.61 ± 0.2	-4.92 ± 0.5

Figure 3.6 Each sample's calculated fraction of river water (Frw), fraction of seawater (Fsw), and fraction of sea ice melt (Fsim), with points distinguished by early winter (circles) vs. late winter (squares). End-members that were used to calculate the fractions for winter samples are presented in the adjacent table.

3.4.3 Distribution of nutrients

Identifying that zero salinity is representative of La Grande waters in our data, and increasing salinity coincides with increasing ambient seawater contribution, the plume of La

Grande River clearly was the dominant control on the distribution of nutrients along the coast during winter. Nitrate concentrations in surface waters decreased with distance from the river mouth (Figure 3.3c, g) and also decreased vertically with increasing depth in the water column (Figure 3.4c, h) reflecting the plume structure. La Grande River had a winter nitrate concentration of 4.53 μM, which lies within the higher range of nine previously sampled Hudson Bay rivers (average of 3.77 ± 2.1 μM) (Kuzyk et al., 2010). The ambient seawater had a nitrate concentration of 3.18 ± 0.2 μM (n=5) (Table 3-1), which was lower than what was measured in subsurface (30-50 m), residual winter waters (Granskog et al., 2011) at the entrance to James Bay in October 2005, (~ 5-7 μM, Kuzyk et al., 2010). These comparisons show that the ambient seawater we observe in NEJB in 2016/2017 is lower in nitrate than expected based on previous measurements at the mouth of James Bay. This may have to do with denitrification and other associated processes. In contrast to nitrate, phosphate concentrations were near zero in La Grande River during winter (0.09 and 0.13 μM, Table 3-1) and were relatively high in the ambient seawater (0.66 ± 0.04 μM, n = 5, Table 3-1). Surface phosphate concentrations were near the limit of detection (maximum 0.07 μM) in the core plume area near the river mouth and northward as far as Kakachischuan Point (Figure 3.3d, h). Phosphate concentrations increased with depth, from near-zero values in the surface layer to maximum concentrations of 0.6 μM in early winter and 0.72 μM in late winter (Figure 3.4).

Nutrient-salinity relationships for the early winter and late winter periods (Figure 3.5b, c, d) show that nitrate was conservatively mixed during late winter ($R^2 = 0.67$, $p < 0.001$) but during early winter, some inshore locations had unexpectedly low nitrate concentrations in comparison to our other observations (< 2.7 μM, with salinity 2-18,

Figure 3.5c). There was no significant relationship between nitrate and salinity for combined winter periods. Phosphate-salinity relationships were strongly positive during both early winter and late winter ($R^2 = 0.95$ and 0.98, $p < 0.001$ respectively; Table 3-2) indicating conservative mixing. Silicate concentrations decreased with increasing salinity during winter ($R^2 = 0.28$, $p < 0.001$, Table 3-2). Silicate also demonstrated a similar seasonal relationship with salinity as nitrate where the strength of the relationship is stronger and has greater significance in late winter ($R^2 = 0.85$, $p < 0.001$, Table 3-2) than in early winter ($R^2 = 0.17$, $p = 0.04$, Table 3-2). The inshore sites with low nitrate were not anomalous for phosphate, however relatively low silicate concentrations were found here as well (where salinity > 10).

During summer, nutrient distributions along the coast reflected both water-mass mixing and nutrient uptake. Surface nitrate concentrations generally were very low (< 0.6 μM and often at the limit of detection). The highest surface nitrate concentrations during summer were 2.4 μM at one offshore site and 2.6 μM - 3.05 μM in La Grande River (Figure 3.3k). In contrast to nitrate, there was no discernable spatial pattern in surface phosphate concentrations during summer and the range of concentrations (0 - 0.53 μM) was similar to the winter periods (Figure 3.2l). However, phosphate-salinity relationships clearly show departure from conservative mixing (weaker positive linear relationship, Table 3-2) consistent with phosphate uptake during summer, similar to the observed nitrate uptake. Silicate concentrations had no discernable relationship with salinity in summer, but were low overall compared to the early and late winter periods (Figure 3.5d). These lower concentrations of silicate during summer are consistent with an increase in diatom production during the open water season. With the lack of silicate data for low salinity samples, we are unable to determine what La Grande is contributing to the coastal waters in summer in regard

to silicate, but we expect concentrations to remain high with a slight decrease similar to nitrate, as this has been observed across many high latitude rivers (Holmes et al., 2012; Le Fouest et al., 2013). This decrease would be dependent upon the phytoplankton community requirements and composition, i.e., a large population of diatoms would consume the silicate. Overall, the summer nutrient condition reflects a combination of water mass mixing, and biological uptake, whereas the winter nutrient distribution is driven by the stratification of the coastal waters.

3.4.4 Nutrient ratios and assessment of potential nutrient limitation

The Redfield N:P molar ratio (16:1) is one way of assessing the limiting nutrient in a given system in terms of planktonic producers (Redfield, 1958). Ratios less or greater than 16, respectively, indicate that nitrate or phosphate supply is limited relative to the expected average nutrient demand of phytoplankton. Eelgrass or *Zostera marina*, which is abundant in this region (Lalumiere et al., 1994), takes up NP in a ratio of 20 and overall seagrass species have been found to have a mean NP ratio of 24 (Duarte, 1990). This implies greater nitrogen demand (relative to phosphate) by eelgrass than phytoplankton.

Our samples vary widely with respect to the Redfield ratio (black line in Figure 3.7a) depending on both salinity and season. The saltiest samples are characterized by NP ratios of about 4.9 in all seasons, whereas the freshest samples are characterized by NP ratios of about 79 (although values ranged 0 - 237 across all seasons where salinity < 10, n = 42). During winter, nitrate would be the limiting nutrient upon the beginning of the ice-melt season in about half of the coastal samples, with salinities mostly >10. The other half of the samples, in which phosphate would become the limiting nutrient, are surface waters within the La Grande River plume where surface salinity was < 10. During summer, almost all the samples

indicate nitrate is generally the limiting macronutrient (Figure 3.7a). Thus, our nutrient ratio data indicate that nitrate is the limiting element in NEJB coastal waters during summer; both for phytoplankton and eelgrass species, assuming no other nutrient supplements such as direct uptake via roots. Our conclusions are consistent with the pronounced drawdown of nitrate to values near the detection limit in virtually all samples during summer, the very fresh sample right at the river mouth being an exception (Figure 3.7a).

Our finding of nitrate being the limiting nutrient for primary production in water samples with salinity > 10 is consistent with the nitrate limitation observed across many Arctic surface waters between 2004-2016, where the majority of NP ratio calculations fall under 10 (Ardyna et al., 2020). In more coastal regions, like the Beaufort Sea and Mackenzie Shelf, NP ratios in surface waters are relatively close to the Redfield ratio between 13 and 15 (Macdonald et al., 1987; Tremblay et al., 2008). Interior Hudson Bay is known to be generally oligotrophic and its offshore surface waters have an average NP ratio of 2.29 indicating nitrogen is the nutrient in lowest supply (Ferland et al., 2011). The higher salinity waters of the NE coast of James Bay demonstrates oligotrophic conditions, when comparing the waters that enter from Hudson Bay and those that have cycled through to the study area.

It is interesting to note that the SiP relationship is significant when examining just samples with salinity 18-20 ($p = 3.8x10^{-5}$, $R^2 = 0.69$, $n = 19$). A similarly strong SiP relationship was reported by Macdonald et al. (1987) on the Mackenzie Shelf. It suggests uptake of Si together with P during summer as expected with diatom production. A cluster of samples with salinities > 20 have lower SiP ratios than fresher samples and lower silicate, which we associate with a lack of river water addition (Figure 3.7c). The affected samples are the nitrate-limited samples based on the NP relationship (Figure 3.7a).

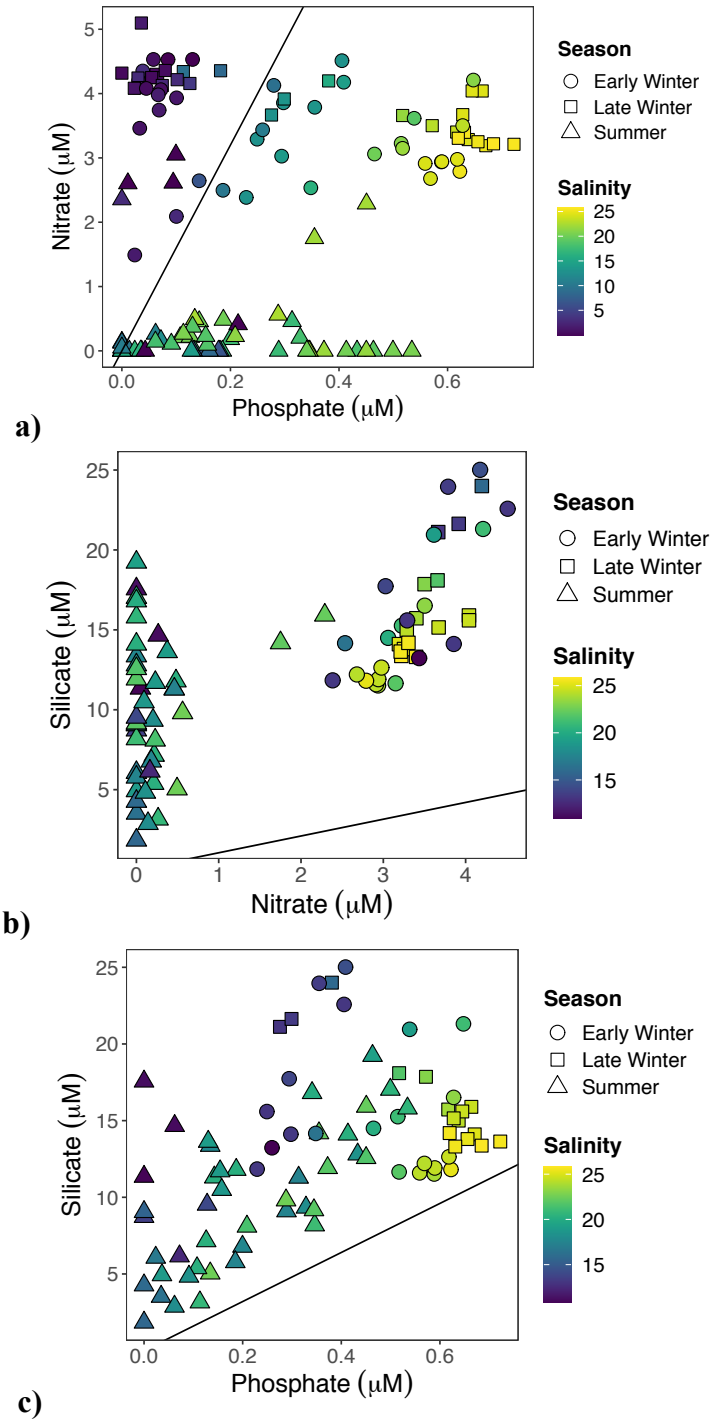

Figure 3.7 Nutrient relationships coloured by salinity and with shapes representing sampling season (circle = EW, square = LW, triangle = Summer). (a) N:P relationship with the Redfield Ratio (16:1) represented by black solid line. (b) Si:N relationship with the Brzezinski (1985) diatom composition ratio (1.05) represented by the black line. (c) Si:P relationship with the corresponding Si vs P ratio 16:1 based on above N:P and Si:N ratios, represented by the black line. Samples with salinity <10.5 in figures (b) and (c) have been omitted due to unreliable silicate values.

We conclude that in this saltier water (interpreted as ambient seawater), phosphate is not limiting when compared to nitrate, however it is potentially limiting when compared to silicate. Based on previous Si:N ratios recorded in literature, which can vary within the water column and temporally (1.05-2.0, Brzezinski, 1985; Tremblay et al., 2008, 2015), our data (Figure 3.7b,c) suggest that silicate (Si) would not be the potentially limiting nutrient, regardless of location or season.

3.4.5 Surface water nutrient stocks and contributions of source waters

Although our data suggest N is the potentially limiting nutrient for primary production across most of the coastal waters we measured, except within the La Grande plume, and that river water and seawater supply N, it remains difficult to appreciate the importance of La Grande River inputs to nutrient dynamics in the coastal domain because both the supply and demand for nutrients vary seasonally (see Table 3-1) and spatially. To quantitatively assess the contribution of La Grande River nutrient inputs and compare them across space and time, we calculated two types of nutrient stocks (nitrate and phosphate) for the surface layer (top 5 m) of the water column: (i) observed stocks, based on measured nutrient concentrations integrated over a 5-m water column; and (ii) expected stocks. The expected stocks represent expected fractional nutrient additions from RW and SW components based on observed nutrient concentrations within RW and SW (Table 3-1); they can be thought of as estimates of the 'initial' nutrient stocks prior to biological uptake. We chose the top 5 m of the water column, which represents the plume thickness in winter, and shows the greatest seasonal variation in freshwater content. Furthermore, eelgrasses in NEJB are generally confined to < 5 m water depth (Lalumiere et al., 1994). Only phosphate and nitrate are quantified as these are the two identified potential limiting nutrients in and out of

the core of the plume. Six offshore locations (Sites 1-6, Fig. 3.8) that were sampled repeatedly, at least once in winter and once in summer (± 3 km between seasons), were selected along the coast at locations extending from 53 km north to 20 km south of the La Grande River mouth. Sites 1-3 lie north of La Grande, Sites 4 and 5 are located near the La Grande River mouth with Site 5 located to the west of a set of islands, and Site 6 is located south of the River (Figure 3.8). We avoided locations that we interpreted as having been influenced by small streams during summer, based on high residuals in the salinity- $\delta^{18}O$ regression relationship.

We opted to use salinity alone to calculate the RW and SW stock calculations. This decision follows from our conclusion that, within a particular season, the La Grande River is the major control on salinity and $\delta^{18}O$ variations *among our sampling stations*, explaining 93%-98% of the variance. We assume all sites are equally affected by seasonal sea-ice melt additions because they occur at a regional scale. Any local sea ice melt is also assumed to be circulated out by riverine induced estuarine circulation, as residence time based on discharge rates in summer is around one day. Furthermore, with small local rivers just as likely as ice melt to cause residual variation in the salinity- $\delta^{18}O$ relationship during summer, a fully resolved system would involve four components (SW, RW, SIM, and smaller local rivers), which has no unique solution when only two tracers are available. Based on the three end-member mixing model (RW, SW, SIM) applied to winter data in section 3.4.2, variation among our sampling stations due to differences in brine addition was not more than 10%-15% at most (see Figure 3.6).

In Figure 3.9, we show the calculated stocks of RW and SW in the top 5 m of each site and nutrient stocks expected from conservative mixing of RW and SW for late winter

and summer. For comparison, we also plot observed nutrient stocks for the six sites (black diamonds). Expected nutrient stocks are very different between late winter and summer reflecting the 1.5-fold higher river discharge in winter (4600 m^3 s^{-1} vs. 3200 m^3 s^{-1}) and the storage of this freshwater in the surface layer of a highly stratified water column under the ice cover (Figure 3.4; and see also Peck et al., submitted).

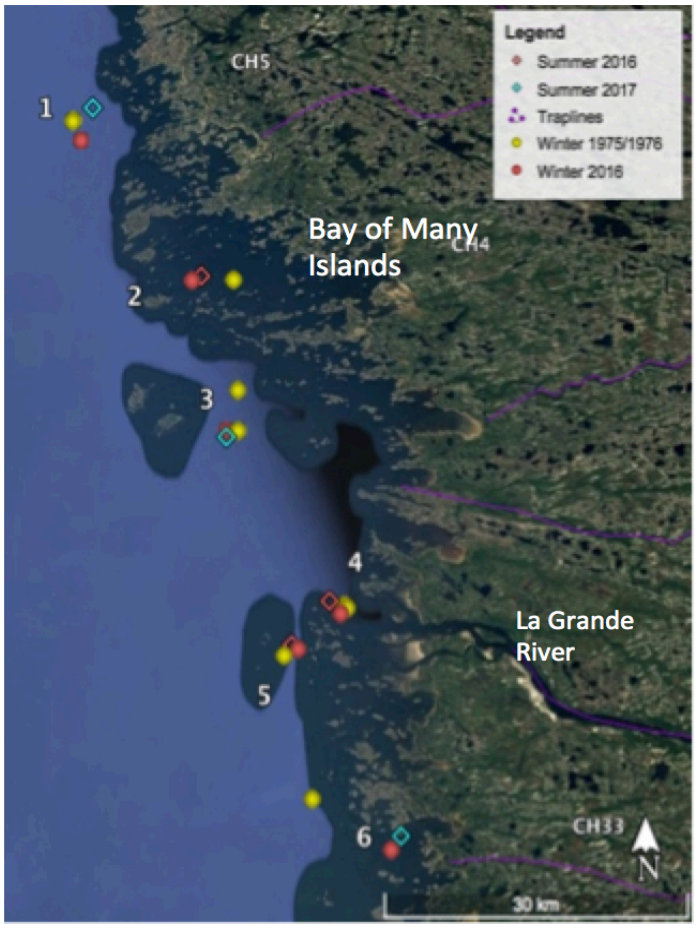

Figure 3.8 Map of six selected sites for inventory calculations. Red points represent 2016 sites, and blue points represent 2017 sites. Yellow points represent stations from winter 1975/1976. Map sourced from Google Earth Pro.

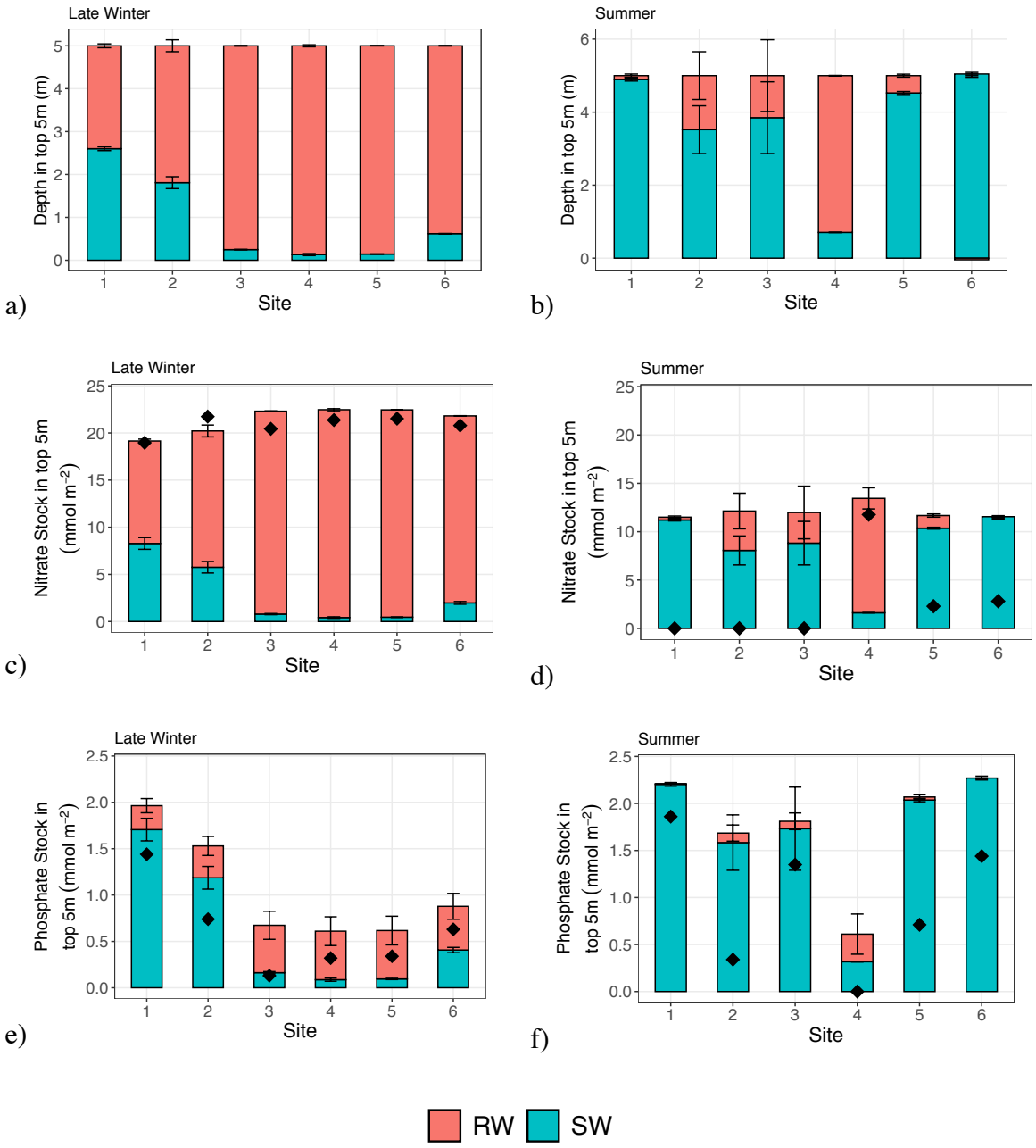

Figure 3.9 Calculated depth of each water type (RW and SW) at each station in (a) late winter and (b) summer. Calculated initial nutrient stocks in the top 5 m of the water column during late winter and summer (nitrate – c,d; phosphate – e,f; with colours showing the contribution of each water type (red – RW, blue – SW). Black diamonds on each bar show the actual measured stocks of nutrients at each site. Error bars are representative of standard deviation, calculated out through a series of error propagation equations.

In late winter, the surface layer of all sites is dominated by RW (Figure 3.9a) and because RW contains significant nitrate, all sites along the coast have large expected nitrate stocks (~20-24 mmol m^{-2}). The implication here is that even outside the core of the plume, the RW is a dominant source of nitrate for the under-ice water column for a large stretch of the coast. SW-derived nitrate in the surface layer increases northward – the main direction of plume flow and hence entrainment - but at most contributes 40% of the total expected nitrate stock at the northernmost site (site 1, Figure 3.9c). The observed stocks of nitrate in late winter are similar to the expected stocks (Figure 3.9c) consistent with no significant biological drawdown at this time of year.

In contrast to nitrate, during winter there is wide variation in phosphate stocks, spatially. The phosphate stocks are high at the northern sites because of strong SW supply and low at the sites nearer or south of the river mouth (sites 3, 4, 5, and 6) due to the very low RW phosphate supply (Figure 3.9e). However, across all sites, the observed phosphate stocks in late winter are lower than expected. Possible explanations include biological uptake of phosphate (e.g., by perennial eelgrass) or an abiotic loss mechanism such as sorption onto oxides in surface sediment (Sundby et al., 1992, van Raaphorst and Kloosterhuis, 1994) or sorption with iron during flocculation around the halocline in estuarine mixing zones (Macdonald et al., 1987). The largest difference in observed phosphate is seen at site 2, just outside of Bay of Many Islands, which is known to host productive eelgrass beds (Lalumiere et al., 1994). However, this is also the frontal area of the plume, where salinity increases rapidly with distance, and thus flocculation-induced P losses could be expected.

In summer, the expected nitrate stocks are about half those in late winter (Figure 3.9d); they are similar across all the sites and supplied mostly by SW except at site 4 at the

river mouth. This exceptional dominance of RW-derived nitrate at site 4 is consistent with the P limitation and thus N excess we observe in low salinity (< 10) waters (Figure 3.7a) but may also be related to the relatively short residence time of La Grande waters in this area in both winter (~2.5 weeks) and in summer (~0.6 days). This lends to the importance of considering the stocks but also the renewal rate near the river mouth. The observed nitrate stocks during summer are much lower than the expected stocks with the exception of the river mouth site 4 (Figure 3.9d). During summer, the observed nitrate stocks are completely drawn down to zero north of the mouth of La Grande, and nearly to zero south of the mouth. Phosphate stocks in summer are higher than those in late winter and supplied almost entirely by SW (Figure 3.9f). The exception is the RW-dominated site 4, which has a very low summer phosphate stock which is supplied by 50% RW and 50% SW. Because sampling occurred late in the growing season (August), we expected to see low observed nutrient stocks in relation to the calculated expected stocks (which represent pre-biological uptake). Phosphate stocks are drawn down relative to the expected stocks but with varying degrees of drawdown from site to site. This difference between nitrate (which was completely drawn down) and phosphate reinforces the notion of nitrate limitation north of La Grande in summer.

3.4.6 Comparison of pre- and post-development nutrient stocks

In the interest of assessing the effects of La Grande River development on freshwater and nutrient dynamics in the NEJB coastal domain (cf., Maavara et al. 2020), historical data were compiled for the river and estuary waters based on Messier et al. (1986, n = 16), and for the surrounding marine environment prior to hydroelectric activities (1974-1976) based on Marine Environmental Data Service (MEDS; https://www.meds-sdmm.dfo-mpo.gc.ca/isdm-

gdsi/index-eng.html). Additionally, data was also compiled from the Fisheries and Marine Service Technical Report no. 650 (Grainger and McSween, 1976), which identified fourteen sites in the La Grande estuary and six sites in offshore James Bay with applicable nutrient data.

The first notable difference in the oceanographic data was the low maximum salinity detected in the study area in recent years compared to pre-diversion measurements both in winter and summer. In the 1974-1976 MEDS data set, the summer salinity ranged 23-25 in deepwater near the mouth of La Grande, whereas we saw a maximum summer salinity of 22.2. Winter salinity reached a maximum of 28 in 1975-1976, which is well above the maximum of 26 that we observed. The comparison of deepwater salinities in 2016-2017 and 1974-1976 suggests that James Bay has been affected by large-scale freshening during recent decades. A freshening trend during the last 20-30 years also has been identified tentatively from stable and clumped $\delta^{13}C$ isotope trends in brachiopod shell calcite studied in west Hudson Bay (Brand et al., 2014). Lacking historical $\delta^{18}O$ data, it is not possible to attribute the regional freshening to increased presence of RW and/or SIM. Despite the freshening, late winter nitrate concentrations associated with James Bay seawater were similar in the pre-diversion period (~2.6 μM) and our data (3.18 ± 0.2 μM, n = 5, Table 3-1). Late winter phosphate concentrations are also very similar between the two periods (0.68 μM pre-diversion, and 0.66 ± 0.04 μM, n = 5, Table 3-1). For river water, we were only able to find nutrient data for the winter from the pre-diversion period. Messier et al. (1986) give average pre-diversion values of 1.6 μM nitrate and 0.15 μM phosphate for the La Grande River in winter (Table 3-3).

Using the historical seawater and river water nutrient data, together with surface

salinity measured in late winter 1975-1976, we calculated expected nutrient stocks for the pre-development period using the same method described previously (section 3.4.5). Because the base salinity of the seawater in this area in late winter of 1975-1976 was 28, we calculate RW contributions to the surface (top 5 m) layer of up to 50% (Figure 3.10a). Sites are indicated on Figure 3.8 as yellow points. Site 3, had two corresponding pre-diversion sites and thus the mean of the salinity and nutrient data were taken. The pre-development nitrate stocks were about half those seen in our data (compare Figure 3.10c and d). Although the SW-derived nitrate stocks were larger because of the greater SW contribution to the surface layer, the lower nitrate concentration in the RW plus overall lower RW contribution to the surface layer led to much lower nitrate stocks relative to our data. In contrast, the phosphate stocks were at least one-third greater than those seen in our data. Stock distribution patterns north and south of the river mouth pre-and post-development are similar for phosphate but reversed for nitrate, which used to be lowest at the river mouth and increased to the north and the south and now shows the opposite pattern because of the large plume together with the higher concentrations of N in river water. Ongoing work suggests that nitrate concentrations in La Grande River water have increased following regulation (de Melo et al., in review).

Table 3-3 Pre-diversion (1974-1978) average observations for salinity and nutrients in La Grande River water and east James Bay seawater in winter. Seawater nutrient values are taken from one station at the deepest sampling depth (36.5 m)

Water Type	Salinity	Nitrate (μM)	Phosphate (μM)	Silicate (μM)
La Grande R.	0[a]	1.6[b] (1.6-2.1; n=16)	0.15[b] (0.05-0.32; n=16)	43.3[b] (31.6-56.6; n=16)
Seawater	28[a]	2.6[c]	0.68[c]	12.8[c]

[a]MEDS data
[b]Messier et al., 1986
[c]Grainger and McSween, 1976

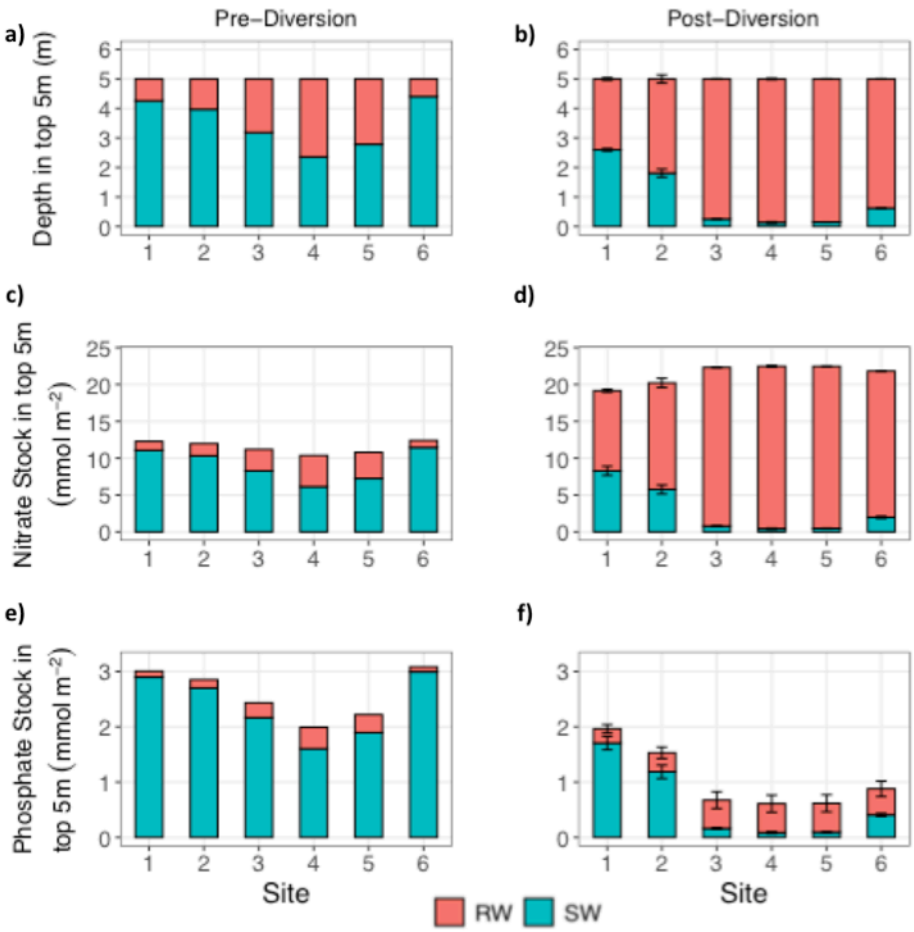

Figure 3.10 Calculated depth of each water type (RW and SW) at each station (a) pre-diversion (1975-1976) and (b) post-diversion (2016-2017) in late winter. Pre-diversion (c) nitrate and (e) phosphate stocks in the top 5m of the water column compared to post-diversion (d) nitrate and (f) phosphate stocks apportioned by RW (red) and SW (blue) contributions.

3.4.7 Implications for nutrient dynamics and primary production in the coastal domain

Nutrient distributions in the northeast James Bay coastal domain have been modified both in space and time by the changes in La Grande River discharge. Freshening of the study region's source seawater is more likely due to large-scale phenomena (regional climate change or altered circulation patterns), rather than local changes based on salinity maxima observations between our present data, and data collected historically, prior to diversion. This overall freshening also may have modified the nutrient distributions. The new data, which

include a second freshwater tracer ($\delta^{18}O$), indicates that sea-ice melt plays a major role in the regional-scale freshening of James Bay surface waters between winter and summer. The previous contribution of SIM to summer water masses, and the possibility of changes in SIM explaining the decrease in ambient seawater salinity between the 1970s and today, which affects both summer and winter water masses, is not something we can assess because of the lack of historical $\delta^{18}O$ data. These new data we present here provide a baseline for future work on SIM contributions. With the majority of freshwater that is released into James Bay being exported from the Hudson Bay system within 4 years (Ridenour et al., 2019), there is time for the ambient salinity to have adjusted to changes in river discharge or the sea-ice cycle that occurred over the period 1980-2012. The salinity of waters entering James Bay from Hudson Bay may have varied during these three decades, as well, because there have been fluctuations in the Arctic freshwater flux (cf., Yang et al., 2016). We have the best opportunity of reconstructing the locally driven changes because of the well-documented changes in the La Grande plume itself, which has been a topic of great interest within the local communities who are directly impacted by the changes.

Comparing the RW content and nutrient stocks of the surface layer pre- vs. post-development (Figure 3.10), it is clear that the major driver of change in N and P stocks is the vastly increased RW content in the winter surface layer. The higher base salinity in the pre-development period would tend to lead us to *overestimate* the RW content at that time; thus the increase in RW content in the surface layer post-development may be larger than that implied by the stocks in Figure 3.10.

The change in RW (and thus also N and P) content of the surface layer is due to the augmented flows associated with river development/regulation *in combination with* the

presence of landfast ice cover. Because of the lack of wind mixing, under-ice river plumes including the winter plume of the La Grande tend to be much larger and more strongly stratified than open-water plumes for equivalent discharge (Ingram and Larouche, 1987; Li and Ingram, 2007). Changes in river discharge that affect coastal areas during the period of ice cover have amplified effects on nutrient dynamics because of the way the river water is retained under the ice and near the coast with relatively little mixing with ambient seawater. This conclusion is important to keep in mind because other recent works have emphasized the importance of the altered nutrient composition of river water following damming (Maavara et al., 2020). Maavara and co-workers reported that altered reservoir cycling of nutrients alters the NP ratios in regulated river runoff and potentially increases P limitation in coastal waters. Our data show increased NP ratios in La Grande River following development. However, the altered nutrient ratios in the river water play a minor role in modifying coastal nutrient dynamics relative to the effects of increasing river discharge during the ice-covered period. Ultimately, the disposition of the river plume along the coast, which is dictated by season (i.e. ice cover, open water), together with river discharge, constrains the way nutrient stocks are utilized and/or cycled. The impact of the La Grande plume on nutrient dynamics is more a hydrographic phenomenon than a product of altered reservoir biogeochemistry.

During winter, the high flows along with reduced mixing under the ice cover lead to the development of a large, highly stratified plume, which is much larger today ($\geq$ 1200 km^2) than it was under the natural winter flow conditions of the 1970s (~200 km^2; Ingram and Larouche 1987; Peck et al., submitted), and resultantly increased RW content captured in the sea ice in this plume region. Our data show that riverine nutrient supply dominates the

nutrient stocks within the fresh surface layer that extends across this region. The surface layer has high nitrate and silicate/low phosphate conditions with phosphate being the nutrient in lowest supply. We conclude that the development has led to a larger area of potential phosphate limitation of primary production in late winter, assuming light penetrates under the ice cover enough for photosynthetic activity at that time of year, and that primary production distribution is not affected by low surface salinity itself and the physical structure of the overlying ice (cf., Gosselin et al., 1985, 1986). After a residence time of a few weeks, the large nitrate stocks that characterize the plume presumably would be exported from NE James Bay into southern Hudson Bay and possibly augmenting primary production in some downstream area.

Although we do not have data for spring, either pre- or post-development, we speculate that the calculated expected nutrient stocks for late winter under current conditions (Figure 3.9) might more represent the stocks that used to occur in spring when there was a natural spring freshet. In the past, under a natural flow regime, the present winter mode (i.e., river-dominated nitrate supply) would have existed during spring, being initiated by the high spring freshet river flows and lasting until ice breakup, which is typically sometime in late May or early June (Taha et al., 2019). In 2016-2017, the late winter (March-April) discharge averaged ~3900-4600 $m^3 s^{-1}$, which is quite similar to June discharge with natural conditions in 1975-1977 (3800 $m^3 s^{-1}$) and in the upper part of the range of freshet flows for 1960-1978 (2400-6100 $m^3 s^{-1}$; Messier et al., 1986). These discharge measurements emphasize the comparability of the pre-development freshet and the present day winter period. Thus, the large nitrate stocks that we presently see in late winter presumably used to occur in late May, when spring freshet occurred. So little light is available under the sea-ice cover (Ehn, pers.

comm.) that it can be assumed the growing period for phytoplankton begins only after the ice retreats. This would be expected to closely follow spring freshet as it is synced to the landfast ice breakup in James Bay (Taha et al., 2019). Thus, we propose that the start of the growing season along the NEJB coast would have been characterized by nutrient replete conditions in the past but is now characterized by strongly nitrate-limited conditions because the peak flows have been shifted to be out of sync with the retreat of the ice. All else being equal, rooted vascular plants like eelgrass that can access sedimentary nutrient stores should have the competitive advantage relative to phytoplankton under the present-day spring nutrient regime. However, if eelgrass cannot access sediment nutrient stores (or these stores are not present), or if nutrient competition is heightened by heterotrophic bacterial uptake enhanced by warmer water temperatures, then nutrient limitation of eelgrass right at the start of the growing season could also arise. Spring nutrient stocks should be assessed together with sedimentary nutrient supply to eelgrass.

The larger ROFI, wherein the surface layer contains a mixture of river and sea water, surrounding the highly stratified region of the under-ice plume has also increased in area with the increase in winter river discharge (Ingram and Larouche 1987; Peck et al., submitted). For example, the area within the salinity 20 isohaline measured about 800 km^2 in 1976 under winter flows of 460 m^3s^{-1} and > 2300 km^2 in 1984 under winter flows of 3000 m^3s^{-1}. Our data show that late winter stocks of nutrients in this region of freshwater influence originate from a combination of river water and seawater, that nitrate is the nutrient in lowest supply, and that the late winter stock of nitrate has increased compared to pre-development conditions because of an increased stock of nitrate that is RW-derived. If the photosynthetic activity of ice algae is N-limited in the large ROFI in the NEJB coastal domain, then additional RW

would support increased production by the ice algal community during late winter post-development, as these algae are well adapted to low light conditions and thrive with ice cover (Michel et al., 1988; 1996). The larger nitrate stock we observe presently may support up to two times more primary production in the late winter period during the period when the river flows remain very high. This is to say if light is not the limiting factor in primary production at this time, as is observed in areas that experience ice-cover (Tremblay and Gagnon, 2009).

For the summer period, the implications of development for primary production follow from the discharge being lower than under natural conditions. Nitrate is the nutrient in lowest supply (except for a small area at the river mouth) and dominated by marine SW supply. Lacking summer nutrient data from the 1970s, we can only speculate that the lower salinity of the marine source waters at the present time may be tied to lower nitrate concentrations in these source waters, as well. Thus, even with a more weakly stratified water column because of reduced river outflow, there may be weaker surface nitrate replenishment and lower primary production by microalgae. The conditions should give rooted vascular plant species like eelgrass a competitive advantage over species without an alternative nutrient supply.

3.5 Conclusions

In this study we have presented new tracer data (salinity and previously unmeasured $\delta^{18}O$) along with new data for nitrate, phosphate, and silicate, for the northeast James Bay coastal region. Seasonal and spatial differences of parameters in the different water types that make up the coastal water mass (RW, SW, and SIM) were identified and quantified. Fractions of the three water types were calculated using the seasonal sets of end members. La Grande was shown to be the dominant source of freshening along the coast, with SIM only

composing 10-15% of the summer ambient seawater. Ambient seawater in summer freshens considerably (maximum 22.45 from 25.61 in winter), which is most likely occurring on a bay-wide scale as opposed to being influenced by local SIM. Local SIM may account for some of this freshening at depth with mixing throughout the summer, however based on the short residence time of waters in this area during summer, it is not likely that any local SIM has remained by the time of sampling even in deep waters as the water column is thoroughly mixed. This seasonal freshening has been observed as far back as the 1970s, implying that the water that enters James Bay in the west is freshened considerably (from ~30 to 25) by summer, and freshens further, to 23, by the time water circulates and exits in the east (Prinsenberg, 1984).

The drivers and fate of nutrient supply in these coastal waters are dependent upon the seasonality of the sea-ice cycle as well as the regulated discharge of La Grande. In winter, the La Grande plume dominates nutrient conditions within its extent, where nitrate concentrations and associated stocks are higher than that supplied by the ambient seawater. Nitrate, phosphate and even silicate to a degree, demonstrate conservative mixing in winter, but in summer there is a departure from these trends due to water mass mixing, and nutrient uptake from the increase in primary production, expected during the open water season.

The determination of limiting nutrients reflects the shift in this estuarine like area between the riverine and coastal water mass domains, where phosphate is limiting primary production in the lower salinity (< 10) waters, and nitrate is limiting in the more saline waters. Silicate is always in excess when compared to nitrate and phosphate, thereby asserting nitrate as the limiting nutrient in this region when salinity > 10.

With the six selected offshore sites along the coast, representing the latitudinal extent of our study area, we are able to further identify that La Grande River has a drastic impact on nutrient stocks during winter. Nitrate stocks are nearly double in winter than those seen in summer, and phosphate stocks, which are mainly controlled by the SW component, are lowest in winter when the plume extends over almost the entire region.

With regulation of La Grande, the conditions observed in winter currently are comparable, discharge-wise, to the natural spring freshet, and current summer, likewise with natural winter conditions. This shifting of the nutrient supply, which is impacted differently throughout the sea-ice cycle, carries significant implications for production (including species and community composition, timing of blooms) in the NEJB coastal region. The overall degree of dominance between La Grande inflow and ambient James Bay seawater has changed historically, and seasonally, which has impacted the overall nutrient regime of the region, and as discussed, the primary production it supports.

References

Anderson, J. T., & Roff, J. C. (1980). Seston Ecology of the Surface Waters of Hudson Bay. Canadian Journal of Fisheries and Aquatic Sciences, 37(12), 2242–2253. https://doi.org/10.1139/f80-269

Andrews, J., Babb, D., & Barber, D. G. (2018). Climate change and sea ice: Shipping in Hudson Bay, Hudson Strait, and Foxe Basin (1980–2016). Elem Sci Anth, 6(1), 19. https://doi.org/10.1525/elementa.281

Ardyna, M., Mundy, C. J., Mills, M. M., Oziel, L., Lacour, L., Verin, G., … Raimbault, P. (2020). Environmental drivers of under-ice phytoplankton bloom dynamics in the Arctic Ocean. Elementa Science of the Anthropocene, 8(30), 1–21.

Barber, D. G., Harasyn, M. L., Babb, D. G., Capelle, D., McCullough, G., Dalman, L. A., … Sydor, K. (2021). Sediment-laden sea ice in southern Hudson Bay: Entrainment, transport, and biogeochemical implications. Elementa: Science of the Anthropocene, 9(1). https://doi.org/10.1525/elementa.2020.00108

Brand, U., Came, R. E., Affek, H., Azmy, K., Mooi, R., & Layton, K. (2014). Climate-forced change in Hudson Bay seawater composition and temperature, Arctic Canada. Chemical Geology, 388, 78–86. https://doi.org/10.1016/j.chemgeo.2014.08.028

Brzezinski, M. A. (1985). The Si:C:N ratio of marine diatoms: Interspecific variability and the effect of some environmental variables. Journal of Phycology, 21, 347–357.

Burt, W.J., Thomas, H., Miller, L., Granskog, M., Papakyriakou, T.N., et al. 2016. Inorganic Carbon Cycling and Biogeochemical Processes in an Arctic Inland Sea (Hudson Bay). Biogeosciences 13(16): 4659-4671. doi:10.5194/bg-13-4659-2016.

Cooper, L. W., McClelland, J. W., Holmes, R. M., Raymond, P. A., Gibson, J. J., Guay, C. K., & Peterson, B. J. (2008). Flow-weighted values of runoff tracers (δ18O, DOC, Ba, alkalinity) from the six largest Arctic rivers. Geophysical Research Letters, 35(18), 3–7. https://doi.org/10.1029/2008GL035007

Curtis S, Allen L. 1976. The Waterfowl Ecology of the Quebec Coast of James Bay. Canadian Wildlife Service: 72.

Déry, S. J., Mlynowski, T. J., Hernández-Henríquez, M. A., & Straneo, F. (2011). Interannual variability and interdecadal trends in hudson bay streamflow. Journal of Marine Systems, 88(3), 341–351. https://doi.org/10.1016/j.jmarsys.2010.12.002

Déry, S. J., Stadnyk, T. A., MacDonald, M. K., & Gauli-Sharma, B. (2016). Recent trends and variability in river discharge across northern Canada. Hydrology and Earth System Sciences, 20(12), 4801–4818. https://doi.org/10.5194/hess-20-4801-2016

Duarte, C. (1990). Seagrass nutrient content. Marine Ecology Progress Series, 67(2), 201–207. https://doi.org/10.3354/meps067201

Eastwood, R. A., Macdonald, R. W., Ehn, J. K., Heath, J., Arragutainaq, L., Myers, P. G., … Kuzyk, Z. A. (2020). Role of River Runoff and Sea Ice Brine Rejection in Controlling Stratification Throughout Winter in Southeast Hudson Bay. Estuaries and Coasts, 43(4), 756–786. https://doi.org/10.1007/s12237-020-00698-0

Etkin, D. A. (1991). Break-up in Hudson Bay: Its sensitivity to air temperatures and implications for climate warming. Climatological Bulletin 25(1): 21-34.

Ferland, J., Gosselin, M., & Starr, M. (2011). Environmental control of summer primary production in the hudson bay system: The role of stratification. Journal of Marine Systems, 88(3), 385–400. https://doi.org/10.1016/j.jmarsys.2011.03.015

Galbraith, P. S., & Larouche, P. (2011). Sea-surface temperature in Hudson Bay and Hudson Strait in relation to air temperature and ice cover breakup, 1985-2009. Journal of Marine Systems, 88(3), 463–475. https://doi.org/10.1016/j.jmarsys.2011.06.006

Gosselin, M., Legendre, L., Demers, S., & Ingram, R. G. (1985). Responses of Sea-Ice Microalgae to Climatic and Fortnightly Tidal Energy Inputs (Manitounuk Sound, Hudson Bay). Canadian Journal of Fisheries and Aquatic Sciences, 42(5), 999–1006. https://doi.org/10.1139/f85-125

Gosselin, M., Legendre, L., Therriault, J.-C., Demers, S., & Rochet, M. (1986). Physical control of the horizontal patchiness of sea-ice microalgae. Marine Ecology Progress Series, 29, 289–298. https://doi.org/10.3354/meps029289

Grainger, E. H. (Fisheries and M. S.), & McSween, S. (Fisheries and M. S.). (1976). Marine zooplankton and some physical-chemical features of James Bay related to La Grande hydro-electric development. Ste. Anne de Bellevue, QC.

Granskog, M. A., Kuzyk, Z. Z. A., Azetsu-Scott, K., & Macdonald, R. W. (2011). Distributions of runoff, sea-ice melt and brine using δ18o and salinity data - a new view on freshwater cycling in hudson bay. Journal of Marine Systems, 88(3), 362–374. https://doi.org/10.1016/j.jmarsys.2011.03.011

Hernández-Henríquez, M. A., Mlynowski, T. J., & Déry, S. J. (2010). Reconstructing the Natural Streamflow of a Regulated River: A Case Study of La Grande Rivière, Québec, Canada. Canadian Water Resources Journal, 35(3), 301–316. https://doi.org/10.4296/cwrj3503301

Hochheim, K. P., & Barber, D. G. (2010). Atmospheric forcing of sea ice in Hudson Bay during the fall period, 1980-2005. Journal of Geophysical Research: Oceans, 115(5), 1–20. https://doi.org/10.1029/2009JC005334

Hochheim, K., & Barber, D. (2014). An update on the ice climatology of the Hudson Bay system. Arctic, Antarctic, and Alpine Research, 46(1), 66–83. https://doi.org/10.1657/1938-4246-46.1.66

Holmes, R. M., McClelland, J. W., Peterson, B. J., Tank, S. E., Bulygina, E., Eglinton, T. I., … Zimov, S. A. (2012). Seasonal and Annual Fluxes of Nutrients and Organic Matter from Large Rivers to the Arctic Ocean and Surrounding Seas. Estuaries and Coasts, 35(2), 369–382. https://doi.org/10.1007/s12237-011-9386-6

Hudon, C., Morin, R., Bunch, J., & Harland, R. (1996). Carbon and nutrient output from the Great Whale River (Hudson Bay) and a comparison with other rivers around Quebec. Canadian Journal of Fisheries and Aquatic Sciences, 53(7), 1513–1525. https://doi.org/10.1139/f96-080

Ingram, R. G., & Larouche, P. (1987). Changes in the under-ice characteristics of la grande rivière plume due to discharge variations. Atmosphere - Ocean, 25(3), 242–250. https://doi.org/10.1080/07055900.1987.9649273

Ingram, R. G., Wang, J., Lin, C., Legendre, L., & Fortier, L. (1996). Impact of freshwater on a subarctic coastal ecosystem under seasonal sea ice (southeastern Hudson Bay, Canada). I. Interannual variability and predicted global warming influence on river plume dynamics and sea ice. Journal of Marine Systems, 7(2–4), 221–231. https://doi.org/10.1016/0924-7963(95)00006-2

Kuzyk, Z. A., Macdonald, R. W., Granskog, M. A., Scharien, R. K., Galley, R. J., Michel, C., … Stern, G. (2008). Sea ice, hydrological, and biological processes in the Churchill River estuary region, Hudson Bay. Estuarine, Coastal and Shelf Science, 77(3), 369–384. https://doi.org/10.1016/j.ecss.2007.09.030

Kuzyk, Z. Z. A., Macdonald, R. W., Tremblay, J. É., & Stern, G. A. (2010). Elemental and stable isotopic constraints on river influence and patterns of nitrogen cycling and biological productivity in Hudson Bay. Continental Shelf Research, 30(2), 163–176. https://doi.org/10.1016/j.csr.2009.10.014

Lalumière, R., Messier, D., Fournier, J. J., & Peter McRoy, C. (1994). Eelgrass meadows in a low arctic environment, the northeast coast of James Bay, Québec. Aquatic Botany, 47(3–4), 303–315. https://doi.org/10.1016/0304-3770(94)90060-4

Landy, J. C., Ehn, J. K., Babb, D. G., Thériault, N., & Barber, D. G. (2017). Sea ice thickness in the Eastern Canadian Arctic: Hudson Bay Complex & Baffin Bay. Remote Sensing of Environment, 200(August), 281–294. https://doi.org/10.1016/j.rse.2017.08.019

Lapoussière, A., Michel, C., Gosselin, M., Poulin, M., Martin, J., & Tremblay, J. É. (2013). Primary production and sinking export during fall in the Hudson Bay system, Canada. Continental Shelf Research, 52, 62–72. https://doi.org/10.1016/j.csr.2012.10.013

Le Fouest, V., Babin, M., & Tremblay, J. E. (2013). The fate of riverine nutrients on Arctic shelves. Biogeosciences, 10(6), 3661–3677. https://doi.org/10.5194/bg-10-3661-2013

Li, S. S., Ingram, R. G. (2007). Isopycnal deepening of an under-ice river plume in coastal waters: Field observations and modeling. Journal of Geophysical Research: Oceans 112(C7). doi:https://doi.org/10.1029/2006JC003883.

Maavara T, Akbarzadeh Z, Van Cappellen P. (2020). Global Dam-Driven Changes to Riverine N:P:Si Ratios Delivered to the Coastal Ocean. Geophys Res Lett 47(15): e2020GL088288. doi:https://doi.org/10.1029/2020GL088288

Macdonald, R. W., Wong, C. S., & Erickson, P. E. (1987). The distribution of nutrients in the southeastern Beaufort Sea: Implications for water circulation and primary production. Journal of Geophysical Research: Oceans, 92(C3), 2939–2952. https://doi.org/10.1029/JC092iC03p02939

Macdonald, R. W., D. W. Paton, and E. C. Carmack (1995), The freshwater budget and underice spreading of Mackenzie River water in the Canadian Beaufort Sea based on

salinityand 18O/16O measurements in water and ice, Journal of Geophysical Research, 100(C1), 895-919.

Matthes, L. C., et al. (2021), Environmental drivers of spring primary production in Hudson Bay, Elementa: Science of the Anthropocene, 9(1), doi:10.1525/elementa.2020.00160.

de Melo, M.L., M.-L. Gérardin, C. Fink-Mercier, and P.A. del Giorgio. 2022. Patterns in riverine carbon, nutrient and suspended solids export to the Eastern James Bay: links to climate, hydrology and landscape features. *Biogeochemistry*: In review.

Messier D, Ingram RG, Roy D. (1986). Chapter 20: Physical and biological modifications in response to La Grande hydroelectric complex. Elsevier Oceanography Series 44:403-424.

Messier D, Lepage S, de Margerie S. (1989). Influence du couvert de glace sur l'étendue du panache de La Grande Rivière (baie James). Arctic 42(3): 278-284.

Michel, C., L. Legendre, S. Demers, J.-C. Therriault. (1988). Photoadaptation of sea-ice microalgae in springtime: photosynthesis and carboxylating enzymes. Mar. Ecol. Prog. Ser. 50: 177-185.

Michel, C., L. Legendre, R.G. Ingram, M. Gosselin, M. Levasseur. (1996). Carbon budget of ice algae under first-year ice: evidence of a significant transfer to zooplankton grazers. J. Geophys. Res. 101: 18,345 -18,360.

Östlund, H. G., & Hut, G. (1984). Arctic ocean water mass balance from isotope data. Journal of Geophysical Research, 89(4), 6373–6381.

Pavlov, A. K., Stedmon, C. A., Semushin, A. V., Martma, T., Ivanov, B. V., Kowalczuk, P., & Granskog, M. A. (2016). Linkages between the circulation and distribution of dissolved organic matter in the White Sea, Arctic Ocean. Continental Shelf Research, 119, 1–13. https://doi.org/10.1016/j.csr.2016.03.004

Peck, C. J., Kuzyk, Z. Z. A., Heath, J. P., Lameboy, J., Ehn, J. K. (submitted). Under-ice hydrography of the La Grande River plume in relation to a ten-fold increase in wintertime discharge.

Prinsenberg, S. J. (1984). Freshwater contents and heat budgets of James Bay and Hudson Bay. Continental Shelf Research, 3(2), 191–200. https://doi.org/10.1016/0278-4343(84)90007-4

Prinsenberg, S. J. (1988). Ice-Cover and Ice-Ridge Contributions to the Freshwater Contents of Hudson Bay and Foxe Basin. Arctic, 41(1), 6–11.

Redfield, A. C. (1958). The biological control of chemical factors in the environment. American Scientist, 46(3), 205–221. Retrieved from https://www-jstor-

org.uml.idm.oclc.org/stable/pdf/27827150.pdf?refreqid=excelsior%3Af11611d1b19a1553954ceaab2c8b383c

Ridenour, N. A., Hu, X., Jafarikhasragh, S., Landy, J. C., Lukovich, J. V., Stadnyk, T. A., … Barber, D. G. (2019). Sensitivity of freshwater dynamics to ocean model resolution and river discharge forcing in the Hudson Bay Complex. Journal of Marine Systems, 196(May), 48–64. https://doi.org/10.1016/j.jmarsys.2019.04.002

Roff, J. C., & Legendre, L. (1986). Physico-chemical and biological oceanography of hudson bay. In I. P. Martini (Ed.), Elsevier Oceanography Series (Vol. 44, pp. 265–292). New York: Elsevier Science Publishers. https://doi.org/10.1016/S0422-9894(08)70907-3

Saucier, F.J., Senneville, S., Prinsenberg, S., Roy, F., Smith, G., Gachon, P., Caya, D., Laprise, R. (2004). Modelling the sea ice–ocean seasonal cycle in Hudson Bay, Foxe Basin and Hudson Strait, Canada. Climate Dynamics 23, 303–326.

Sundby, B., Gobeil, C., Silverberg, N., & Mucci, A. (1992). The phosphorus cycle in coastal marine sediments. Limnology and Oceanography, 37(6), 31–75. Retrieved from http://www.jstor.org/stable/30001658

Taha, W., Bonneau-Lefebvre, M., Cueto Bergner, A., & Tremblay, A. (2019). Evolution From Past to Future Conditions of Fast Ice Coverage in James Bay. Frontiers in Earth Science, 7(October), 1–20. https://doi.org/10.3389/feart.2019.00254

Tan, F. C., & Strain, P. M. (1980). The distribution of sea ice meltwater in the eastern Canadian Arctic. Journal of Geophysical Research, 85(C4), 1925–1932. https://doi.org/10.1029/jc085ic04p01925

Tremblay, J.-É., & Gagnon, J. (2009). The effects of irradiance and nutrient supply on the productivity of Arctic waters: a perspective on climate change. In J. C. J. Nihoul & A. G. Kostianoy (Eds.), Influence of Climate Change on the Changing Arctic and Sub-Arctic Conditions (pp. 73–89). Springer.

Tremblay, J. É., Simpson, K., Martin, J., Miller, L., Gratton, Y., Barber, D., & Price, N. M. (2008). Vertical stability and the annual dynamics of nutrients and chlorophyll fluorescence in the coastal, southeast Beaufort Sea. Journal of Geophysical Research: Oceans, 113(7), 1–14. https://doi.org/10.1029/2007JC004547

Tremblay, J. É., Anderson, L. G., Matrai, P., Coupel, P., Bélanger, S., Michel, C., & Reigstad, M. (2015). Global and regional drivers of nutrient supply, primary production and CO2 drawdown in the changing Arctic Ocean. Progress in Oceanography, 139, 171–196. https://doi.org/10.1016/j.pocean.2015.08.009

van Raaphorst, W., & Kloosterhuis, H. T. (1994). Phosphate sorption in superficial intertidal sediments. Marine Chemistry, 48(1), 1–16. https://doi.org/10.1016/0304-4203(94)90058-2

Yang Q, Dixon TH, Myers PG, Bonin J, Chambers D, et al. 2016. Recent increases in Arctic freshwater flux affects Labrador Sea convection and Atlantic overturning circulation. Nature Communications 7(1): 10525. doi:10.1038/ncomms10525.

4.0 Winter nutrient distributions and freshwater relationships in northwest and southeast costal regions of Hudson Bay

Abstract

Hudson Bay is the largest inland sea in North America, and despite the increasing interest in oceanographic studies here over the past two decades, the Hudson Bay Riverine Coastal Domain (RCD) is still poorly understood, especially in winter. In recent decades, these areas have experienced atypical ice conditions, along with an overall shortening of the sea-ice season, and trends of increasing riverine discharge. The two coastal regions that are the focus of this study are northwest Hudson Bay (NWHB), encompassing the sub-regions of Repulse Bay/Naujaat and Chesterfield Inlet, and southeast Hudson Bay (SEHB), encompassing the sub-regions of Sanikiluaq, Kuujuaraapik, Umiujaq, and Inukjuak. We present new nutrient and freshwater tracer data for water samples collected during ice-covered conditions for both NWHB and SEHB. We examine the oxygen isotope ratio – salinity relationship within each region and sub-region to identify the dominant sources of freshwater and then compare the nutrient concentrations and ratios and determine how sea-ice and river water influence the nutrient regime. Our aim is to test the hypothesis that, despite having the same source seawater, excess river water in winter in coastal SEHB leads to more limited nutrient recharge compared to the ice-dominated NWHB, which was recently identified as a productive hotspot in spring. The winter SEHB coastal water mass is largely influenced by riverine input from local rivers (Great Whale River and the Nastapoca River), but also from the "upstream" James Bay outlet and has an average salinity of 26. Our findings show that although the freshwater budget in NWHB is generally brine-dominated in winter, the waters do not experience stronger nutrient recharge in terms of maximum nutrient

concentrations than SEHB. In both areas, nitrate concentrations did not exceed 5 μM during winter and phosphate concentrations averaged 1 μM. Despite much more river water in SEHB in winter, and evidence that river inflow was supplying silicate, the concentrations in coastal waters in winter were similar between regions. Only during a single sampling event in February 2019 was a nutrient-rich water mass observed along the NWHB coast in winter. Based on its properties - isotopically depleted (-2.1‰), rich in phosphate (1.2 μM), and poor in nitrate (3.6 μM), we infer that river water-rich Hudson Bay outflow, and nitrogen-poor as a result of denitrification, re-circulated into NWHB. A similar water mass was not detected in SEHB despite a larger data set. We suspect the signal originated in southern Hudson Strait based on previous observations of a P-rich/N-poor water mass in this area. Similar high phosphate concentrations were observed in the 1960s in NWHB but accompanied by higher nitrate concentrations. This study overall, demonstrates the properties of two regions of the Hudson Bay RCD and how sea-ice and river water may interact to influence the distribution of nutrients, while also identifying unusual nutrient concentrations in NWHB.

4.1 Introduction

The shallow Arctic Riverine Coastal Domain (RCD) remains a critical gap in our understanding of Arctic ecosystems (Macdonald, 2000; Carmack et al., 2015). Despite the RCD being a contiguous feature, serving as a means of transportation for riverine discharge, similar in function to a conveyor belt through Arctic and subarctic coastal regions, local point-source river outlets contribute to spatial variation in RCD properties. This spatial variability is accompanied by large seasonal variability due to the strong seasonality of northern river discharge as well as the seasonal sea-ice cycle, which withdraws freshwater from the ocean surface when it forms and releases freshwater when (and where) it melts. The

sea-ice formation process can even lead to river water being transported with brine, when it is ejected during formation, down to great water depths, if riverine water is present under the ice cover (cf., Granskog et al., 2011). In addition to the freshwater distribution dynamics of freezing and melting sea ice, landfast ice cover modifies how river water is dispersed and incorporated in the coastal domain (cf., Macdonald et al., 1995; Kuzyk et al., 2008). In the RCD river runoff may not always be the main contributor to variations in freshwater distribution, rather, in places where river runoff is relatively minor, variations may be caused by the formation and melt of ice, or by changes in the freshwater content of source seawater.

The importance of broader oceanographic setting on determining properties in the RCD also cannot be ignored. Well-studied RCDs such as the Mackenzie Estuary along the Arctic Ocean (Macdonald et al., 1987; Carmack and Macdonald, 2002; Simpson et al., 2008) and the Great Whale River in southeast Hudson Bay (Hudon et al., 1996; Ingram et al., 1996; Li and Ingram, 2007) differ in ways that reflect their vastly different oceanographic and ice regimes. Differences among the characteristics of inflow shelves, outflow shelves, and interior shelves of the Arctic Ocean described in previous literature (Carmack and Wassman, 2006) presumably also may underlie differences observed in RCDs. For example, in the Arctic Ocean and its surrounding seas, Pacific-origin seawater contains a much larger freshwater component than seawater of Atlantic origin so the balance of these two sources may produce the largest seasonal and inter-annual variations in freshwater content (Jones et al., 1998). In other places, it is the combination of local and imported (advected) sea ice meltwater that determines the freshwater quantity and distribution (Tan and Strain, 1996).

Within the RCD, freshwater contributes to a coastal boundary current that is of key importance for physical and chemical processes such as estuarine-like nutrient resupply to

surface waters (cf., Kuzyk et al., 2010). River runoff (but not sea-ice melt) introduces new nutrients and organic matter that stimulate new primary production in coastal waters (Le Fouest et al., 2013). While the direct input of nutrients from river water tends to be lower than the inputs of marine nutrients for shelves and basin areas, they can be significant for coastal waters and estuaries (Bluteau et al., 2021). How freshwater is processed in the RCD (e.g., how long it is held there, the timing and location of its release, and how it is mixed) particularly during the ice-covered season that is complicated by river water-ice interactions (cf., Kasper and Weingartner, 2015), has important implications for shelf and basin processes. In offshore areas, freshwater introduced at the surface of the ocean increases the strength of vertical stratification, which decreases mixing and reduces, for example, surface nutrient renewal. Freshwater delivery by coastal currents has been investigated as an important factor influencing stratification, winter mixing depths, and surface nutrient renewal (Dmitrenko et al., 2005; Steele et al. 2010; Peralta-Ferriz and Woodgate, 2015; Woodgate and Peralta-Ferriz, 2021). It is also thought that through sensitive interactions and climate feedbacks, the Arctic RCD is a focal point for climate-driven change yet it is still among the most difficult areas to represent in models.

In this study, we use new observations of coastal ocean water properties collected during the ice-covered season over a number of years (2016-present) to attempt to synthesize a regional-scale perspective of the coastal oceanography of Hudson Bay. We focus on two sub-regions in northwest Hudson Bay (NWHB) and four sub-regions in southeast Hudson Bay (SEHB) where sampling was achieved through community-based research partnerships. Sub-regions are labeled according to the community/area within each of the two regions, but in our study, each sub-region refers to the general coastal area where sampling and scientific

work was conducted. The data set consists of conductivity-temperature-depth (CTD) profile data, measurements of salinity and the freshwater tracer $\delta^{18}O$ (oxygen isotope ratios of seawater), and dissolved nutrients: nitrate, phosphate, and silicic acid (hereafter silicate). Assuming the localities represent the average conditions of the RCD and its variability in the two regions of interest (NWHB and SEHB; Figure 4.1), we examine the data to test the hypothesis that *the coastal water masses in these two regions, despite common source seawater, have divergent freshwater and nutrient properties because of regional differences in the dominance of sea-ice formation (which withdraws freshwater) vs. freshwater addition by river runoff and sea-ice melt.*

Although there are numerous Cree and Inuit communities along the coast of Hudson Bay where community members have observed environmental changes during recent decades (MacDonald et al., 1997), observations of coastal water properties are extremely scarce and especially during the ice-covered season. A few notable exceptions are the studies of the physics, chemistry and biology of the Great Whale River estuary (Legendre et al., 1981; Gosselin et al., 1985; Ingram et al 1996 and references therein) and the studies in the La Grande River area in northeast James Bay pre-hydroelectric development (Prinsenberg, 1982 and references therein; Messier et al., 1986) and recent work (first chapter of this thesis, Peck et al., submitted). Individual studies have examined the winter oceanography of the Churchill estuary area (Kuzyk et al., 2008), the Nelson estuary area (Kazmiruk et al., 2021), and the Belcher Islands area (Eastwood et al. 2020).

4.2 Study area

Hudson Bay is a large, inland sea with diverse coastal environments (Ingram and Prinsenberg, 1998). Northwest Hudson Bay (NWHB) receives cold inflowing Arctic-derived

waters from Foxe Basin and Hudson Strait. There are various inlets and bays that develop stable landfast ice cover but the 'Kivalliq Polynya' (Bruneau et al. 2021), a persistent lead consisting of open water and broken ice, known in this region as an "ice factory", extends from Roes Welcome Sound (Dmitrenko et al., 2021) southward along the northwest coast (Figure 4.1). Most streams are fully frozen by late winter and the only sizable river is the one that drains Baker Lake and discharges at Chesterfield Inlet. Southeast Hudson Bay (SEHB) represents an entirely different ecoregion, considered similar to James Bay (Stewart and Lockhart, 2005). The majority of Hudson Bay's river runoff is discharged along the south coast of the bay and in James Bay (Déry et al. 2011; 2016) with cyclonic circulation carrying the runoff eastward, producing large stocks of river water in summer in SEHB (Granskog et al., 2011; Burt et al., 2016). Even during winter, this region receives river-water rich outflow from James Bay, which maintains shallow stratification southeast of the Belcher Islands throughout winter (Eastwood et al., 2020). Sea ice melt water also accumulates disproportionately compared to the amount of ice produced in SEHB (Granskog et al 2011; Eastwood et al 2020) because of the cyclonic water circulation and the eastward and southward drift of sea ice throughout winter (Landy et al. 2017; Barber et al. 2021).

4.2.1 Northwest Hudson Bay

In coastal northwest Hudson Bay, we focused our observations in two locations: Naujaat (formerly Repulse Bay, and labeled as RB in this study) and Chesterfield Inlet (CI) (Figure 4.1), both in the Kivalliq region of Nunavut. This northwestern region is known to have high biodiversity and is home to large populations of marine animals such as whales, walrus, seals, birds, and polar bears (Stirling, 1997; Gaston et al., 2007). A recent study

found high primary production in this region in spring, which was attributed in part to nutrient-rich conditions (Matthes et al., 2021).

Naujaat is an Inuit hamlet located on the Arctic Circle, on the shore of Repulse Bay, a small bay with a surface area ~1700 km^2, where our sampling was conducted. The bathymetry is relatively deep, with a channel > 240 m that runs parallel to the southern shore of the bay, however the bathymetry has not been mapped in this area. Our sampling occurred during the winter period, as well as June 2019 when the melt period had just started (We distinguish this as "late winter"). This bay is fully ice-covered in winter, with the landfast ice extending southeast from the community of Naujaat towards Roes Welcome Sound, which is located between Southampton Island and the mainland (Figures 4.1 and 4.2a). Despite some previous oceanographic work conducted in northern Hudson Bay surrounding Southampton Island, and on the northeast coast (Roff and Legendre, 1986; Tan and Strain 1996, Harvey et al., 1997, Ferland et al., 2011; Lapoussiere et al., 2013), there have been no in depth studies conducted in the area surrounding Naujaat (RB).

Chesterfield Inlet is a long inlet (~200 km) extending westward to a large freshwater lake (Baker Lake). A multidisciplinary study was conducted in the inlet in summer 1978 (Budgell, 1976; Budgell, 1982) and a biological oceanographic study was conducted at a site about 40 km north of the hamlet of Chesterfield Inlet during February-April 1988 (Welch et al. 1985). During summer, the inlet is a partially mixed estuary. The entrance area where we sampled has complex bathymetry with maximum water depths of ~100 m. Tidal forcing is strong with current speeds reaching 2 m s^{-1} (Budgell, 1976; Budgell, 1982). Our sampling occurred during typical winter periods, when the inlet was fully ice-covered and the landfast ice extended eastward (offshore) for a distance of about 15 km from the community.

4.2.2 Southeast Hudson Bay

In southeast Hudson Bay (SEHB), we focused our observations in four locations or sub-regions: Sanikiluaq (SK), Kuujuaraapik (KJ), Umiujak (UM), and Inukjuak (IN), stretching between 55.1°N and 58.l7°N. Sanikiluaq is the only sub-region not located along the southeastern coast, but within the Belcher Islands. Sampling in this sub-region was conducted on both east and west sides of the Islands. The Nastapoka (near UM) and Great Whale (at KJ) Rivers are the two largest local riverine freshwater contributors to this coastal domain (with mean annual discharges of 8.0 km^3 and 19.8 km^3 respectively (Déry et al., 2011), not taking into consideration the riverine influence felt along this coast from James Bay outflow (Eastwood et al., 2020). The southeastern coastal areas encompassed in our study are relatively shallow, not greater than 100 m in depth. Sampling took place during typical winter periods (January-February, and March-April), when this area is fully covered with landfast ice, which extended offshore (westward) generally around 10 km from shore. Sampling stations were located no more than 9 km from shore in any of the four sub-regions. Much more work has been conducted in this region (Maestrini et al., 1986; Hudon et al., 1996; Ingram et al., 1996; Kuzyk et al., 2010; Granskog et al., 2011; Lapoussiere et al., 2013) in comparison to NWHB, however there still remain gaps in data collection during in the winter months.

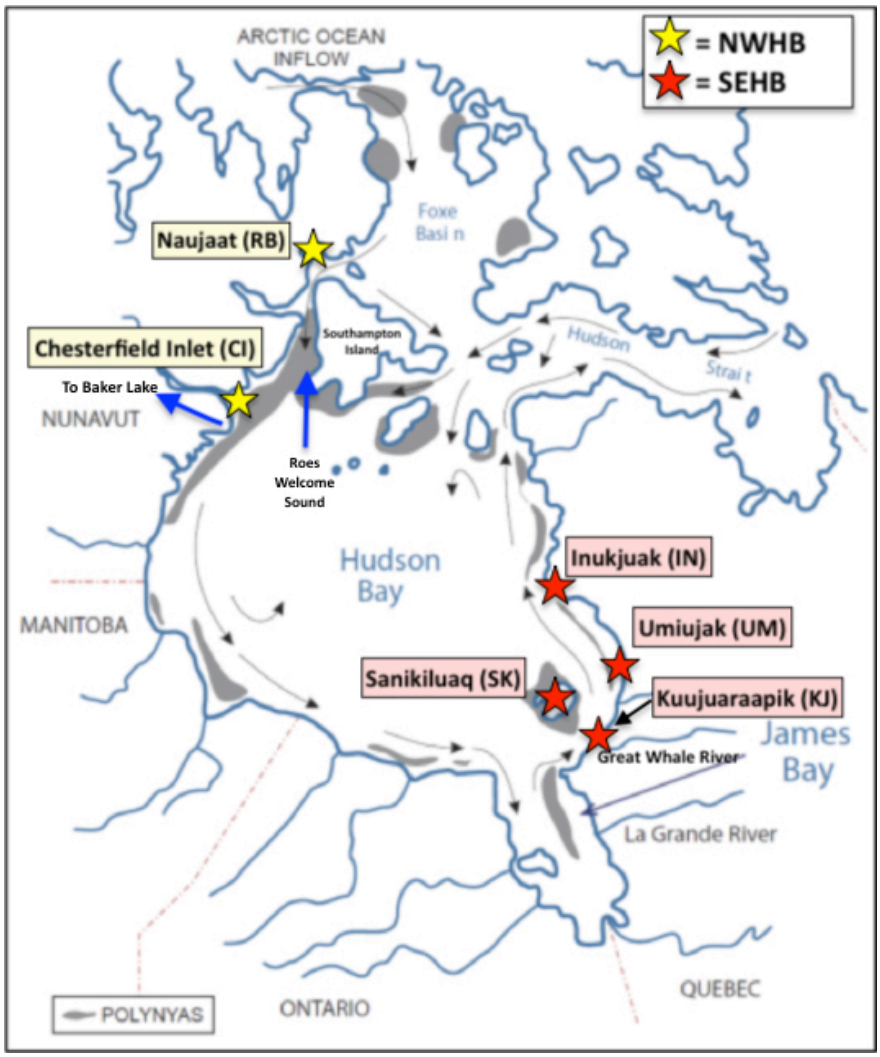

Figure 4.1 Map of the two coastal regions of this study (NWHB and SEHB), with sub-regions indicated by coloured stars. Grey shading indicates location of polynyas. Black arrows indicate the general circulation pattern of surface waters. Blue arrows show features of the region.

4.3 Methods

4.3.1 Sample Collection

All field sampling was done with the help of community research partners who contributed to study design as well as sampling efforts. Field sampling was done during two times of year representing early winter (January, February), and late winter into early spring (March-April for SEHB and May-June for NWHB, and for the purpose of this study will be

termed ‘late winter’) across both regions in the overall study area (Figure 4.2). An attempt to revisit the same location of stations was made, but ultimately depended on sea-ice extent from year to year. For example, the floe edge location in Repulse Bay varied seasonally and between the years of the study, so a station visited in 2018 may not have been accessible in 2019.

A total of four trips were taken for sampling in NWHB (two in 2018 and two in 2019) with ten stations visited in 2018 and seven stations in 2019 (Figure 4.2a, b). Sampling in Chesterfield Inlet (CI) took place during the two trips of 2018 but not in 2019. Sampling was accomplished at a total of seventeen sites in 2016 and thirty stations in 2017 in all sub-regions of SEHB across two sampling trips per year (early winter and late winter) (Figure 4.2c). The spatial distribution of sample sites was dictated by the extent and condition of the land fast ice during winter months as skidoos were used for transportation. NWHB stations for the most part were returned to during subsequent trips, with slight variance in latitude and longitude. Upon arrival at a site, a hole was drilled through the landfast ice with an auger, slush was cleared from the water and instruments were deployed through the hole. Once at a site, conductivity, temperature, depth (CTD) profiles were taken with either, but most often with both, an Idronaut Ocean Seven 304 Plus or a Sontek Castaway CTD in SEHB. In 2018 and 2019 (NWHB) these profiles were taken with either, or both the Castaway instrument by Sontek and an RBRconcerto^3. The Castaway CTD has a depth limit of 100 m. The accuracies of the Castaway results as stated by the manufacturer are ±0.05°C for temperature, 0.25% ± 5 µS/C for conductivity, and ±0.1 for salinity. The accuracies of the Idronaut instrument as stated by the manufacturer are ±0.002°C for temperature and ±0.003 mS/cm for conductivity.

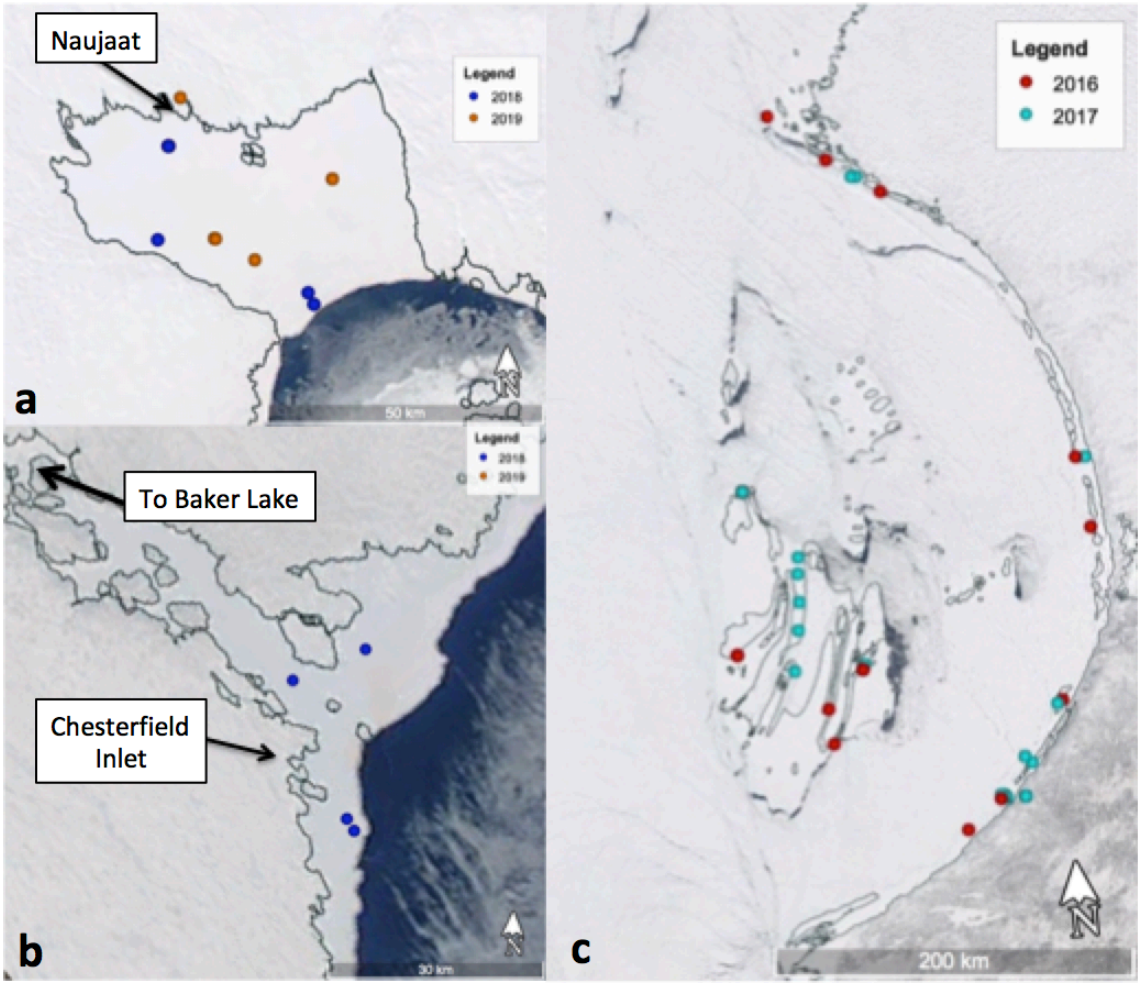

Figure 4.2 Distribution of sampling locations on the landfast sea ice in the vicinity of (a) Naujaat/Repulse Bay, (b) Chesterfield Inlet, and (c) SEHB communities. Some stations are replicated from year to year and are layered on top of each other. Approximate locations of the communities of Chesterfield Inlet and Naujaat are indicated.

The accuracies of the RBR as stated by the manufacturer are ±0.003 mS/cm for conductivity, ±0.002°C for temperature, and ±0.05% full scale for pressure (depth). Various depths in the water column were sampled at each site through the hole in the ice with the use of a Kemmerer water sampler, which was deployed with a pre-marked rope (in 1 m intervals). Specific depths that were sampled were decided while at a station based upon the bottom depth of the station and the halocline observed, if one was present, via the Castaway

CTD, which visualized the patterns immediately after deployment and retrieval. Surface (variable but generally 1-2 m from the bottom of the ice) and bottom samples (generally within 5 m of the bottom) were collected and samples above and below the halocline, if one was present at the site, and the site was deeper than 5 m. Water samples were collected and stored in brown–opaque Nalgene bottles which were prepared prior to water sampling by acid-washing them with 10% HCl, rinsing three times with MilliQ water, and letting dry completely overnight.

4.3.2 Sample Analysis

Water samples were subsampled from the Nalgene bottles in a temporary clean lab set up (where risk of contamination was minimized) within a few hours of being gathered in the field and generally within the hour after returning to the lab. The samples were preserved as necessary and brought back to the University of Manitoba. All samples were later analyzed in various university laboratories for parameters including nutrients (nitrate, phosphate, and silicate), salinity, and oxygen isotope ratio ($\delta^{18}O$). $\delta^{18}O$ samples were collected into new 20 mL scintillation vials with no headspace, tightly capped, and then sealed around the cap with parafilm, and stored at 4°C. The samples were analyzed at Ján Veizer Stable Isotope Laboratory (formerly GG Hatch) at the University of Ottawa using a Gasbench attached to a DeltaPlus XP isotope ratio mass spectrometer (ThermoFinnigan, Germany). Subsamples (0.6 mL) were pipetted into an Exetainer, and, together with internal standards, flushed with a gas mixture of 2% CO_2 in helium using the Gasbench. Exetainers were left to equilibrate at +25°C for 18 h minimum. Values are expressed in standard $\delta^{18}O$ notation with the V-SMOW (Vienna Standard Mean Seawater) as reference value and units expressed as per mille (‰). Analytical precision was ± 0.15‰. Salinity samples were

collected into new or otherwise triple-rinsed and dried 125 mL Boston Round glass bottles, tightly capped and then covered with parafilm around the cap. Salinity was measured using a Guildline Autosal 8400 salinometer with a precision better than 0.002 at the Marine Productivity laboratory at the Freshwater Institute (FWI) – Department of Fisheries and Oceans (DFO), Winnipeg. Samples were standardized against IAPSO Standard Sea Water. Nutrient samples were collected by filtering the water sample through a pre-combusted glass fiber filter (Whatman GF/F, 25 mm, nominal pore size 0.7 um) held in an acid-washed syringe style filter holder. The filtrate was collected in triplicate into 15 mL Sarstedt polypropylene vials that had been pre-cleaned for at least 8 hours in a 10% HCl acid bath. The vials were rinsed three times with the sample water, filled with 12-13 mL of filtered sample water, sealed, then frozen at -20°C. The concentrations of phosphate (PO_4^{3-}), nitrate and nitrite (NO_3^-, NO_2^-), and silicic acid ($Si(OH)_4$) were determined using a Bran and Luebbe Autoanalyzer III following standard colorimetric methods adapted from Hansen and Koroleff (2007) at Jean-Éric Tremblay's lab at the Université Laval, Québec. Nutrient analytical detection limits are 0.02 μM for NO_2^- , 0.03 μM for NO_3^-, 0.05 μM for PO_4^{3-}, and 0.1 μM for $Si(OH)_4$. Despite slow thawing, samples with salinity between 0 and ~10 had unusually low concentrations of silicic acid, which furthermore exhibited a positive linear relationship with salinity. We suspect that for the fresher samples (salinity ≤ 10), silicic acid was not properly recovered from frozen samples after thawing (c.f., Macdonald and McLaughlin, 1982). All silicate values reported for samples with salinity ≤ 10 were subsequently removed from the dataset. Eleven silicate values total were excluded from the dataset (ten samples from KJ and one sample from UM).

4.3.3 Data Analysis

Bottle salinity was matched with CTD salinity readings to ensure the sample depths that were recorded were accurate. This was done to avoid discrepancies potentially caused by currents altering the depth at which the Kemmerer ultimately closed because the CTD and Kemmerer sampler were deployed independently.

Initial looks at the data were done through Ocean Data View (ODV) software (Version 4.7.10) and some figures were also generated through ODV. Basic statistical analysis of raw data was conducted with the use of R, within the RStudio interface (Version 1.3.1073). All data for properties (salinity, $\delta^{18}O$, nitrate, phosphate, and silicate) were analyzed using analysis of variance (ANOVA, aov function in the R *stats* package - Version 4.0.2) to identify whether there were significant differences between regions and sub-regions based on the property distribution. Linear models were created with the *stats* package (Version 4.0.2), to assess the overall relationship between salinity and $\delta^{18}O$, as well as the relationships between salinity-nutrients, and $\delta^{18}O$-nutrients. These were also analyzed to determine if there were significant differences between regions and sub-regions using regression analysis and analysis of variance (ANOVA). Data was visualized in figures generated with the use of the package *ggplot2* Version 3.3.5.

4.4 Results

4.4.1 Properties in NWHB Coastal Waters

In early winter of 2018 and 2019, the salinity range at NWHB stations was small, varying by less than 2 units (31.7 – 33.1). The low end of the salinity range (< 32.5) was found only at CI stations, presumably reflecting outflow from Baker Lake (Thelon and Kazan River confluence), which is ~40 km inland at the head of the inlet (Figure 4.2). The $\delta^{18}O$

values at NWHB sites ranged from -2.83‰ to -0.98‰ with the lowest values again at CI stations. There was no depth dependence for salinity or $\delta^{18}O$ over the shallow depth range (~50 m) of the CI stations, nor over the large depth range (~250 m) of the RB stations.

In late winter, the salinity range in NWHB increased slightly with several CI samples having salinity near 31 (Figure 4.3, lower panel). There was a slight increase in the maximum salinity in RB in late winter and lower salinity (down to ~31) in a few surface samples. One RB sample that was more depleted in $\delta^{18}O$ and lower in salinity than the rest (Figure 4.3) came from a deep inlet just east of the community of Naujaat (Figure 4.2a), where a small stream is present, which freezes almost completely during winter. Between early winter and late winter, $\delta^{18}O$ shifted towards more negative values at CI but did not change significantly at RB.

Concentrations of nitrate, phosphate, and silicate in NWHB were similar in early winter and late winter varying from 0 to 5.2 μM, 0.2 to 4.4 μM, and 2 to 13 μM, respectively through both time periods (Figure 4.3). Nutrient concentration ranges were similar at Repulse Bay and Chesterfield Inlet despite the lower salinity and $\delta^{18}O$ at the latter site.

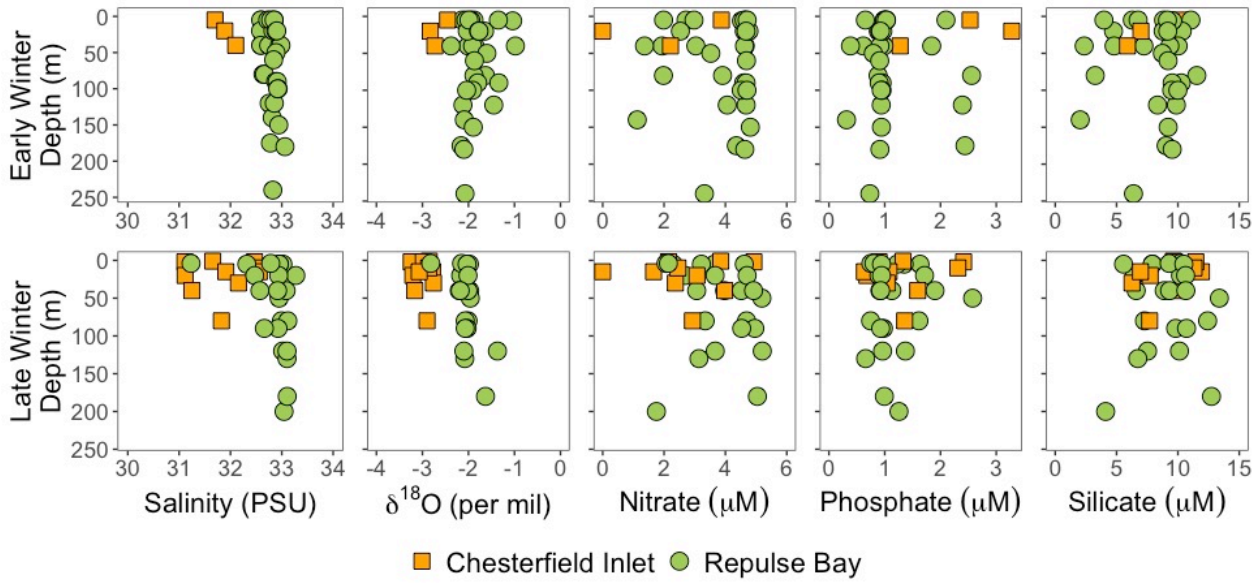

Figure 4.3 Vertical profiles of salinity, $\delta^{18}O$, nitrate, phosphate, and silicate in early winter and late winter for sites in NWHB. Points are coloured and shaped by sub-region (orange square = CI and green circle = RB).

4.4.2 Properties in SEHB Coastal Waters

In SEHB in early winter (EW), a stratified water column existed at a number of locations. Surface waters with salinity < 10 and $\delta^{18}O$ values < -12‰ were found at KJ and UM stations (Figure 4.4). At SK stations to the east and south of the Belcher Islands, surface waters had slightly lower salinity and $\delta^{18}O$ values than the corresponding subsurface waters. Those subsurface waters were similar to those seen throughout SEHB in early winter, with average salinity of about 30 and average $\delta^{18}O$ value of about -4‰ (Figure 4.4). At IN, there were no depth-related trends in salinity or $\delta^{18}O$ in early winter. Late winter (LW) water properties for all sub-regions were similar to those seen in early winter, with the exception of a small decrease in subsurface salinity and $\delta^{18}O$ at KJ.

Nutrient concentrations differed between sub-regions and showed a slight range increase from EW to LW (Figure 4.4). Nitrate concentrations ranged from 1.1 to 5.2 μM with lower concentrations in low salinity and low $\delta^{18}O$ surface waters and the shallow subsurface

in the KJ sub-region (Figure 4.4). The same was true of phosphate and indeed the freshest samples at KJ contained only about 1 µM phosphate. Highest concentrations of nitrate (~5 µM) and phosphate (up to about 1.1 µM) occurred in deeper waters (50-80 m). Silicate concentrations quantified in samples with salinity > 10 were quite variable but increased slightly with depth at SK and KJ stations (not statistically significant) (Figure 4.4).

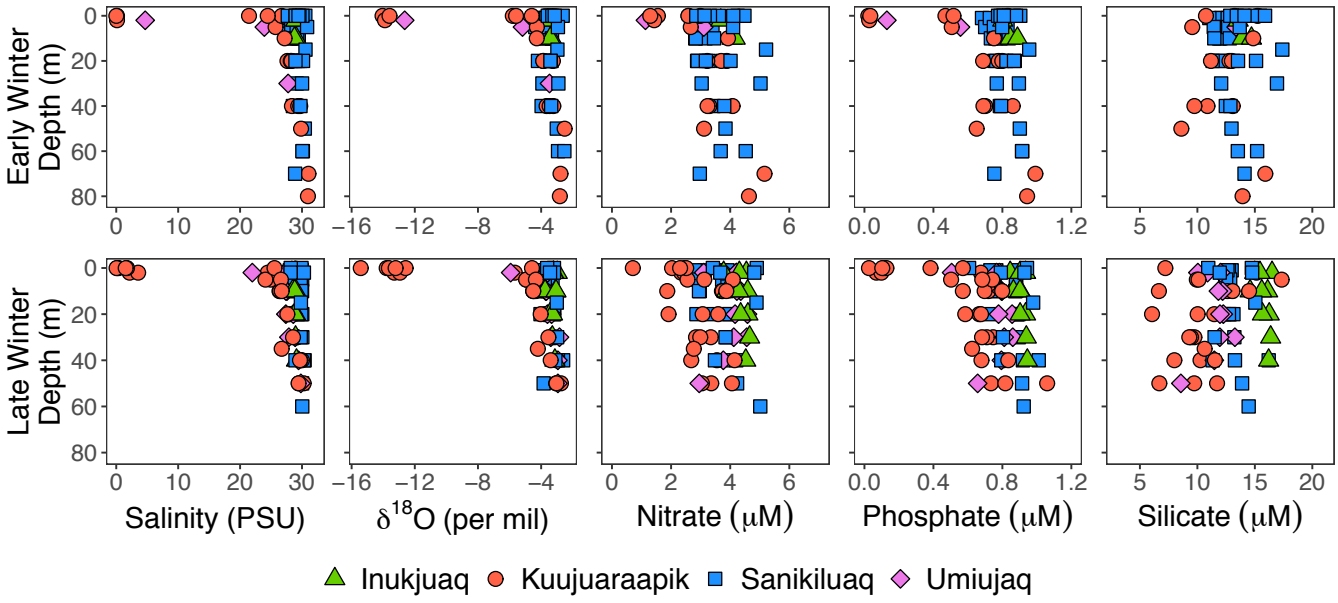

Figure 4.4 Vertical profiles of salinity, $\delta^{18}O$, nitrate, phosphate, and silicate in early winter and late winter for the sub-regions of SEHB. Points are coloured and shaped by sub-region.

4.4.3 Comparison of properties within and between regions

In Figure 4.5, we use boxplots to summarize the differences in water properties within and between the sub-regions. Early winter and late winter data were combined, as there is no statistically significant difference between seasons for all properties. Salinity was significantly higher at both NWHB sub-regions CI and RB compared to all SEHB sub-regions and $\delta^{18}O$ was significantly higher at RB (but not CI) than at all the SEHB sites.

Among the SEHB sub-regions, salinity and $\delta^{18}O$ were mostly similar across sites but salinity and $\delta^{18}O$ were both higher at IN compared to KJ (Figure 4.5). Nitrate was similar at IN, RB, UM, with KJ, SK, and CI being slightly lower and more comparable to each other. Phosphate was significantly higher at CI and RB than at any of the SEHB sites. It was also lowest at KJ relative to IN, SK, and UM. Silicate was lowest at CI and RB, moderate at KJ, SK, and UM, and highest at IN when considering mean concentrations, however the highest concentrations were observed in KJ and SK (~17.4 µM).

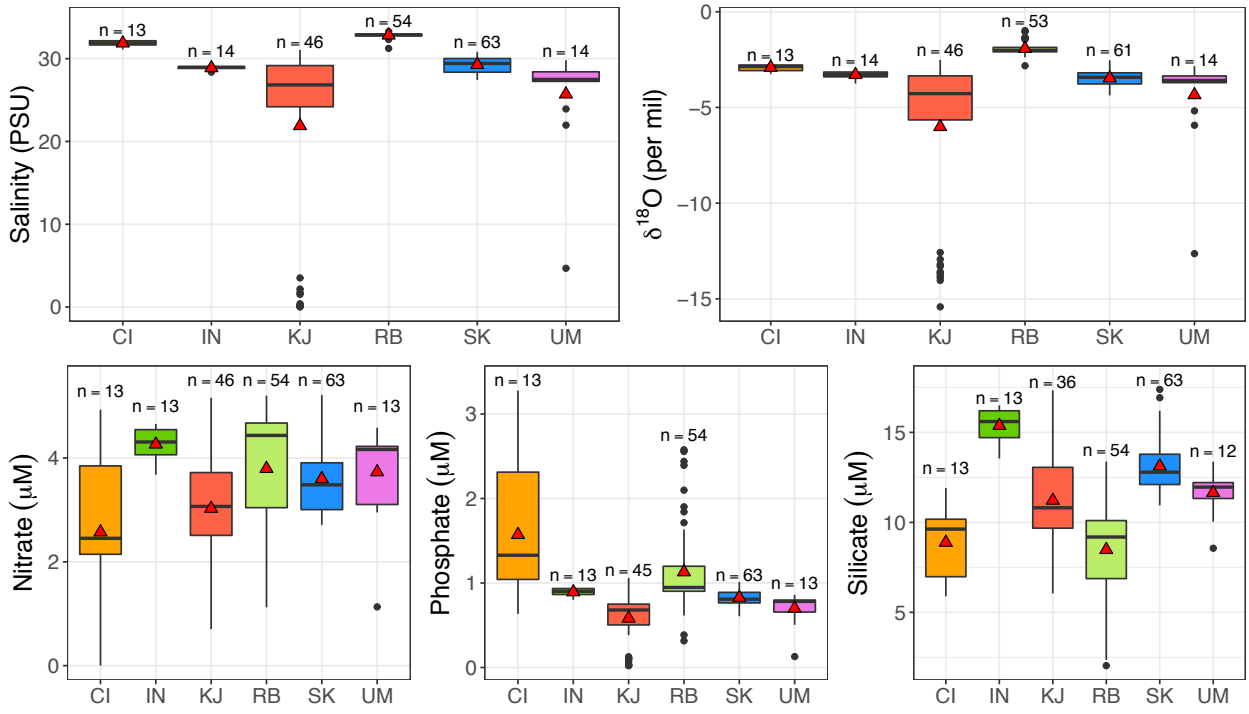

Figure 4.5. Boxplots of salinity, $\delta^{18}O$, nitrate, phosphate, and silicate concentrations coloured and grouped by sub-region. Sample count is indicated by the n value above each boxplot. Red triangle and black horizontal lines show the respective mean and median of each data grouping. CI = Chesterfield Inlet, IN = Inukjuak, KJ = Kuujuaraapik, RB = Naujaat (formerly Repulse Bay), SK = Sanikiluaq, and UM = Umiujaq.

4.4.4 Salinity - $\delta^{18}O$ relationship

Figure 4.6 shows the relationship between salinity and $\delta^{18}O$ for the combined NWHB and SEHB coastal water data set; colour coding distinguishes the different sub-regions. The overall regression relationship for salinity vs. $\delta^{18}O$ for the entire data set is described by the linear equation: $y = 0.36 (\pm 0.003)*x - 13.9 (\pm 0.1‰)$ and there is a very good fit ($R^2=0.98$, $p < 0.001$). We excluded the one zero-salinity $\delta^{18}O$ value that fell below -15‰ from the regression analysis believing it to have been contaminated by snow during sampling. The statistics of the salinity- $\delta^{18}O$ regression relationships for SEHB sub-regions are summarized in Table 4-1 in order to highlight the linearity of the SEHB samples. The NWHB and SEHB coastal regions are distinct along the salinity gradient with RB and CI at the high end of the salinity scale (31.1-33.3) and the SEHB sites lying below a maximum salinity of 31.3. The regions overlap along the $\delta^{18}O$ axis because of the CI samples having $\delta^{18}O$ values as low as -3.2‰ and SEHB sites having values up to -2.5‰ (Figure 4.6b).

All samples from the sub-regions of SEHB lie along the apparent RW-SW mixing line with little deviation. In contrast, CI samples exhibit an almost horizontal pattern with salinity varying by about 2.5 units but $\delta^{18}O$ remaining between -3.1‰ and -2.5‰ (Figure 4.6b). RB samples show a vertical pattern with salinity staying roughly constant (within less than one unit) while $\delta^{18}O$ varies between -2.5‰ to -1.0‰. For the NWHB region alone, there is no significant linear relationship between salinity and $\delta^{18}O$ for either RB, CI or the two sites combined (Figure 4.6b).

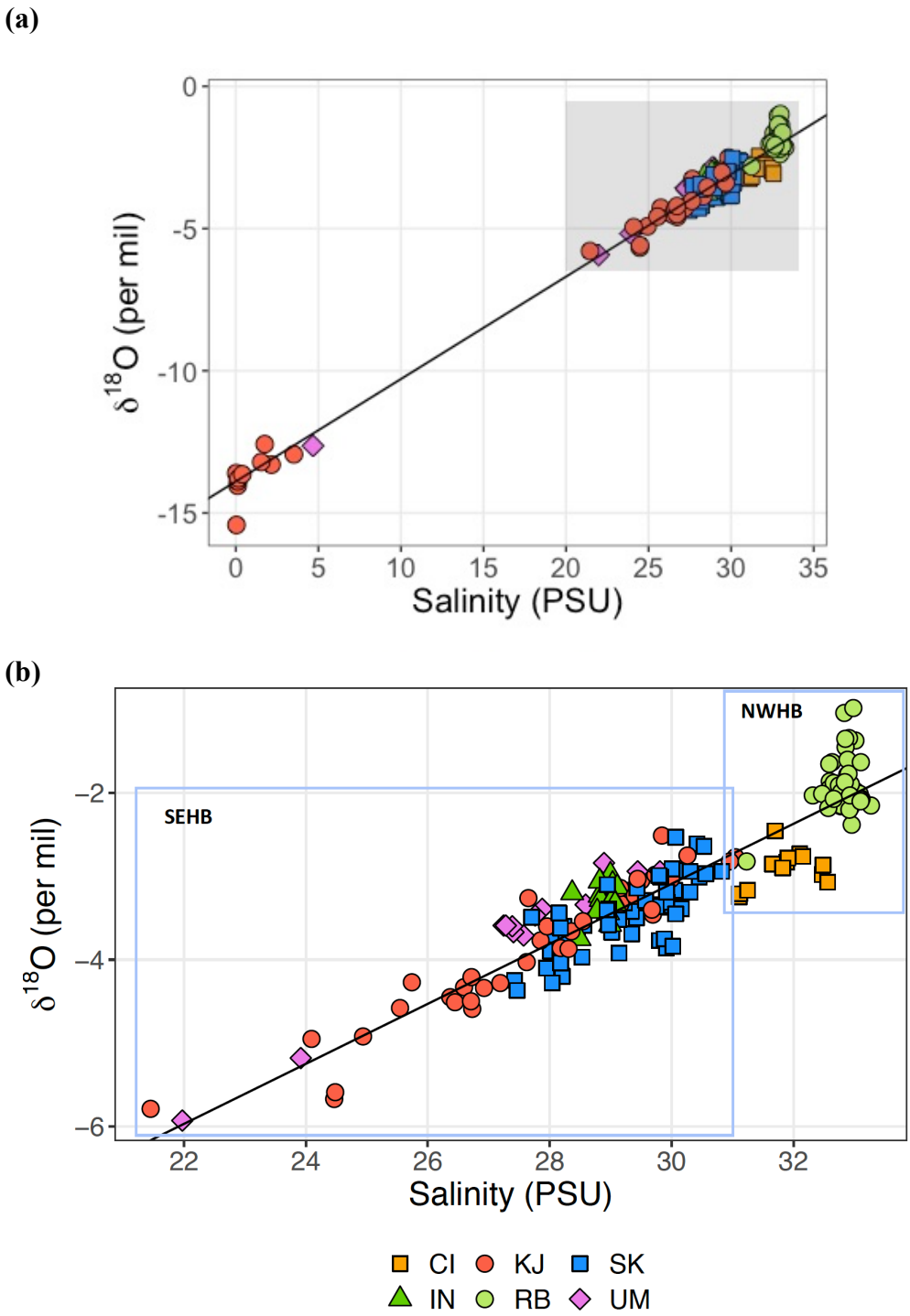

Figure 4.6 (a) Relationship between salinity (S) and $\delta^{18}O$ for the combined set of winter samples across the six study sites. The zero-salinity sample with the most negative $\delta^{18}O$ value was excluded from the regression. The regression equation is $\delta^{18}O = 0.36\ (\pm 0.003)*S - 13.9‰\ (\pm 0.1‰)$, $r^2=0.98$. The lower panel (b) is an enlargement of the shaded area in the upper panel (a). Blue lined boxes enclose the SEHB and NWHB data on the lower plot.

Table 4-1 Results of statistical analysis of the regression relationship between $\delta^{18}O$ and salinity for each sub-region of SEHB. Asterisk (*) indicates a statistically significant relationship.

Sub-Region	Slope (SE)	Intercept (SE)	p-value	R^2	n
KJ	0.36 (0.004)	-13.84 (0.09)	< 0.001*	0.995	46
SK	0.36 (0.04)	-13.87 (1.1)	< 0.001*	0.583	61
UM	0.40 (0.01)	-14.51 (0.16)	< 0.001*	0.997	14
IN	0.30 (0.26)	-12.01 (7.6)	0.276	0.097	14

4.4.5 Salinity – nutrient relationships

The three nutrients exhibit different relationships with salinity during the combined early and late winter periods. Nitrate is not significantly related to salinity in either region or sub-region except for KJ, where a weak positive relationship exists because of the low nitrate concentrations (< 2.7 μM) in low salinity waters (< 10) (Figure 4.7a). For phosphate, there is a strong positive relationship with salinity for the KJ sub-region because of the very low phosphate (< 0.2 μM) in low salinity waters (Figure 4.7b). There is also a significant relationship of increasing phosphate with salinity across all SEHB samples ($R^2 = 0.84$, $p < 0.001$, $n = 135$). The large variation in phosphate concentrations in NWHB samples (1-3.3 μM) is not related to salinity, $p = 0.3$ (Figure 4.7b). For silicate, there are conflicting weak relationships with salinity for different sub-regions (Figure 4.7c). In the KJ samples, there is a very weak negative trend between silicate and salinity ($R^2 = 0.04$, slope = -0.24, $n = 34$,), whereas for the SK samples, there is a weak positive trend ($R^2 = 0.27$, slope = 0.82, $n = 61$).

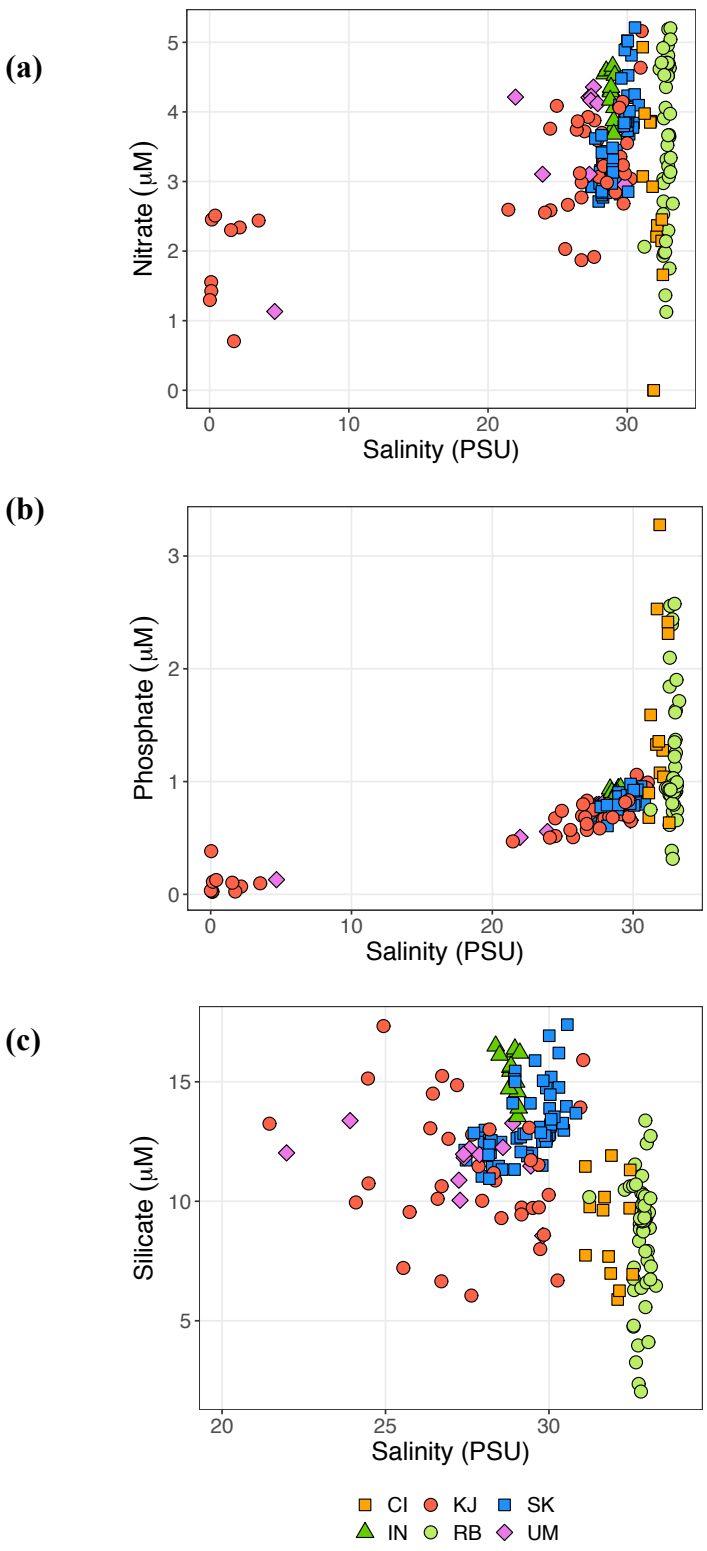

Figure 4.7. Relationships between salinity and (a) nitrate, (b) phosphate, and (c) silicate for combined early and late winter data across all sites. Note the different salinity scale in (c).

4.4.6 $\delta^{18}O$ – nutrient relationships

Although general trends in $\delta^{18}O$-nutrient plots are comparable to those in salinity-nutrient plots, there are a few interesting differences. The wide range of nitrate concentrations can be seen to be independent of variation in $\delta^{18}O$ across the range of -6‰ and -1‰ (Figure 4.8a). In contrast, phosphate looks mostly conservative at low $\delta^{18}O$ values but a group of high-phosphate samples can be seen at $\delta^{18}O$ values between -3‰ to -1.6‰ (Figure 4.8b). With silicate, an overall negative trend with $\delta^{18}O$ is evident in Figure 4.8c and at relatively high $\delta^{18}O$ values there exists a subset of samples with very low silicate (< 5 μM), which coincide with the lower nitrate concentrations (< 2.5 μM) and lower phosphate concentrations (< 0.9 μM).

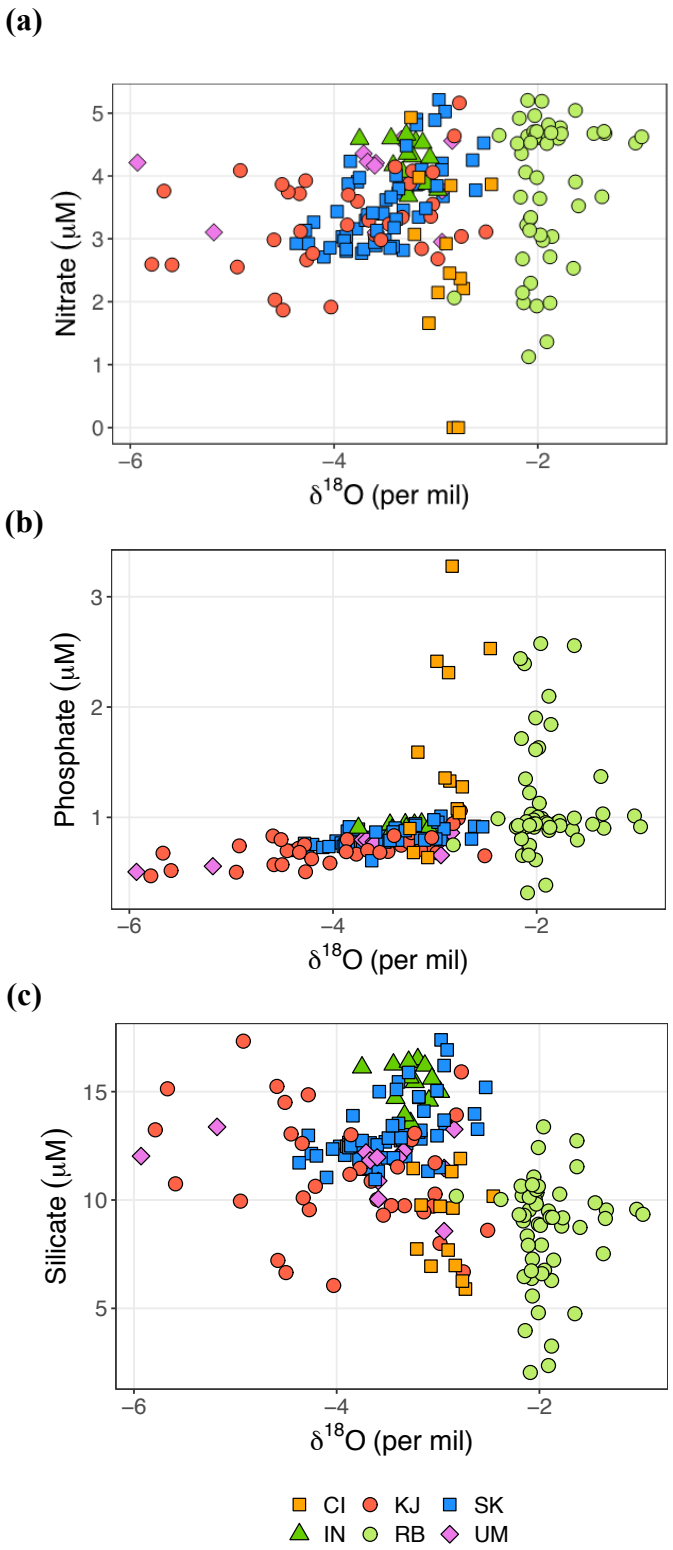

Figure 4.8. Relationships between $\delta^{18}O$ and (a) nitrate, (b) phosphate, and (c) silicate for combined early and late winter data across all sites. Data presented coincides with samples with a salinity > 20.

4.4.7 Nutrient – nutrient relationships

With respect to Redfield ratio for C:N:P of phytoplankton composition (106:16:1), nitrate is the potentially limiting element for primary production across almost all SEHB and all of NWHB (Figure 4.9a). With the global average Si:N consumption ratio of phytoplankton being 1.05:1 (Brzezinski, 1985), silicate is found in excess almost always in comparison to nitrate (Figure 4.9b); however, when compared against phosphate, which isn't typically compared but has been reported in the western Canadian Arctic where consumption ratio of Si:P is 26:1 (Tremblay et al., 2008), silicate would be the limiting element after nitrate is depleted at almost all sites (Figure 4.9c). Roughly half of the high-salinity samples from the NWHB region are much higher than what would be expected at the nitrate and silicate values observed (Figure 4.9a, c). The ratios at which these nutrients would be expected to be regenerated through oxidation of marine organic matter (regarding N:P and Si:P) are relatively higher than what is observed in this specific group of samples from NWHB, prompting questions of nutrient sources in this area.

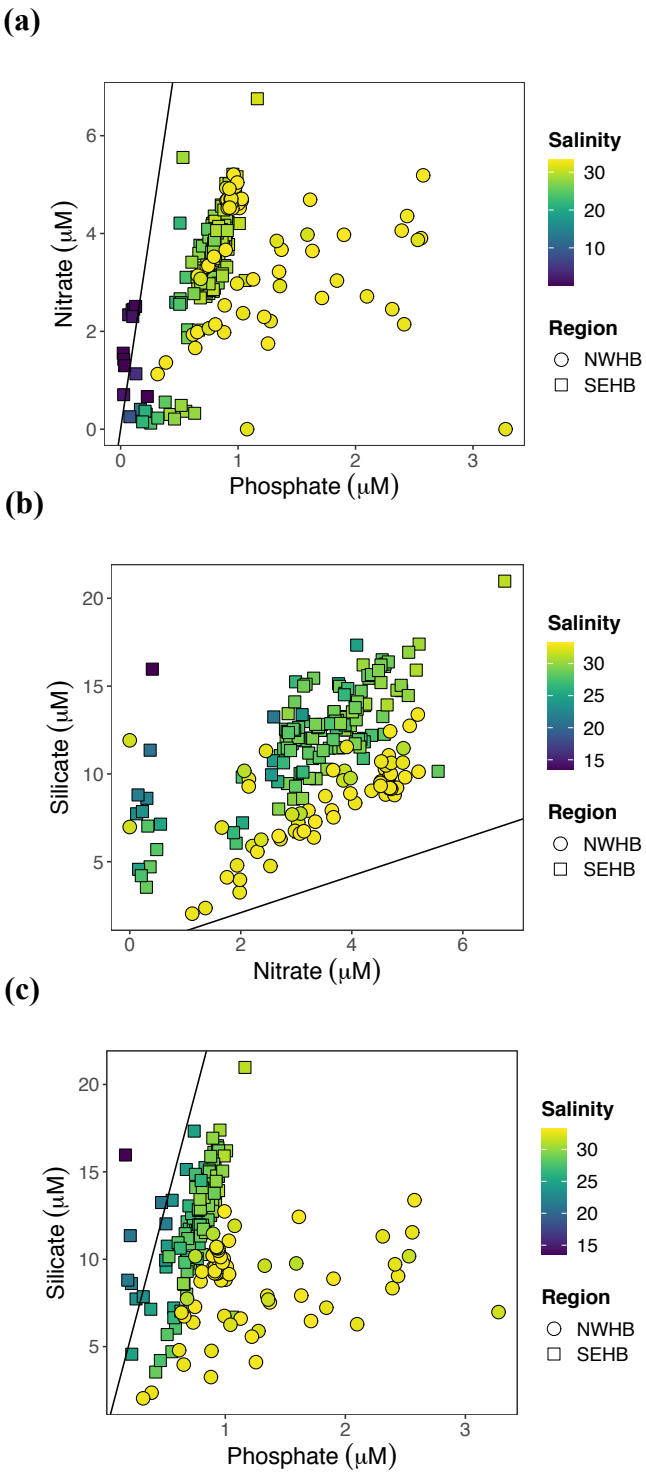

Figure 4.9. Relationships between (a) nitrate and phosphate, (b) nitrate and silicate, and (c) silicate and phosphate with lines showing Redfield and Brzezinski ratios (N:P = 16:1, Si:N = 1.05:1), and the Si:P consumption ratio established by Tremblay et al. 2008 for Arctic regions (26:1).

4.5 Discussion

4.5.1 Freshwater content of coastal waters in winter

One of the main causes of regional- and local-scale differences in nutrient distributions in Hudson Bay coastal waters during winter is freshwater content, which, in Hudson Bay, is primarily comprised of river water (RW) and sea-ice melt (SIM) (cf., Granskog et al., 2011; Burt et al., 2016). SEHB coastal water samples are characterized by distinctly lower salinity than those in NWHB, with no overlap in range. Based on the low $\delta^{18}O$ values accompanying the lower salinity in these samples, we can confirm the freshwater present in SEHB coastal samples in winter is predominantly RW. In general, RW is strongly isotopically depleted relative to SIM (cf., Östlund and Hut, 1984), and in Hudson Bay, the end-member values of these freshwater sources (salinity and $\delta^{18}O$) have been estimated at about 0, -14.0‰ (RW) and 5, 0‰ (SIM) (Granskog et al., 2011).

As expected for mixing between seawater and a RW end-member, our coastal water samples spanning a salinity range of 0-33 fit well along a linear regression line in a plot of salinity vs. $\delta^{18}O$ ($R^2 = 0.98$, $p < 0.001$) (Figure 4.6a). At the low end of the salinity scale in Figure 4.6a, a cluster of the freshest samples include those influenced directly by outflow of eastern Hudson Bay rivers, including the Great Whale and Nastapoca Rivers, which have previously been identified as strong local freshwater influences (Freeman et al., 1982; Ingram et al., 1996). The freshwater end-member implied by the overall regression relationship for both regions (-13.9‰ ± 0.1‰) is slightly enriched compared to previously reported $\delta^{18}O$ values of between -14.86‰ and -14.17‰ for these rivers (Granskog et al. 2011; Burt et al., 2016). $\delta^{18}O$ values for these rivers might be isotopically enriched (i.e., higher) during low-flow winter periods because of evaporative enrichment of lake water, which contributes to base flow (cf., Smith et al., 2015). Alternatively, the apparent freshwater end-member of the

overall relationship might be elevated as a result of the influence of more isotopically enriched sources, such as the Nelson River in southwest Hudson Bay (annual average value of -10.64‰ (Smith et al., 2015)) and/or the La Grande River in northeast James Bay (winter value of -13.28‰ (Eastwood et al., 2020), see also Chapter 3 in this thesis (winter value of -14.07 ± 0.30‰)).

In the SEHB region, even sites without direct local winter river influence such as SK and IN have distinctly lower salinity than NWHB sites. Influence of river water in SEHB winter coastal samples is not surprising because Hudson Bay rivers discharge 630-870 km^3 annually and many major rivers discharge into the southern half of the bay and James Bay, which is 'upstream' of our SEHB region in so far as the general cyclonic circulation in Hudson Bay is concerned (cf., Saucier et al., 2004; Ridenour et al., 2019a). Despite a large proportion of river discharge coming during the spring freshet here, new river water residence times have been estimated to be as long as 18 years (Ridenour et al., 2019b), previously estimated to be 3-4 years (Jones and Anderson, 1994).

Because of the modified hydrograph of the La Grande, there is significant winter river discharge into eastern James Bay each winter: ~48 km^3 yr^{-1} or about 21% of the annual total (de Melo et al., submitted). Previous work showed that the SK area, with the exception of stations located northwest of the islands, is influenced during winter by river water-rich outflows from James Bay (Eastwood et al. 2020; Petrusevich et al., 2018). Based on our salinity-$\delta^{18}O$ regression relationships for the SEHB sub-regions (Table 4-1) we can see that the apparent freshwater end-members (intercepts) for KJ (-13.84‰) and SK (-13.87‰) are within range of the La Grande River $\delta^{18}O$ values mentioned above, with UM not far off (-14.51‰). This indicates that James Bay winter outflow may be a cause of the low salinity

and $\delta^{18}O$ observed at these three sub-regions. However, IN does not share the same apparent zero-salinity end-member, however, sample size is low and the regression relationship is very weak (Table 4-1).

In NWHB the sea-ice cycle plays a much more important role in the water mass composition. The relatively salty, isotopically enriched composition of the NWHB coastal samples reflects the dominant influence of Arctic-derived seawaters that enter Hudson Bay in this area and outside of localized areas like Chesterfield Inlet, these water masses do not get extensively transformed by meteoric input in winter, in contrast to SEHB. Previous studies have estimated the salinity and $\delta^{18}O$ of Hudson Bay's source seawater at 32.8 ± 0.1 and -1.5 ± 0.2‰, respectively (Granskog et al., 2011). Our salinity-$\delta^{18}O$ regression relationship implies a $\delta^{18}O$ value of -2.1‰ for water of salinity 32.8 but variability in $\delta^{18}O$ can be seen among the high salinity samples, both above and below the regression line (Figure 4.6a,b). This variability in $\delta^{18}O$ in high salinity samples is at odds with the notion of uniform source seawater to Hudson Bay. There has been some previous discussion of the influence of multiple source waters in northern Hudson Bay. Jones and Anderson (1994) described salinity = 33.1 and a minimum in alkalinity for waters that overflow from Foxe Basin and fill the deep offshore basins of Hudson Bay, and they characterized a second source seawater as one formed by Hudson Strait Bottom Water (salinity = 33.4) mixing with river runoff from both Hudson Bay Winter Surface Water and Hudson Bay Intermediate Water to produce water masses of variable salinity. Either time variation in Hudson Bay Winter Surface Water that outflows into west Hudson Strait, or spatial variation in the mixtures of Hudson Bay Winter Surface Water and Hudson Strait Bottom Water that are formed and re-circulated back to NWHB could explain the $\delta^{18}O$ variations seen our data set.

There is some freshening and especially lowering of $\delta^{18}O$ values (Figure 4.6b) that may be attributed to riverine input in CI samples close to the mouth of the inlet. Here, there is a horizontal salinity - $\delta^{18}O$ relationship that we attribute to mixing of fresh, isotopically depleted river water with salty, isotopically enriched brine. The samples are saltier than would be expected from their $\delta^{18}O$ values based on the salinity-$\delta^{18}O$ regression relationship, and overlap with SEHB samples (Figure 4.6b). Previously, horizontal relationships were observed in Foxe Basin and attributed to addition of isotopically heavy sea ice meltwater (Tan and Strain, 1996) but those observations were made during summer, whereas our observations were made at a time of no obvious melt. The "Kivalliq Polynya" in northwestern Hudson Bay (Figure 4.1a) may be expected to be a site of near-continual ice growth during winter and consequently continuous brine rejection (Aagaard et al., 1981; Bruneau et al., 2021). The area of the polynya is highly variable but it contributes on average 182 km^3 of new ice during winter, which is expected to be formed from near pure seawater and thus produce the equivalent brine (Bruneau et al., 2021). The placement of CI samples in relation to the salinity- $\delta^{18}O$ mixing line (Figure 4.6b) is associated with brine rejection, which is consistent with the location of the Kivalliq Polynya and the constant brine production through winter. We assume here that the overall water mass is the same as the water mass we observe in RB but transformed as it circulates through Roes Welcome Sound along the coast of the Bay, freshened by riverine inputs (the main one in this area being Baker Lake) which provide the more depleted $\delta^{18}O$ values, and the slightly lower salinity (Figure 4.6b).

A vertical salinity - $\delta^{18}O$ relationship like we see at RB stations is not typically observed but has been observed at one station at the western end of Hudson Strait (see station

45, Figure 1 in Tan and Strain, 1996). They attributed the variation in $\delta^{18}O$ with hardly any variation in salinity to the presence of a subsurface water mass containing brine, which was particularly unusual as their observations came from the summer period. However, a brine-rich subsurface water mass is not unexpected for Repulse Bay in winter. Furthermore, this area is extremely dynamic because of the convergence of water masses from Foxe Basin, west Hudson Strait, and Hudson Bay (cf., description in Jones and Anderson, 1994). Different degrees of mixing between winter water masses of Hudson Bay and Hudson Strait inflow could readily produce water masses similar in salinity but divergent in $\delta^{18}O$ because of varying degrees of river water and brine influence (cf., Eastwood et al., 2020).

While our NWHB study area is influenced by river runoff near Chesterfield Inlet, local sea-ice processes (i.e. brine rejection during sea-ice formation) are an important influence that increases the salinity of coastal waters while having little influence on the $\delta^{18}O$ of the samples, thus partially masking the effect of river water content in the water mass. We see a much greater influence from riverine inputs in the southeastern region, with evidence of freshening and strong isotopic depletion along the salinity-$\delta^{18}O$ mixing line.

4.5.2 Influence of river water on nutrient concentrations and ratios

The assessment of freshwater source contributions to the regional and local water masses is important for discussing the winter nutrient distributions. Specifically, we expected that as the water mass is transformed with increasing riverine input as it is between NWHB to SEHB, the nutrient content and composition would change as well. However, surprisingly, the nitrate concentrations do not show a regional difference: NWHB samples have a slightly larger range in nitrate than SEHB concentrations within a smaller salinity range, but overall the maximum nitrate concentrations at depth are the same between the two regions (5.2 μM,

Figure 4.7a and 4.8a). This nitrate maximum is relatively low in comparison to concentrations that have been measured in Hudson Bay deep waters (7-15 μM) (Ferland et al., 2011), both inshore and offshore (cf., Kuzyk et al., 2010). Tremblay and Gagnon (2009) remark that the typical vertical resupply of nitrate, when turbulence occurs in the water column in fall, does not occur in the inshore areas of shallow Arctic shelves due to the lack of deep nutrient reservoirs. This may be similar to the shallow Hudson Bay coastal regions of our study, where the majority of sites have a depth < 100m. The nitrate concentrations in low-salinity, riverine-influenced waters are among the lowest of the SEHB region (0.9 - 2.5 μM, Figure 4.7a). This is expected, as river waters are generally a poor source of nitrate to coastal waters with some exceptions (see Chapter 3 of this thesis; Macdonald et al., 1987; Bluteau et al., 2021). It is interesting that the values we observe are not lower throughout this region in comparison to a much less riverine dominated area like NWHB (Figure 4.8a), considering RW addition would work to dilute the SEHB coastal water mass (within the RCD) and consequently dilute the nutrients. The nitrate concentrations specifically are also consistent throughout the water column and a nutricline does not appear (Figure 4.4). With estuarine circulation, associated vertical mixing may explain an increase of nitrate to the surface from deeper waters (Kuzyk et al., 2010), which would reflect the properties found in the winter coastal water mass of SEHB. Another possibility would be considering ammonium addition by rivers which would convert to nitrate in the coastal waters (Le Fouest et al., 2013), which would reflect the higher than anticipated concentrations, as in this study we do not measure ammonium. However, this scenario would imply lower phosphate in SEHB samples, which is not what we see (most SEHB and NWHB samples measure ~1 μM phosphate, Figures 4.7b and 4.8b). The implication here is that RW does not serve solely in

the sense of addition and nutrient dilution, but rather there must be an RW-associated process that would work to increase nutrients.

Phosphate is often regarded as a conservative tracer as it does not transform readily through the system apart from being consumed and renewed. Our SEHB phosphate data demonstrates a strong positive linear trend with salinity, ($R^2 = 0.84$, p-value < 0.001). This is generally the trend observed in estuarine areas where there is a large salinity gradient, as river waters contain little to no phosphate, in large part due to the biogeochemical processes that occur within the river (Macdonald et al., 1987), where bioavailable P is either used up or bound to iron oxides before entering the coastal system (Slomp, 2011). We observe regional differences in phosphate concentrations, where NWHB samples depart from the strong linear relationship between phosphate and salinity/$\delta^{18}O$ observed in SEHB, and have a large range of concentrations reaching maximum values above 3 μM (Figures 4.7b & 4.8b). The SEHB deepwater samples characterized by high salinity, high $\delta^{18}O$ match well in terms of phosphate concentrations with previously measured Hudson Bay deepwater samples (1.3-2.1 μM), but the high values measured in NWHB surpass any previous records of SEHB or offshore bay waters (Ferland et al., 2011). Perhaps the most interesting result comes from CI, where there is slightly more RW influence than RB, which we would anticipate having lower phosphate concentrations, however we observe some of the highest concentrations of the entire study area. Despite these high values, there remains a cluster of samples from RB that continues almost horizontally from SEHB phosphate-$\delta^{18}O$ relationship (Figure 4.8b) and also has similar NP ratios ~5 (Figure 4.9b).

Silicate also demonstrates a regional difference where concentrations are slightly lower in NWHB than what is observed in SEHB, consistent with our expectations for how

the greater influence of RW in SEHB should influence nutrient concentrations. Silicate is much more scattered and has much weaker relationships (not statistically significant) with both salinity and $\delta^{18}O$, compared to the other nutrients. However, the general pattern indicates a positive relationship between silicate concentrations and magnitude of RW influence (decreasing $\delta^{18}O$) when considering the river-influenced sites KJ, UM and CI (Figure 4.8c). Rivers are known to provide high silicate concentrations to coastal waters (Turner et al., 2003), and in Hudson Bay specifically, silicate has been found at its highest levels in summer near the mouth of James Bay (~9 μM) (Lapoussiere et al., 2013), agreeing with our dataset. A slight (non-significant) negative tendency between RW content and silicate emerges when looking at SK and RB sites, which probably points to the RW in these samples having been cycled for several years within the Hudson Bay system and losing the high silicate that it carried upon initial discharge to Hudson Bay (Figure 4.8c). This is an example of the long residence time of RW in Hudson Bay complicating the interpretation of $\delta^{18}O$-nutrient relationships.

Throughout the entire study area, silicate remains in excess compared to nitrate, and there is evidently some variation that does not relate to variations in RW. For example, silicate concentrations in CI samples remain similar to those in RB, when we would expect higher silicate in CI because of the higher RW component. These lower than expected silicate concentrations might be attributable to diatom species composition, their nutrient consumption ratios, or simply, diatom population sizes, which have been shown to vary year to year in Hudson Bay (Ferland et al., 2011). The nutrient ratios used in this study to compare to our data are averages that apply globally or to the Arctic and likely do not reflect our

regions with accuracy, however they are useful when determining progression of nutrient limitation (i.e. which nutrient will be depleted in the system first).

4.5.3 Comparison to previous nutrient observations

The high phosphate and relatively low nitrate observed in NWHB in this study prompt the question of if these nutrient levels have been seen before in this region. Despite the limited historical data from Hudson Bay, there is nutrient (nitrate and phosphate) and salinity data from summer 1961 in the NWHB region, which was accessed through the Marine Environmental Data Service (MEDS; https://www.meds-sdmm.dfo-mpo.gc.ca/isdm-gdsi/index-eng.html). In order to assess whether the concentrations and ratios we observe in this study are consistent through the last six decades, we combine, in Figure 4.10, the MEDS data, with our NWHB winter data, along with data gathered during the summer of 2018 and 2019 SIMEP (Southamption Island Marine Ecosystem Project) Cruises, which were used to compare and verify our observed concentrations. Stations vary between the three datasets, as ours only contains sites inshore around RB and CI, but the SIMEP and MEDS datasets have stations surrounding Southampton Island in NWHB.

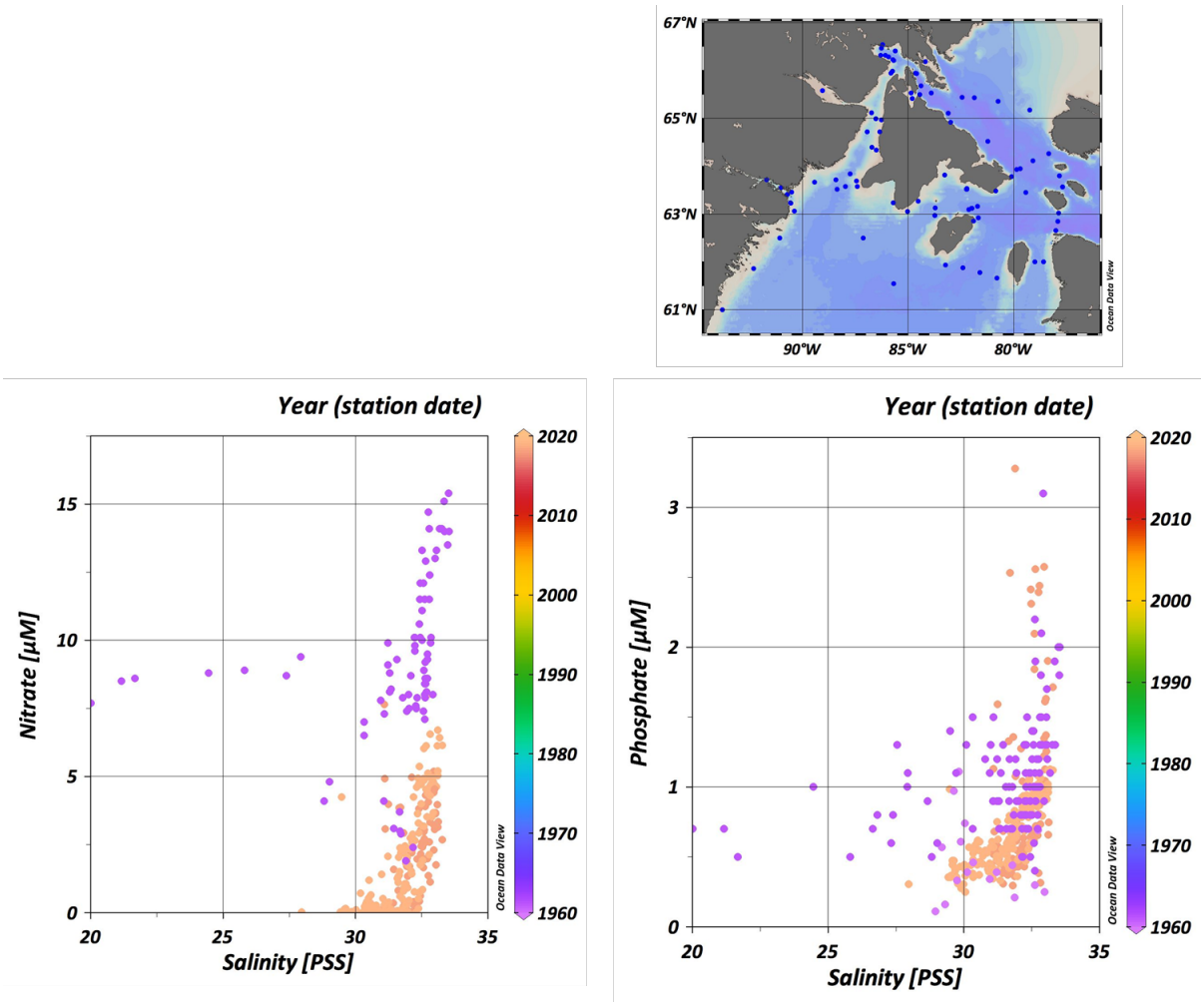

Figure 4.10. Comparison of nitrate and phosphate observations in northwest Hudson Bay over the 1961 – 2020 time period (Data Source: Marine Environmental Data Service for summer 1961 data; Southampton Island Marine Ecosystem Project for summer 2018 and 2019 data).

Salinity compared from the 1960s to today remain within the same range, with some exceptions from the 1960s reaching down to 20, however this is from a station located much farther up the Inlet at Chesterfield Inlet than we have data for. Strikingly, when comparing the historical dataset to the most recent data (our presented data and SIMEP), we immediately see a large shift downward of nitrate concentrations, where in 1961, maximum concentrations of nitrate reached just above 15 µM (Figure 4.10), comparable to the HB deepwater values seen by Ferland et al. (2011). The only station from 1961 overlapping our

nitrate concentrations is located the farthest south along the west coast downstream of Chesterfield Inlet (Figure 4.10, see map). The phosphate range, on the other hand, matches between years and has a similar maximum (above 3 μM) (Figure 4.10). These comparisons show us that the high phosphate we observe within our data in NWHB has been seen before; however there seems to be a large decrease in nitrate from 1961 until present day. Determining why there is such a large shift in nitrate concentrations in this region requires further study and speculation.

4.5.4 Other influences on nutrient distributions

The high phosphate concentrations (2-3 μM) that are found in some of our NWHB samples have unexpectedly low NP ratios (~2:1), indicating much lower nitrate than anticipated with the observed levels of phosphate. Data from 1961 (Figure 4.10) point towards an overall shift downward in nitrate concentrations in the NWHB area. This could potentially explain the similarity we observe in nitrate concentrations seen between NWHB and SEHB, where we would expect to see a lower nitrate load in a more RW dominated water mass (SEHB), than a region that does not experience dilution from RW input (NWHB). The high phosphate / low nitrate characteristics are observed at both the RB and CI sites, at a number of individual stations and various depths; however, they occur only among samples with relatively low $\delta^{18}O$ (below about -1.5‰). Additionally, high phosphate (up to 11 μM) with nitrate < 7 μM have been observed (with NP ratios < 1) along the southern coast of Hudson Strait (Lisa Miller, personal communication), associated with Hudson Bay outflow.

There are a few plausible explanations for what we observe in NWHB. First, there could be strong differences in preformed nutrients that were present in surface water in the fall/early winter just after the productive season ended, which could sink with the beginning of ice formation. In other words, strong N depletion relative to P was produced in surface waters and has persisted in that water mass during nutrient regeneration processes. Another reason for variance in nutrient ratios is difference in nutrient regeneration from organic matter (cf., Redfield, 1963; Brzezinski, 1985; Tremblay et al., 2008). Nutrients should on average regenerate at the ratio of 106C: 16N: 1P: ~16Si or a similar ratio reflecting the specific composition of the organic matter undergoing remineralization, provided it occurs under oxygenated conditions. It has also been noted that remineralization ratios in the Canadian Arctic are 13.3N: 1P: ~26Si (Tremblay et al., 2008).

It is well known that Pacific-source water in the Arctic is characterized by a large residual pool of P due to biogeochemical processes that affect the N supply (Yamamoto-Kawai et al., 2006; Tremblay et al., 2008; Tremblay et al., 2014), The most important process causing the P excess is denitrification in sediment, which occurs on the Bering shelf and possibly other Arctic shelves (Devol et al., 1997; Tanaka et al., 2004). Indeed, Atlantic and Pacific waters have similar slopes for their N versus P relationships, however the intercepts differ, which is considered to be a result of the different rates of denitrification between the two oceans (Pacific sees more denitrification) (Yamamoto-Kawai et al., 2008). Specific nutrient ratios and concentrations have been used to identify different water masses in the past (Jones et al., 1998; Yamamoto-Kawai et al., 2008). Residual signals could be transported to Hudson Bay with Arctic outflow and indeed that probably explains the typical NP ratios we observe, which are slightly below Redfield. However, in the high P samples from

NWHB, our NP ratios are very low in comparison to those in most studies of North American Arctic Ocean shelves. During the time of year of our study (winter), with ice-cover present, we also do not anticipate high rates of primary production, including ice algae (Ferland et al., 2011), which could explain a large depletion of N relative to P like we observe (cf., Maestrini et al., 1986). A water mass that is influenced by denitrification in sediments is most likely the source of the P-rich and N-poor water we observe in NWHB.

4.6 Conclusions

This study provides a modern assessment of the oceanographic properties of two coastal regions (NW and SE) of Hudson Bay, which highlights the coastal areas surrounding six communities: Naujaat (RB), Chesterfield Inlet (CI), Sanikiluaq (SK), Kuujuaraapik (KJ), Umiujaq (UM) and Inukjuak (IN). With new tracer data ($\delta^{18}O$ and salinity) and in most areas providing the only oxygen isotope ratio tracer data ever gathered, we determine that despite the common source seawater, regional and even sub-regional differences in salinity and $\delta^{18}O$ are observed. The winter SEHB coastal water mass is largely influenced by riverine input from local rivers (Great Whale River and the Nastapoca River), but also from the "upstream" James Bay outlet. The NWHB coastal water mass is overall influenced more so by the sea-ice cycle, in regards to sea-ice formation and brine production in winter. Utilizing $\delta^{18}O$ allowed us the ability to comment on RW influence and also helped us to identify the difference in water mass composition between RB and CI, for example. Contrary to the hypothesis, these two regions do not have divergent nutrient properties but rather are very similar. The largest ranges of nitrate and phosphate are observed in NWHB, but SEHB sub-regions remain within the same range. Silicate concentrations overlap between both regions, however the more riverine influenced areas experience higher concentrations, as expected. In

this study we also determine nitrate is the potentially limiting nutrient through the majority of both regions (apart from the salinity < 10 samples). The NP and SiP ratios in these coastal regions are also much lower than expected, when comparing to previously recorded concentrations and the classic nutrient regeneration ratios for marine environments. High phosphate (~3 μM) in NWHB has been observed previously (1961); however, high nitrate that previously accompanied the high phosphate is not observed in recent sampling efforts. Further study within these regions, specifically NWHB, is needed to assess whether low NP ratios are the new normal or if it was an anomaly during our study period. This study overall helps to assess basic oceanographic properties so as to provide a baseline for future work in these regions which is increasingly important to understand for local community members who are experiencing rapid and in some cases unpredictable environmental change.

References

Aagaard, K., Coachman, L. K., & Carmack, E. (1981). On the halocline of the Arctic Ocean. *Deep Sea Research Part A, Oceanographic Research Papers*, *28*(6), 529–545. https://doi.org/10.1016/0198-0149(81)90115-1

Barber, D. G., Harasyn, M. L., Babb, D. G., Capelle, D., McCullough, G., Dalman, L. A., … Sydor, K. (2021). Sediment-laden sea ice in southern Hudson Bay: Entrainment, transport, and biogeochemical implications. *Elementa: Science of the Anthropocene*, *9*(1). https://doi.org/10.1525/elementa.2020.00108

Bluteau, C. E., Galbraith, P., Bourgault, D., Villeneuve, V., & Tremblay, J.-É. (2021). Nutrient transport pathways in the Lower St. Lawrence Estuary: seasonal perspectives from winter observations. *Ocean Science Discussions*, *17*, 1509–1525. https://doi.org/10.5194/os-2021-59

Bruneau, J., Babb, D., Chan, W., Kirillov, S., Ehn, J., Hanesiak, J., & Barber, D. G. (2021). The ice factory of Hudson Bay: Spatiotemporal variability of the Kivalliq Polynya. *Elementa*, *9*(1), 1–17. https://doi.org/10.1525/elementa.2020.00168

Brzezinski, M. A. (1985). The Si:C:N ratio of marine diatoms: Interspecific variability and the effect of some environmental variables. *Journal of Phycology*, *21*, 347–357.

Budgell, W. P. (1976). Tidal propogation in Chesterfield Inlet, N.W.T. *Fisheries and Environment Canada, Canada Centre for Inland Waters, Manuscript Report Series, 3,* xiv+99.

Budgell, W.P. (1982). Spring-neap variation in the vertical stratification of Chesterfield Inlet, Hudson Bay. Nat. Can. (Que.) 109: 709–718.

Burt, W.J., Thomas, H., Miller, L., Granskog, M., Papakyriakou, T.N., et al. 2016. Inorganic Carbon Cycling and Biogeochemical Processes in an Arctic Inland Sea (Hudson Bay). *Biogeosciences* **13**(16): 4659-4671. doi:10.5194/bg-13-4659-2016.

Carmack, E. C., & Macdonald, R. W. (2002). Oceanography of the Canadian shelf of the Beaufort Sea: A setting for marine life. *Arctic*, *55*(SUPPL. 1), 29–45. https://doi.org/10.14430/arctic733

Carmack, E., & Wassmann, P. (2006). Food webs and physical-biological coupling on pan-Arctic shelves: Unifying concepts and comprehensive perspectives. *Progress in Oceanography*, *71*(2–4), 446–477. https://doi.org/10.1016/j.pocean.2006.10.004

Carmack, E., Winsor, P., & Williams, W. (2015). The contiguous panarctic Riverine Coastal Domain: A unifying concept. *Progress in Oceanography*, *139*, 13–23. https://doi.org/10.1016/j.pocean.2015.07.014

Déry, S. J., Mlynowski, T. J., Hernández-Henríquez, M. A., & Straneo, F. (2011). Interannual variability and interdecadal trends in hudson bay streamflow. *Journal of Marine Systems*, *88*(3), 341–351. https://doi.org/10.1016/j.jmarsys.2010.12.002

Déry, S. J., Stadnyk, T. A., MacDonald, M. K., & Gauli-Sharma, B. (2016). Recent trends and variability in river discharge across northern Canada. *Hydrology and Earth System Sciences*, *20*(12), 4801–4818. https://doi.org/10.5194/hess-20-4801-2016

Dmitrenko, I., Kirillov, S., Eicken, H., & Markova, N. (2005). Wind-driven summer surface hydrography of the eastern Siberian shelf. *Geophysical Research Letters*, *32*(14), 1–5. https://doi.org/10.1029/2005GL023022

Dmitrenko, I. A., Kirillov, S. A., Babb, D. G., Kuzyk, Z. Z. A., Basu, A., Ehn, J. K., … Barber, D. G. (2021). Storm-driven hydrography of western Hudson Bay. *Continental Shelf Research*, *227*, 1–16. https://doi.org/10.1016/j.csr.2021.104525

Eastwood, R. A., Macdonald, R. W., Ehn, J. K., Heath, J., Arragutainaq, L., Myers, P. G., … Kuzyk, Z. A. (2020). Role of River Runoff and Sea Ice Brine Rejection in Controlling Stratification Throughout Winter in Southeast Hudson Bay. *Estuaries and Coasts*, *43*(4), 756–786. https://doi.org/10.1007/s12237-020-00698-0

Ferland, J., Gosselin, M., & Starr, M. (2011). Environmental control of summer primary production in the hudson bay system: The role of stratification. *Journal of Marine Systems*, *88*(3), 385–400. https://doi.org/10.1016/j.jmarsys.2011.03.015

Freeman, N. G., Roff, J. C., & Pett, R. J. (1982). Physical, chemical, and biological features of river plumes under an ice cover in James and Hudson Bays. *Le Naturaliste Candien*, *109*, 745–764.

Gaston, A. J., Smith, S. A., Saunders, R., Storm, G. I., & Whitney, J. A. (2007). Birds and marine mammals in southwestern Foxe Basin, Nunavut, Canada. *Polar Record*, *43*(1), 33–47. https://doi.org/10.1017/S0032247406005651

Gosselin, M., Legendre, L., Demers, S., & Ingram, R. G. (1985). Responses of Sea-Ice Microalgae to Climatic and Fortnightly Tidal Energy Inputs (Manitounuk Sound, Hudson Bay). *Canadian Journal of Fisheries and Aquatic Sciences*, *42*(5), 999–1006. https://doi.org/10.1139/f85-125

Granskog, M. A., Kuzyk, Z. Z. A., Azetsu-Scott, K., & Macdonald, R. W. (2011). Distributions of runoff, sea-ice melt and brine using δ18o and salinity data - a new view on freshwater cycling in hudson bay. *Journal of Marine Systems*, *88*(3), 362–374. https://doi.org/10.1016/j.jmarsys.2011.03.011

Harvey, M., Therriault, J., & Simard, N. (1997). Late-summer distribution of phytoplankton in relation to water mass characteristics in Hudson Late-summer distribution of phytoplankton in relation to water mass characteristics in Hudson Bay and Hudson Strait (Canada). *Canadian Journal of Fisheries and Aquatic Sciences*, *54*, 1937–1952. https://doi.org/10.1139/cjfas-54-8-1937

Hudon, C., Morin, R., Bunch, J., & Harland, R. (1996). Carbon and nutrient output from the Great Whale River (Hudson Bay) and a comparison with other rivers around Quebec. *Canadian Journal of Fisheries and Aquatic Sciences*, *53*(7), 1513–1525. https://doi.org/10.1139/f96-080

Ingram R.G., & Prinsenberg S. Coastal oceanography of Hudson bay and surrounding eastern Canadian arctic waters. A.R. Robinson, K.N. Brink (Eds.), The Sea, Vol. 11. The Global Coastal Ocean Regional Studies and Synthesis, Harvard University Press, Cambridge, Massachusetts and London (1998), pp. 835-861

Ingram, R. G., Wang, J., Lin, C., Legendre, L., & Fortier, L. (1996). Impact of freshwater on a subarctic coastal ecosystem under seasonal sea ice (southeastern Hudson Bay, Canada). I. Interannual variability and predicted global warming influence on river plume dynamics and sea ice. Journal of Marine Systems, 7(2–4), 221–231. https://doi.org/10.1016/0924-7963(95)00006-2

Jones, E. P., & Anderson, L. G. (1994). Northern hudson bay and foxe basin: Water masses, circulation and productivity. *Atmosphere - Ocean*, *32*(2), 361–374. https://doi.org/10.1080/07055900.1994.9649502

Jones, E. P., Anderson, L. G., & Swift, J. H. (1998). Distribution of Atlantic and Pacific waters in the upper Arctic Ocean: Implications for circulation. *Geophysical Research Letters*, *25*(6), 765–768.

Kasper, J. L., and T. J. Weingartner (2015), The Spreading of a Buoyant Plume Beneath a Landfast Ice Cover, *J. Phys. Oceanogr.*, *45*(2), 478-494, doi:10.1175/jpo-d-14-0101.1.

Kazmiruk, Z. V., D. W. Capelle, C. M. Kamula, S. Rysgaard, T. Papakyriakou, and Z. A. Kuzyk (2021), High biodegradability of riverine dissolved organic carbon in late winter in Hudson Bay, Canada, *Elementa: Science of the Anthropocene*, *9*(1), doi:10.1525/elementa.2020.00123.

Kuzyk, Z. A., Macdonald, R. W., Granskog, M. A., Scharien, R. K., Galley, R. J., Michel, C., … Stern, G. (2008). Sea ice, hydrological, and biological processes in the Churchill River estuary region, Hudson Bay. *Estuarine, Coastal and Shelf Science*, *77*(3), 369–384. https://doi.org/10.1016/j.ecss.2007.09.030

Kuzyk, Z. Z. A., Macdonald, R. W., Tremblay, J. É., & Stern, G. A. (2010). Elemental and stable isotopic constraints on river influence and patterns of nitrogen cycling and biological productivity in Hudson Bay. *Continental Shelf Research*, *30*(2), 163–176. https://doi.org/10.1016/j.csr.2009.10.014

Landy, J. C., Ehn, J. K., Babb, D. G., Thériault, N., & Barber, D. G. (2017). Sea ice thickness in the Eastern Canadian Arctic: Hudson Bay Complex & Baffin Bay. *Remote Sensing of Environment*, *200*(August), 281–294. https://doi.org/10.1016/j.rse.2017.08.019

Lapoussière, A., Michel, C., Gosselin, M., Poulin, M., Martin, J., & Tremblay, J. É. (2013). Primary production and sinking export during fall in the Hudson Bay system, Canada. *Continental Shelf Research*, *52*, 62–72. https://doi.org/10.1016/j.csr.2012.10.013

Le Fouest, V., Babin, M., & Tremblay, J. E. (2013). The fate of riverine nutrients on Arctic shelves. *Biogeosciences*, *10*(6), 3661–3677. https://doi.org/10.5194/bg-10-3661-2013

Legendre, L., Ingram, R. G., & Poulin, M. (1981). Physical control of phytoplankton production under sea ice (Manitounuk Sound, Hudson Bay). *Can. J. Fish. Aquat. Sci. 38*: 1385-1392

Li, S. S., Ingram, R. G. (2007). Isopycnal deepening of an under-ice river plume in coastal waters: Field observations and modeling. *Journal of Geophysical Research: Oceans 112*(C7). doi:https://doi.org/10.1029/2006JC003883.

MacDonald, M., Arragutainaq, L., & Novalinga, Z. (1997). *Voices from the Bay: Traditional Ecological Knowledge of Inuit and Cree in the Hudson Bay Bioregion*. Canadian Arctic Resource Committee.

Macdonald, R.W., McLaughlin, F.A. (1982). The effect of storage by freezing on dissolved inorganic phosphate, nitrate and reactive silicate for samples from coastal and estuarine waters. *Water Res 16*(1): 95-104.

Macdonald, R. W., Wong, C. S., & Erickson, P. E. (1987). The distribution of nutrients in the southeastern Beaufort Sea: Implications for water circulation and primary production. *Journal of Geophysical Research: Oceans*, *92*(C3), 2939–2952. https://doi.org/10.1029/JC092iC03p02939

Macdonald, R. W., D. W. Paton, and E. C. Carmack (1995), The freshwater budget and underice spreading of Mackenzie River water in the Canadian Beaufort Sea based on salinityand 18O/16O measurements in water and ice, *Journal of Geophysical Research, 100*(C1), 895-919.

Macdonald, R. W. (2000). Arctic Estuaries and Ice: A Positive-Negative Estuarine Couple. In E. L. Lewis, P. E. Jones, P. Lemke, T. D. Prowse, & P. Wadhams (Eds.), *The Freshwater Budget of the Arctic Ocean* (pp. 383–407). Springer Netherlands.

Maestrini, S. Y., Rochet, M., Legendre, L., & Demers, S. (1986). Nutrient limitation of the bottom-ice microalgal biomass (southeastern Hudson Bay, Canadian Arctic). *Limnology and Oceanography*, *31*(3), 969–982.

Matthes, L. C., et al. (2021), Environmental drivers of spring primary production in Hudson Bay, *Elementa: Science of the Anthropocene*, *9*(1), doi:10.1525/elementa.2020.00160.

de Melo, M.L., M.-L. Gérardin, C. Fink-Mercier, and P.A. del Giorgio. 2022. Patterns in riverine carbon, nutrient and suspended solids export to the Eastern James Bay: links to climate, hydrology and landscape features. *Biogeochemistry*: In review.

Messier D, Ingram RG, Roy D. (1986). Chapter 20: Physical and biological modifications in response to La Grande hydroelectric complex. *Elsevier Oceanography Series* 44:403-424. Östlund, H. G., & Hut, G. (1984). Arctic ocean water mass balance from isotope data. *Journal of Geophysical Research*, *89*(4), 6373–6381.

Östlund, H. G., & Hut, G. (1984). Arctic ocean water mass balance from isotope data. Journal of Geophysical Research, 89(4), 6373–6381.

Peck, C. J., Kuzyk, Z. Z. A., Heath, J. P., Lameboy, J., Ehn, J. K. (submitted). Under-ice hydrography of the La Grande River plume in relation to a ten-fold increase in wintertime discharge.

Peralta-Ferriz, C., & Woodgate, R. A. (2015). Seasonal and interannual variability of pan-Arctic surface mixed layer properties from 1979 to 2012 from hydrographic data, and the dominance of stratification for multiyear mixed layer depth shoaling. *Progress in Oceanography*, *134*, 19–53. https://doi.org/10.1016/j.pocean.2014.12.005

Petrusevich, V. Y., I. A. Dmitrenko, I. E. Kozlov, S. A. Kirillov, Z. A. Kuzyk, A. S. Komarov, J. P. Heath, D. G. Barber, and J. K. Ehn (2018), Tidally-generated internal waves in Southeast Hudson Bay, *Cont. Shelf Res.*, *167*, 65-76, doi:https://doi.org/10.1016/j.csr.2018.08.002.

Prinsenberg, S. J. (1982), Present and future circulation and salinity in James Bay, *Le Naturaliste Canadien, 109*, 827-841.

Redfield, A. C. (1958). The biological control of chemical factors in the environment. *American Scientist*, *46*(3), 205–221. Retrieved from https://www-jstor-org.uml.idm.oclc.org/stable/pdf/27827150.pdf?refreqid=excelsior%3Af11611d1b19a1553954ceaab2c8b383c

Ridenour, N. A., Hu, X., Sydor, K., Myers, P. G., & Barber, D. G. (2019a). Revisiting the Circulation of Hudson Bay: Evidence for a Seasonal Pattern. *Geophysical Research Letters*, *46*(7), 3891–3899. https://doi.org/10.1029/2019GL082344

Ridenour, N. A., Hu, X., Jafarikhasragh, S., Landy, J. C., Lukovich, J. V., Stadnyk, T. A., … Barber, D. G. (2019b). Sensitivity of freshwater dynamics to ocean model resolution and river discharge forcing in the Hudson Bay Complex. *Journal of Marine Systems*, *196*(May), 48–64. https://doi.org/10.1016/j.jmarsys.2019.04.002

Roff, J. C., & Legendre, L. (1986). Physico-chemical and biological oceanography of Hudson Bay. In I. P. Martini (Ed.), *Elsevier Oceanography Series* (Vol. 44, pp. 265–292). New York: Elsevier Science Publishers. https://doi.org/10.1016/S0422-9894(08)70907-3

Saucier, F.J., Senneville, S., Prinsenberg, S., Roy, F., Smith, G., Gachon, P., Caya, D., Laprise, R. (2004). Modelling the sea ice–ocean seasonal cycle in Hudson Bay, Foxe Basin and Hudson Strait, Canada. Climate Dynamics 23, 303–326.

Simpson, K. G., Tremblay, J. E., Gratton, Y., & Price, N. M. (2008). An annual study of inorganic and organic nitrogen and phosphorus and silicic acid in the southeastern Beaufort Sea. Journal of Geophysical Research, 113. https://doi.org/10.1029/2007JC004462

Slomp, C. P. (2011). Phosphorus Cycling in the Estuarine and Coastal Zones: Sources, Sinks, and Transformations. In E. Wolanski & D. S. McLusky (Eds.), *Treatise on Estuarine and Coastal Science* (pp. 201–229). Elsevier. https://doi.org/10.1016/B978-0-12-374711-2.00506-4

Smith, A., C. Delavau, & Stadnyk, T. (2015). Identification of geographical influences and flow regime characteristics using regional water isotope surveys in the lower Nelson River, Canada. *Canadian Water Resources Journal /Revue canadienne des ressources hydriques* 40: 23–35.

Steele, M., Zhang, J., Ermold, W., (2010). Mechanisms of summertime upper Arctic Ocean warming and the effect on sea ice melt. *Journal of Geophysical Research: Oceans 115*(C11), C11004. http://dx.doi.org/10.1029/2009JC005849.

Stewart, D.B., and W.L. Lockhart. 2005. An Overview of the Hudson Bay Marine Ecosystem. Can. Tech. Rep. Fish. Aquat. Sci. 2586: vi + 487 p.

Stirling, I. (1997). The importance of polynyas, ice edges, and leads to marine mammals and birds. *Journal of Marine Systems*, *10*(1–4), 9–21. https://doi.org/10.1016/S0924-7963(96)00054-1

Tan, F. C., & Strain, P. M. (1996). Sea ice and oxygen isotopes in Foxe Basin, Hudson Bay, and Hudson Strait, Canada. *Journal of Geophysical Research C: Oceans*, *101*(C9), 20869–20876. https://doi.org/10.1029/96JC01557

Tremblay, J. É., Simpson, K., Martin, J., Miller, L., Gratton, Y., Barber, D., & Price, N. M. (2008). Vertical stability and the annual dynamics of nutrients and chlorophyll fluorescence in the coastal, southeast Beaufort Sea. *Journal of Geophysical Research: Oceans*, *113*(7), 1–14. https://doi.org/10.1029/2007JC004547

Tremblay, J. E., Raimbault, P., Garcia, N., Lansard, B., Babin, M., & Gagnon, J. (2014). Impact of river discharge, upwelling and vertical mixing on the nutrient loading and productivity of the Canadian Beaufort Shelf. *Biogeosciences*, *11*(17), 4853–4868. https://doi.org/10.5194/bg-11-4853-2014

Tremblay, J.-É., & Gagnon, J. (2009). The effects of irradiance and nutrient supply on the productivity of Arctic waters: a perspective on climate change. In J. C. J. Nihoul & A. G. Kostianoy (Eds.), *Influence of Climate Change on the Changing Arctic and Sub-Arctic Conditions* (pp. 73–89). Springer.

Turner, R. E., Rabalais, N. N., Justic, D., & Dortch, Q. (2003). Global patterns of dissolved N, P and Si in large rivers. *Biogeochemistry*, *64*(3), 297–317. https://doi.org/10.1023/A:1024960007569

Welch, H. E. (1985). Introduction to limnological research at Saqvaqjuac, northern Hudson Bay. *Canadian Journal of Fisheries and Aquatic Sciences*, *42*(3), 494–505. https://doi.org/10.1139/f85-067

A. Woodgate, R., & Peralta-Ferriz, C. (2021). Warming and Freshening of the Pacific Inflow to the Arctic From 1990-2019 Implying Dramatic Shoaling in Pacific Winter Water

Ventilation of the Arctic Water Column. *Geophysical Research Letters*, *48*(9), 1–11. https://doi.org/10.1029/2021GL092528

Yamamoto-Kawai, M., Carmack, E. C., & McLaughlin. F. A. (2006). Nitrogen balance and Arctic throughflow. *Nature, 443*((43), doi:10.1038/443043a.

Yamamoto-Kawai, M., McLaughlin, F. A., Carmack, E. C., Nishino, S., & Shimada, K. (2008). Freshwater budget of the Canada Basin, Arctic Ocean, from salinity, δ18O, and nutrients. *Journal of Geophysical Research: Oceans*, *113*(1), 1–12. https://doi.org/10.1029/2006JC003858

5.0 Conclusions and synthesis

The Riverine Coastal Domain (RCD), and particularly the Hudson Bay and James Bay coastal regions, are areas of great importance socially, biogeochemcially, and economically, and have been experiencing significant environmental changes over the last several decades. The Arctic and sub-Arctic climates of Hudson and James Bays set the system up for highly seasonal sea-ice and river discharge cycles. The input of freshwater from sea-ice melt in summer, and the seasonality of the discharge rates of rivers both impact the HB and JB water masses. The distribution of freshwater and how it interacts with coastal seawater (e.g., mixing, freezing, serving as a physical barrier to atmospheric disturbances as ice) affects the distribution of nutrients and how they are utilized or renewed in the RCD. Different source waters, i.e., RW, SIM, and SW, also provide different nutrient conditions.

The lack of recent comprehensive oceanographic data in the coastal regions of northeast James Bay, northwest Hudson Bay and southeast Hudson Bay, especially in winter, has made it difficult to project possible impacts of a changing climate and anthropogenic changes, such as with hydroelectric development and regulation. Addressing this gap, in this thesis I provided new data (oxygen isotope ratio, salinity, and nutrients) for NEJB, SEHB, and NWHB to address the overarching objective of characterizing the relationships between the freshwater cycles and nutrient distributions, with emphasis on ice-covered conditions, when biological processes are reduced. The results and conclusions I presented in this thesis allow for further interpretation of what primary production in these areas could potentially look like, as the freshwater dynamics continue to change.

For the first sub-objective, I used seawater oxygen isotope ratio ($\delta^{18}O$) and salinity data to trace and quantify the three main water masses of the three regions in the study area: local

river water (RW), seawater (SW), and sea-ice melt (SIM). In NEJB, in winter, the coastal water mass is dominated by the under-ice river plume of La Grande River, which is currently the highest discharging river to the Hudson Bay system. La Grande River, which has undergone hydroelectric development, has a reversed hydrograph where the peak discharge, typically seen in spring in natural systems, has been shifted to winter. The presence of landfast ice prevents wind mixing which provides the conditions for the plume to thicken in terms of depth, and for it to expand in surface area over the course of the winter. Areas along the NEJB coast, which previously (under the natural flow regime) had high salinity and seawater-associated nutrient stocks during winter, now have low salinity and river-derived nutrient stocks, with potential implications for primary production in spring when the growing season begins. In summer, this region has much lower riverine influence than in winter, albeit higher than it did under natural conditions because annual discharge of La Grande River has increased some ~30%. The coastal domain sees a freshening of the source-seawater during summer as well, which I interpret as a wide-scale freshening, not attributed to local SIM. Mixing of the water column occurs without the presence of ice-cover, which creates an overall average fresher water mass.

In NWHB, riverine influence in the surface layer was very minimal or non-existent in winter, with slight evidence of riverine-induced freshening at Chesterfield Inlet (CI), where there were water samples with lower $\delta^{18}O$ values compared to Naujaat (RB). In this region, the dominant freshwater processes during winter were those associated with the sea-ice cycle and the source-seawater from which it was derived. SEHB represents an intermediate between NEJB and NWHB. Water in the coastal boundary is circulated around the bay (general cyclonic direction) and is altered by riverine input. In any given winter period, by

the time water makes it to SEHB, the surface water mass has been freshened by both sea-ice melt and riverine inputs (from James Bay and to a lesser extent the Great Whale River), but not to the same low salinity and $\delta^{18}O$ observed in NEJB in winter, as summarized in Figure 5.1.

To address my second sub-objective, I examined the nutrient distributions with respect to the supply provided by the water sources discussed above, as well as identified whether the nutrients and properties were exhibiting conservative or non-conservative behaviour. The nutrient content of source waters (both RW and SW) in NEJB varies by season, with winter concentrations of nitrate, silicate, and phosphate slightly higher than summer, likely impacted by riverine seasonality and the apparent regional freshening of the source seawater. Overall nutrient concentrations of mixed waters, between the two sources, are further depleted in summer - either to or near the limit of detection - due to biological uptake. Nutrient stocks were calculated for winter and summer in NEJB to help understand the influence each water type along this coast had on the nutrient condition, in line with the third sub-objective. The influence of La Grande River on NEJB coastal waters in summer is greatly diminished relative to winter, as identified by the calculated surface pre-production nitrate and phosphate stocks (separated by source water). Nitrate and phosphate stocks, respectively, decreased and increased from winter to summer, with reduction in river discharge. In winter, La Grande River nitrate concentrations (4.53 μM) were higher than those in the ambient seawater (3.18 μM), which was unexpected considering the nitrate concentration of riverine discharge in the Arctic and subarctic is generally not higher than the deep seawater nutrient reservoirs. Phosphate stocks along the NEJB coast in winter were low in the surface because the highly stratified river plume dominated and maintained a surface salinity < 10, which created a

phosphate-limited water mass. Production in the higher salinity waters (> 10) here would be limited by nitrate despite the La Grande's high contribution. Sea ice cover and high flow in any given winter result in a short flushing rate and thus what we observed as high nitrate stocks in winter, was most likely transported out of the NEJB coast and towards the SEHB region before the growing season began.

With evidence of freshwater (RW) moving out of NEJB and continuing along the RCD, it is clear that we will need to understand the freshwater dynamics of JB, in order to assess nutrient distributions in SEHB. With the long residence times of RW calculated for Hudson Bay, it is possible that NEJB RW has been incorporated into the SEHB water mass. Despite RW being the largest freshwater contributor to SEHB in winter, the water characterized by high salinity (> 20) dominated the nutrient supply. The low salinity (< 5) and RW-associated samples in SEHB majorly influenced the density-driven stratification and lack of vertical mixing of the water mass, and therefore influenced the distribution of nutrients. Southeast Hudson Bay SW had comparatively similar nitrate to NEJB RW (~5 μM), which is about two times the concentrations seen in the Great Whale River. One wonders whether a nitrate supplement associated with James Bay outflow partially explains why nitrate concentrations are similar in SEHB and NWHB, despite the negative influence on nitrate provided by the local SEHB rivers like the Great Whale. Phosphate concentrations showed conservative behaviour against salinity (without biological influence) in both SEHB and NEJB; however, maximum phosphate concentrations were higher in SEHB (by ~0.4 μM), consistent with seawater, which is more balanced in its nitrate to phosphate ratio, dominating the overall nutrient supply. Phosphate concentrations were higher still in NWHB during winter, at times reaching values more than three-fold higher than those in NEJB (Figure 5.1). Lack of river

input in part explains the high phosphate concentrations in NWHB but the fact that the most phosphate-rich water samples did not have the highest (most enriched) values of $\delta^{18}O$ implies that this explanation is not complete. Examination of N:P ratios identified that phosphate concentrations were higher than usual, or nitrate was lower than usual, in almost all of the coastal water samples (N:P ~ 5:1), both NWHB and the other regions, but some samples in NWHB reached an extreme minimum where N:P ~ 2:1. The very low N:P ratios prompted the examination of limited data from 1961, accessed through the Marine Environmental Data Service. This comparison of new and historic data revealed that our range of phosphate concentrations had been previously observed, but our nitrate concentrations had almost halved in magnitude compared 1961. However, this comparison is only between two points in time almost 6 decades apart and may not represent an overall shift of the system. The NWHB coastal system was ultimately set up over the winter to become a nitrate limited system once the productive season began, as was SEHB, and coastal waters of NEJB that had salinity > 10. The only area that was a potentially phosphate-limiting system was present in winter within the La Grande plume (salinity < 10), and at a few stations near the Great Whale River that experienced low phosphate and relatively high nitrate. Silicate data for the coastal areas were not scrutinized as closely as phosphate and nitrate. However, winter silicate concentrations were highest in NEJB, and lowest in NWHB, which was expected with the variance of riverine contribution levels between the regions (Figure 5.1).

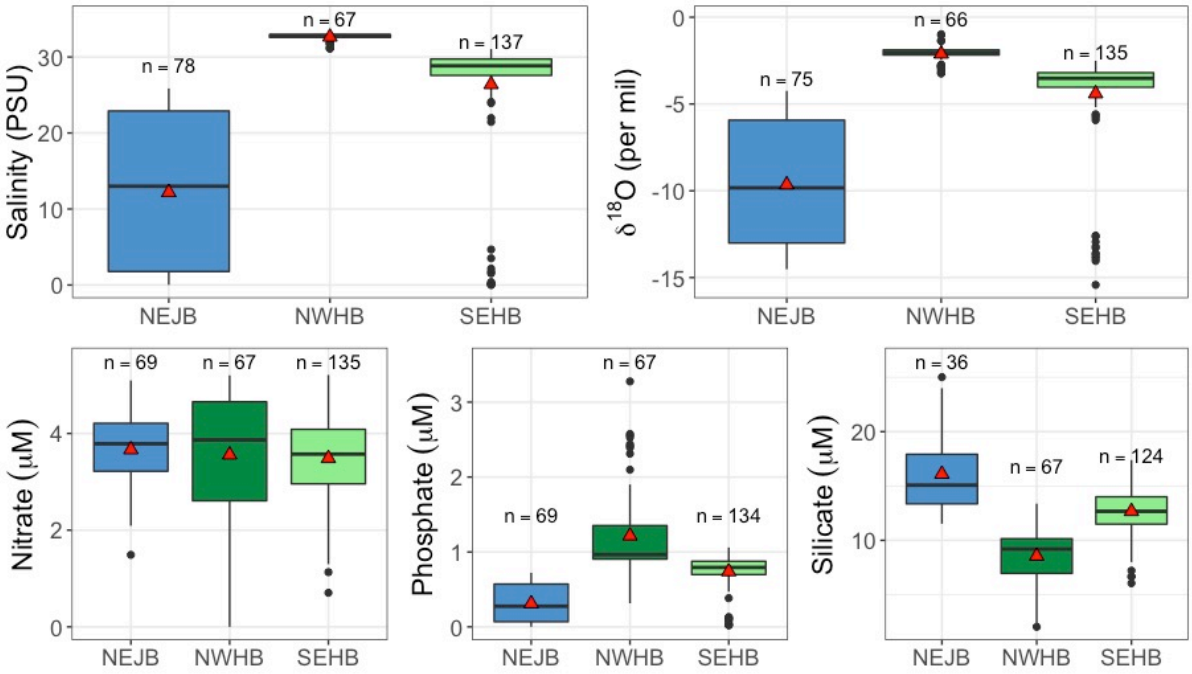

Figure 5.1 Boxplots of winter (EW and LW combined) salinity, $\delta^{18}O$, nitrate, phosphate, and silicate concentrations, coloured and grouped by region (NEJB, NWHB, and SEHB). Sample count is indicated by the n value above each boxplot. Red triangle and black horizontal line indicates the respective mean and median of each data grouping.

The Riverine Coastal Domain (RCD) as described by Carmack et al. (2015) is "a narrow…, shallow…, contiguous feature that is primarily forced by an aggregate of continental runoff sources." The three regions of Hudson Bay and James Bay that were the focus of this thesis provide examples of the vast variability of the RCD in terms of structure and properties. This variability was highly influenced by the seasonal cycles of different freshwater sources. By using the term contiguous, rather than continuous, there is recognition of aggregation of riverine source waters and the associated biogeochemical properties along the RCD in some places and during certain seasons. Identifying NWHB as the starting point, in terms of the general circulation pattern, and NEJB and SEHB as downstream, the expectation is that this shallow, narrow domain accumulates riverine waters and their

associated properties. With the assessment of freshwater sources along these three coastal regions, there was evidence of river water (RW) accumulation along the RCD; however, this accumulation was not directly reflected in an accumulation (and depletion) of nutrients that are abundant (or depleted) in riverine source waters. The accumulation of freshwater downstream of James Bay contributes to the shallow stratification seen in SEHB, throughout any given year. There was no evidence along this coast of cumulative addition or loss of nutrients as a result of the nature of the RCD. This led to the importance of not only considering the variation of freshwater sources along the RCD, but also the properties of the marine waters with which these coastal waters interacted. The deep waters of Hudson Bay are known to have long residence times and resultantly relatively high nutrient concentrations due to the ability of these nutrients to regenerate and accumulate in deep basins. This connection between depth, residence time, and nutrient stock regeneration, highlights the possibility of observing different nutrient conditions in various regions of the Riverine Coastal Domain in the Hudson Bay and James Bay system. The NWHB region is relatively deep, with channels exceeding 250 m, allowing the possibility for deep nutrient regeneration and ultimate renewal to surface waters through physical mixing. The expectation then was to see the deep waters supplying surface waters with higher nutrient concentrations, but surprisingly, the expected deep water nutrient pool was not there. There is a source of high phosphate concentrations to surface waters in NWHB but it is not the local deep basin. We suspect this water type is advected from Foxe Basin or west Hudson Strait. In contrast, the NEJB coastal region is shallow (< 25 m) and has comparatively low nutrient concentrations in what would be considered the source seawater, which may indicate that Hudson Bay

intermediate waters, and not deep waters, cross the broad shallow shelf separating Hudson Bay and our NEJB study area.

Ultimately what this collection of research shows is that regional scale observations, such as those that can be collected from a research vessel during summer, and winter observations from coastal areas, which are best collected from the landfast ice platform with the assistance of Cree and Inuit guides, both contribute to a better understanding of the riverine coastal domain. Both a local and regional context is important for understanding past, present, and future environmental change in the coastal regions of Hudson Bay and James Bay. Other coastal regions of the Hudson Bay – James Bay system, such as the coastal areas of western James Bay not mentioned within this thesis, would benefit from monitoring programs and scientific studies (both in winter and summer). It is difficult, and perhaps not as useful to extrapolate the interpretations and conclusions made for the NWHB, NEJB, and SEHB regions to other geographic regions of the Hudson Bay – James Bay system, without understanding the full context of the ice regime and coastal water mass structure and freshwater composition of a specific coastal area.

This thesis identified the seasonal oceanographic properties of three very different coastal regions of the Hudson Bay – James Bay system: northeast James Bay, northwest Hudson Bay, and southeast Hudson Bay. I analyzed the impact of both the sea-ice cycle, and riverine discharge cycle, taking into consideration the changes both were experiencing in terms of climate change and anthropogenic development, on how nutrients were distributed throughout these highly productive coastal regions of Hudson Bay. With the previous shortcoming of research in these regions, the results will serve as a useful baseline for designing oceanographic monitoring and research efforts moving forward.